DEVELOPMENT OF NOVEL FLUORESCENCE AND NMR REAGENTS FOR MONITORING PROTEIN-PROTEIN INTERACTIONS BETWEEN SURVIVIN AND ITS PROTEIN BINDING PARTNERS

By

Stephanie Cara Bishop

MA, University of Kansas, 2009

Submitted to the graduate degree program in Pharmacology, Toxicology and Therapeutics and the Graduate Faculty of the University of Kansas in partial fulfillment of the requirements for the degree of Doctor of Philosophy.

_____

Chairperson, Jed N. Lampe, Ph.D.

_____

Qi Chen, Ph.D.

_____

Mark Fisher, Ph.D.

_____

Bruno Hagenbuch, Ph.D.

_____

Greg Reed, Ph.D.

Date Defended: 06/08/2015

The Dissertation Committee for Stephanie Cara Bishop certifies that this is the approved version of the following dissertation:

DEVELOPMENT OF NOVEL FLUORESCENCE AND NMR REAGENTS FOR MONITORING PROTEIN-PROTEIN INTERACTIONS BETWEEN SURVIVIN AND ITS PROTEIN BINDING PARTNERS

_____

Chairperson, Jed N. Lampe, Ph.D.

Date approved: 06/11/2015

Abstract

Inhibition of protein-protein interactions is a promising therapeutic strategy for targeting non-enzymatic proteins. One strategy to inhibit protein-protein interactions is to design inhibitors specifically toward the protein-protein interaction interface. To achieve this objective using structure-aided design, knowledge of the structure of the interface of the protein-protein interaction is needed. Augmenting the utility of NMR to determine the structure of larger proteins, and of protein complexes, than is currently achieved with conventional approaches, expands structure-aided design and to evaluate protein-protein interactions for target proteins relevant to human disease such as cancer. A second approach to bring new therapies to the clinic is to identify lead molecules using high-throughput screening. High-throughput screening (HTS) offers the potential to more rapidly and less expensively identify promising molecules that may inhibit a specific protein-protein interaction.

To improve efforts at structure-aided design, we hypothesize that we can expand the utility of fluorescence- and NMR-based approaches to monitor protein-protein interactions by incorporating fluorescent or paramagnetic labels, site-specifically, into a protein of interest. This technology will provide much more structural detail regarding the binding site of a candidate small molecule protein-protein interaction inhibitor. This structural information can then be used in downstream medicinal chemistry efforts to improve inhibitor affinity and specificity. Additionally, site-specific fluorescent and paramagnetic labels can be used in sensitive HTS assays for protein-protein interaction inhibitors.

The lanthanide series of elements, which possess intriguing spectroscopic and paramagnetic properties, was chosen to accomplish these efforts. Lanthanides exhibit luminescence and have excitation and emission maxima unique from biological fluorophores, broad Stokes shifts, and narrow emission bands. In the context of NMR, some lanthanides impart long-range perturbations in the form of paramagnetic relaxation enhancements, pseudocontact chemical shifts, and residual dipolar couplings, which are used to facilitate protein structure determination. Site-specific labeling of the protein of interest was achieved using site-directed mutagenesis, incorporation of the unnatural amino acid paF, followed by copper-free click chemistry with a cyclooctyne-containing lanthanide chelator. Synthesis of the small-molecule lanthanide chelator amenable to copper-free click chemistry-mediated incorporation is described herein.

To improve efforts at identification of candidate protein-protein interaction inhibitors, we hypothesized that a high-throughput fluorescence polarization screening assay could be established. Inhibitors identified in this assay would be further characterized using the lanthanide labeled Survivin protein. A recently-identified cancer target, the Survivin protein, was evaluated using the methodologies described herein. The results demonstrate we were able to fluorescently label the Survivin protein site-specifically using a click chemistry approach. In addition, preliminary fluorescence results indicate that synthesis of a clickable lanthanide chelator was also successful.

Finally, a high-throughput fluorescence polarization-based screening platform for analyzing Survivin protein-peptide interactions was evaluated.

Taken together, the methodologies described herein attempt to augment efforts at structure-aided drug design as well as to produce new technologies to identify promising protein-protein interaction inhibitors, with the ultimate goal of improving our understanding of protein-protein interactions implicated in many human diseases, including cancer.

Dedication

I dedicate my efforts described herein to my friend Bowen Pope (5/2/1979 – 10/24/2009), who continues to inspire me today. Bowen, I thank you for the time that we shared and have only the best memories of our childhood adventures together. The courage, endurance, positive attitude, and strength that you exhibited throughout your fight continue to impact my life. I am so blessed to have known you.

Acknowledgments

I am so grateful to my committee members Dr. Mark Fisher, Dr. Bruno Hagenbuch, Dr. Qi Chen, Dr. Greg Reed, and Dr. Jed Lampe for their countless hours dedicated to my professional development; your invaluable efforts have never gone unnoticed and I hope I have been able to convey my gratitude and appreciation for your suggestions and efforts over the last few years. Thank you so much.

John Karanicolas, Ph.D.: I am immeasurably grateful to you for EVERY interaction we had and for your support of this project. I appreciated your patience, scientific insights, and the opportunity to work with you.

Feng Li, Ph.D., thank you for performing numerous small-molecule mass spectrometry analyses; thank you for our discussions and for your efforts and time. I appreciated it very much.

Antonio Artigues, Ph.D., and Maite Villar, Ph.D., performed whole-protein mass spectrometry analyses as well as tryptic digests on several samples; thank you for your time, efforts, and explanations of the data. I appreciate your efforts very much.

Thank you so much Cody Tully, Rosa Meagher, Dorothy McGregor, Ann Hall, and Randy Stout for all of your time and help with so many tasks. Your efforts have been very much appreciated and have made my time here much easier. Thank you.

I'm grateful to the following sources of financial support: the Madison and Lila Self Graduate Fellowship, the Environmental Toxicology Training Program 5T32ES007079-32, COBRE P20 RR021940-06, and R01 GM099959-01 (John Karanicolas, Ph.D.).

I am indebted to my family for their endless support, in particular to my sister, Jessica, and her family, my parents Rodney Bishop, M.D. and Audrey Bishop, J.D., and my extended family. Jessi, I've been told that Barrett is well-adjusted and kind, which are undoubtedly reflections of the love and compassion you gave him. Thank you so much. You are a blessing in our lives and I am forever grateful.

Thank you to my friends, in particular Ben Woolbright, Ph.D., Mitch McGill, Ph.D., Kelli Boxberger, and Brad Sullivan, Ph.D., for their unwavering support, encouragement, and advice. I enjoyed our science talks and learned a lot from each of you.

Larry Long, Ph.D., I would not have made it to this stage without you. I cannot articulate how much you have helped me. I am so, so grateful for all of your time and efforts. Thank you so much.

Thank you to my son, Barrett, for spontaneously sharing "I love you, Mommy", and for bringing endless joy and purpose to my life. You are a light and a blessing and I love you so much.

Table of Contents **Page**

Abbreviations

ACN: acetonitrile

amu: atomic mass units

ATP: adenosine triphosphate

BGG: bovine gamma globulin

BIR: baculoviral IAP repeat

BLI: biolayer interferometry

c-DTPA: cyclic diethylenetriaminepentaacetic acid (also known as DTPA dianhydride)

CML: chronic myelogenous leukemia

CPC: chromosomal passenger complex

Da: Dalton

DBCO: dibenzylcyclooctyne

DBCO488: dibenzylcyclooctyne + fluorescein small molecule

DMSO: dimethyl sulfoxide

DNA: deoxyribonucleic acid

DOTA: 1,4,7,10-tetraazacyclo-dodecane-1,4,7,10-tetraacetic acid

DTPA: diethylenetriaminepentaacetic acid

E. coli: *Escherichia coli*

EDC: 1-ethyl-3-(3-dimethylamino-propyl)-carbodiimide

EDTA: ethylenediaminetetraacetic acid

EMA: European Medicines Agency

ESI: electrospray ionization

FDA: Food and Drug Administration

FP: fluorescence polarization

FPLC: fast phase liquid chromatography

FRET: Förster resonance energy transfer

GFP: green fluorescent protein

GST: glutathione *S*-transferase

HPLC: high-performance liquid chromatography

HSQC: heteronuclear single quantum coherence

HTS: high-throughput screening

IAP: inhibitor of apoptosis

INCENP: inner centromere protein

IPTG: isopropyl-β-D-1-thiogalactopyranoside

kDa: kiloDalton

LB: Luria-Bertani

LBT: lanthanide binding tag

LED: light-emitting diode

LTQ FT: linear trap quadrupole – Fourier transform

MALDI: matrix-assisted laser desorption/ionization

MALDI-TOF: matrix-assisted laser desorption/ionization – time of flight

mAU: milli absorbance units

MES: 2-(N-morpholino)ethanesulfonic acid

MWCO: molecular weight cutoff

NAD: nicotinamide adenine dinucleotide

NMR: nuclear magnetic resonance

NTA: nitrilotriacetic acid

paF: *para*-azidophenylalanine

PPI: protein-protein interaction

PRE: paramagnetic relaxation enhancement

PCS: pseudocontact chemical shift

RDC: residual dipolar coupling

RNA: ribonucleic acid

SDS-PAGE: sodium dodecyl sulfate-polyacrylamide gel electrophoresis

Smac/DIABLO: second mitochondria-activator of caspases/direct IAP binding protein with low pI

TB: Terrific broth

TCSPC: time-correlated single-photon counting

TFA: trifluoroacetic acid

UV: ultraviolet

ZINC: Zinc is not commercial (compound library)

Chapter 1. Introduction

1.1 Incidence of Cancer

According to the American Cancer Society, more than 1.6 million new cases of cancer will be diagnosed in 2015 in the United States [American Cancer Society, 2015]. Of these, more than 589,000 are expected to be fatal, which corresponds to 1620 people per day. Nearly 1 in 4 deaths in the U.S. is from cancer with heart disease being the only cause of death more prevalent. In 2009, the National Institutes of Health (NIH) reported that the annual healthcare burden was more than $216 billion from all cancers [American Cancer Society, 2015]. Finally, although for most cancers, the one- and five-year survival rates are increasing, some cancers remain exceedingly difficult to treat, and exhibit very high mortality rates [American Cancer Society, 2015]. These staggering statistics indicate that in spite of decades of efforts and many breakthroughs, the need for additional anti-cancer therapies is still pressing. A protein that is being pursued for anti-cancer therapy is Survivin [Ambrosini, *et al.*, 1997, reviewed in Altieri, 2008, Condon, 2011].

1.2 Survivin

1.2.1 Survivin Prevents Apoptosis

Survivin is a 142-amino acid, 16.5 kDa protein expressed predominately in fetal tissues; it is undetectable in terminally-differentiated adult tissues [Ambrosini, *et al.*, 1997, Reed, 2001, Salvesen and Duckett, 2002, Sah, *et al.* 2006] except during mitosis [Giodini, *et al.*, 2002]. *In vivo*, it is normally found as a homodimer with each monomer consisting of both a globular and a single long α-helical domain [Chantalat, *et al.*, 2000, Muchmore, *et al.*, 2000, Verdecia, *et al.*, 2000, Jeyaprakash, *et al.*, 2007]. Survivin is

unusual in that it participates in multiple protein-protein interactions in the cell that are critical to survival and proliferation, while being spatially and temporally distinct. These qualities have made it an attractive drug target.

Initially characterized as a member of the inhibitor of apoptosis protein (IAP) family [Ambrosini, *et al.*, 1997], Survivin is thought to prevent apoptosis by binding caspases, such as caspase-9 [Deveraux, *et al.*, 1998, Chai, *et al.*, 2000, Du, *et al.*, 2000, Liu, *et al.*, 2000, Wu, *et al.*, 2000]. When the cell receives a pro-apoptotic signal, second mitochondria-activator of caspases/direct IAP binding protein with low pI (Smac/DIABLO) is released from the mitochondria [Du, *et al*., 2000; Verhagen, *et al.*, 2000, Adrain, *et al.*, 2001]. Through an incompletely-characterized series of events, Smac/DIABLO competes with caspases for Survivin binding [Sun, *et al.*, 2005, Condon, 2011] at Survivin's **b**aculoviral **i**nhibitor of apoptosis **r**epeat (BIR) domain, which is comprised of amino acids 11 to 80. Survivin sequestration by Smac/DIABLO releases the activator caspases to elicit apoptosis.

1.2.2 Survivin Is Required for Mitosis

Although initially characterized as an IAP, Survivin also binds tubulin and stabilizes growing microtubules [Li, *et al.*, 1998, Giodini, *et al.*, 2002]. Additionally, Survivin is imperative for chromosomal segregation [Skoufias, *et al.,* 2000, Uren, *et al.*, 2000, Jiang, *et al.*, 2001, Wheatley, *et al.*, 2001]. Within the dividing cell, the proteins aurora B, borealin, inner centromere protein (INCENP), and Survivin congregate at the centromere of the chromosome to facilitate proper segregation, ensuring that each daughter cell receives the correct number of chromosomes. The structure of Survivin

within this complex, the chromosomal passenger complex (CPC), has been solved by x-ray crystallography [Jeyaprakash, *et al.*, 2007, Niedzialkowska, *et al.*, 2012]. Recent evidence suggests that the CPC is assembled within the cytosol and then transported into the nucleus via the nuclear pore complex [Zhang and Wang, 2012]. Finally, a contemporary report described the interaction between histone-3 and the BIR domain of Survivin [Jeyaprakash, *et al.*, 2011, Niedzialkowska, *et al.*, 2012], demonstrating that this region binds the nucleosome and facilitates proper chromosomal segregation during division. Thus, the number and variety of Survivin protein-protein interactions represent many possibilities for therapeutic intervention.

1.2.3 Obstacles to Effective Survivin Inhibition

Survivin is upregulated more than 40 fold over healthy tissue in numerous types of cancers [Ambrosini, *et al.*, 1997, Altieri and Marchisio, 1999, Velculescu, *et al.*, 1999]. Consequently, Survivin was identified as a new cancer drug target as early as 1997 [Ambrosini, *et al.*, 1997, reviewed in Altieri, 2008, Condon, 2011] and strategies for Survivin inhibition have included peptide vaccines, an antisense oligonucleotide, Smac mimetics, small-molecule transcriptional repressors, and protein-protein interaction inhibitors [Nakahara, *et al.*, 2007, reviewed in Groner and Weiss, 2014]. Current strategies, however, lack efficacy, giving rise to only moderate outcomes [Giaccone, *et al.*, 2009, reviewed in Groner and Weiss, 2014] and generate different outcomes especially when used in conjunction with other therapies [Carvalho, *et al.*, 2003, Cheung, *et al.*, 2009, reviewed in Groner and Weiss, 2014].

One challenge to inhibiting Survivin function is that it is non-enzymatic; as a consequence, traditional strategies of enzyme inhibition do not apply. In addition, because it lacks a traditional hydrophobic pocket amenable to small-molecule binding, Survivin is considered to be “non-druggable“ [reviewed in Groner and Weiss, 2014]. One strategy to overcome these obstacles is to target Survivin‘s protein-protein interactions, a strategy that is gaining ground in the treatment of many diseases including cancer [Oikawa, *et al.*, 2010], human papilloma virus infection, and hepatitis C virus infection [Zhu, *et al.*, 2010, D’Abramo and Archambault, 2011, Kota, *et al.*, 2012].

To evaluate the consequences of protein partner binding on the protein of interest, fluorescence-based approaches may be utilized. One advantage of fluorescence-based analyses relative to x-ray crystallography and NMR spectroscopy is that fluorescence-based approaches tend to be more sensitive, thereby requiring lower protein concentrations. To study proteins that have a tendency to aggregate at high concentration and/or where over-expression of the protein in high yield is difficult, the improved sensitivity of fluorescence-based analyses is appealing.

1.3 Strategies to Identify or Develop Potential Survivin Protein-Protein Interaction Inhibitors

1.3.1 High-Throughput Chemical Compound Screening to Identify Potential Protein-Protein Interaction Inhibitors

High throughput screening (HTS) of hundreds to thousands of chemical compounds against a target protein or protein-protein interaction is gaining appeal for its efficiency and reduced costs compared to traditional methods [reviewed in Lea and

Simeonov, 2011]. These platforms are advantageous for non-enzymatic protein targets where direct analysis of protein function is difficult [Liu, *et al.*, 2000, Glover, *et al.*, 2003, Nikolovska-Coleska, *et al.*, 2004, Nikolovska-Coleska, *et al.*, 2008]. While enzymatic assays can quantify metabolite production or reactant consumption, proteins that are not enzymes are not amenable to these types of "direct" quantifications. Alternative measures of protein function, such as caspase activity assays, may be utilized for evaluating the activity of certain proteins involved in apoptosis [Hristov, *et al.*, 2014], however, for proteins that are involved in multiple intracellular pathways, ascertaining the consequences of disrupting that protein's function may be inconclusive, i.e., Survivin function in apoptosis, but not mitosis, may be altered. These approaches may require numerous components [reviewed Lea and Simeonov, 2011], making the experimental setup cumbersome and unwieldy. Finally, as increasing interest has developed in targeting and disrupting protein-protein interactions [Arkin, *et al.*, 2004, Oikawa, *et al.*, 2010, Zhu, *et al.*, 2010, D'Abramo and Archambault, 2011, Kota, *et al.*, 2012], alternative strategies have been sought to evaluate the consequences of disrupting target protein function in order to identify inhibitors of protein-protein interactions [reviewed in Lea and Simeonov, 2011]. One high-throughput screening platform to identify protein-protein interaction inhibitors is fluorescence polarization [reviewed in Lea and Simeonov, 2011].

Fluorescence Polarization-based High-Throughput Screening

Fluorescence anisotropy refers to the extent to which a fluorophore is able to freely tumble in the analyzed system [Perrin, 1926]. Fluorescence polarization, P, is

defined as the ratio of the linearly polarized component's intensity divided by the natural light intensity [Lakowicz, 1999]. Anisotropy, r, is a similar ratio, however, it incorporates the total light component's intensity [Lakowicz, 1999].

Briefly, the concept of fluorescence polarization-based HTS, as applied to Survivin as a target, is as follows [reviewed in Lea and Simeonov, 2011]: a small (~<20-mer) synthetic peptide is fluorescently labeled and added to a solution containing Survivin. When the fluorescently-labeled peptide is freely tumbling in solution, i.e. unbound, the resulting fluorescence anisotropy or polarization signal is near zero because the ratio of the parallel and perpendicular fluorescence intensities is averaged out. As an increasing proportion of the fluorescently-labeled peptide binds Survivin protein, the fluorescence anisotropy begins to increase because the rate of fluorophore tumbling slows and thus imparts an average fluorescence polarization that can be measured. When all available fluorescently-labeled peptide is bound to the target protein Survivin, the fluorescence anisotropy signal becomes saturated (100%) because the fluorophore tumbling is at its slowest rate and the largest ratio of vertically to horizontally polarized fluorescence intensity is achieved. A relatively small (<~20-amino acids) peptide is used because if the peptide is too large, then it imparts its own fluorescence polarization even when unbound to a binding partner.

To identify candidate inhibitors of a specific protein-protein interaction, protein and fluorescently-labeled peptide are combined at fixed concentrations, then fluorescence anisotropy or polarization is measured. Small molecule inhibitors will disrupt the protein:peptide binding interaction, eliciting a decrease in the observed fluorescence anisotropy or polarization signal as fluorescently-labeled peptide is

displaced and freely tumbles. Promising small molecule candidate inibitors that elicit decreased fluorescence anisotropy or polarization are then screened for autofluorescence and quenching [Gribbon and Sewing, 2003], two factors that may alter the fluorescence polarization or anisotropy signal independent of disruption of the protein-protein interaction.

1.3.2 Structure-Aided Inhibitor Design

Once a lead candidate has been identified from a HTS assay, structure-aided drug design can be employed to improve the compound's affinity and specificity for its target [reviewed in Madsen, *et al.*, 2002]. This strategy relies on structural information of the 1) target protein small molecule binding pocket or 2) site of a target protein-protein interaction. NMR spectroscopy and x-ray crystallography are well-validated approaches that yield bond distance and atomic arrangements, which are used to determine a protein's structure in dynamic or static conformations, respectively [Wüthrich, 1990, Branden and Tooze, 1998, Wang, *et al.*, 2000, Jorgensen, 2004, Schneider and Fechner, 2005]. If the bond distances and atomic arrangements of the protein of interest are known, small molecules may be engineered to precisely, and with high affinity, bind a therapeutically-relevant pocket of a target protein [He, *et al.*, 2005, reviewed in Madsen, *et al.*, 2002], when the target protein contains such a pocket. As a consequence, the high-resolution 3-dimensional structure of the protein facilitates structure-aided design of molecules to the specific protein target, an example of which is AMN107, an imatinib analog that was designed to overcome imatinib resistance

based on point mutations in the tyrosine kinase implicated in chronic myelogenous leukemia [Weisberg, *et al.*, 2005].

1.4 Limitations of Protein Structure Determination Methods

Although it is sometimes possible to obtain very high resolution structural information, one limitation of x-ray crystallography is that the resulting image represents the crystal structure rather than the solution structure. In comparison, efforts are ongoing to expand the utility of NMR spectroscopy to study protein dynamics, protein-protein interactions, and to resolve "lowly-populated states" [Iwahara and Clore, 2006], states not easily observed using conventional NMR spectroscopy approaches. Understanding conformational dynamics is important to drug development because many times the lowly-populated conformational substates are relevant to a desired pharmacological effect [Lampe, *et al.*, 2010].

1.5 Utility of Lanthanides in Structural Biology

Lanthanides are a series of rare earth metals, most of which carry a +3 charge. Lanthanides have recently found utility in structural biology applications, such as analyzing protein dynamics, because of their unique spectroscopic [Nitz, *et al.*, 2004] and paramagnetic properties, which can be utilized in fluorescence-based approaches and NMR [Su, *et al.*, 2006, Otting, 2008, Allen and Imperiali, 2010, Su and Otting, 2010].

1.5.1 Lanthanide Fluorescence and Biological Utility

Lanthanides exhibit fluorescent properties when the lanthanide ion is chelated in a specific chemical microenvironment. When a chelating group binds and interacts with most of the lanthanide's nine possible coordination sites, the lanthanide is also shielded from any solvent quenching effects that may reduce luminescence [Pietraszkiewicz, *et al.*, 1993]. Lanthanides are relatively insensitive to photobleaching [Pandya, 2006] and have broad Stokes shifts and narrow emission bands [Murphy and Barton, 1993]. Excitation promotes an electron to the triplet excited state [Hemmila, 2005], which is thought to lead to prolonged fluorescence lifetime. The lanthanide terbium generates a millisecond-long lifetime decay [Nitz, *et al.*, 2004], which is orders of magnitude longer than those of other fluorescent entities, enabling time-resolved lifetime analyses and time-resolved distance measurements (via Förster resonance energy transfer (FRET)) between donor and acceptor molecules [Allen, *et al.*, 2006, Sandtner, *et al.,* 2007, Rajapakse, *et al.*, 2009, Hagan and Zuchner, 2011]. In addition, excitation and emission occur at wavelengths in the near infrared range, separate from naturally-occurring biological fluorophores [Werts, *et al.*, 1997, 2000, Hebbink, *et al.*, 2003]. These attributes of lanthanides permit monitoring of the lanthanide-labeled protein in a variety of biological matrices that may contain interfering fluorophores. In addition, FRET distance measurements using lanthanides may be amongst the longest measured [Mathis, 1993], enabling the analysis of longer-range donor-acceptor distances than those using other FRET partners.

Although fluorescence analyses may be performed using tryptophans that are already in the protein of interest [Allen and McLendon, 2006], site-specific introduction of an exogenous fluorophore into the protein of interest may be beneficial. Site-specific

incorporation confers the ability to probe a specific region of the protein of interest where a tryptophan may not exist. Fluorescein and the lanthanide terbium meet many of the aforementioned criteria [Brannon and Magde, 1978, Ge, *et al.*, 2004, Rajapaske, *et al.*, 2009], making them ideal probes for evaluating *in vitro* protein-protein interactions.

1.5.2 Utility of Lanthanides in NMR

Lanthanides are also useful biomolecular NMR probes due to their ability to induce local paramagnetic relaxation enhancement (PRE), pseudocontact chemical shifts (PCS), and residual dipolar couplings (RDC) [reviewed in Clore and Iwahara, 2009]. PRE arises from the paramagnetic center's ability to elicit a local perturbation of the applied magnetic field; PRE is an enhanced relaxation as the proton re-orients its spin in the direction transverse (T_2) to that of the applied magnetic field. PCS result when the paramagnetic center's unpaired electrons relax in the magnetic field and impact neighboring nuclear spins, which are manifest in a chemical shift observed in the NMR spectrum. RDC is a frequency component of the relaxing proton where the dipolar coupling between two spins is incompletely averaged, yielding a residual dipolar coupling, a frequency that can be converted to distance from the paramagnetic center [Saupe and Englert, 1963].

Lanthanide-induced PRE and RDC can yield peak shifts on the order of 4 or more nanometers (nm) [Otting, 2008]. Some lanthanides can induce local and long-range PRE and PCS [Iwahara and Clore, 2006, Otting, 2008, Madl, *et al.*, 2009]. Therefore, PRE, PCS, and RDC facilitate elucidation of dynamics of relatively larger

proteins as well as the role of amino acids involved in a specific protein-protein interaction in NMR [Clore and Iwahara, 2009]. Finally, PRE, RDC, and PCS are determined relative to the paramagnetic center [Solomon, 1955, Bloembergen and Morgan, 1961, Guéron, 1975, Bertini, *et al.*, 2002], therefore, the lanthanide needs to be site-specifically incorporated into the protein of interest.

1.5.3 Small Molecule Lanthanide Chelators

Small molecule lanthanide chelators such as ethylenediaminetetraacetic acid (EDTA) and its derivatives 1,4,7,10-tetraazacyclo-dodecane-1,4,7,10-tetraacetic acid (DOTA) and diethylenetriaminepentaacetic acid (DTPA), (Figure 1.1) have been used for decades for their attomolar lanthanide binding affinity [Cacheris, *et al.*, 1987] and for the superior luminescence intensities of their lanthanide complexes [Brittain, *et al.*, 1976, Horrocks, 1993].

Thiol-reactive derivatives of small molecule lanthanide chelators such as dipicolinic acid, DOTA, and their derivatives have been employed to react with a protein's available cysteines [Poupart, *et al.*, 2006, Su, *et al.*, 2008, Häussinger, *et al.*, 2009, Almeida, *et al.*, 2011, Zhang, *et al.*, 2011]. Where only one reactive cysteine is present, lanthanide chelation for NMR can generate chemical shifts of substantial magnitude and facilitate deconvolution of spectra to yield structural information [Otting, *et al.*, 2008]. In most cases, however, the protein of interest contains multiple cysteines and/or they are critically involved in disulfide bond formation, or other secondary structure stabilizing events and thus cannot be mutated to other amino acids to reduce non-specific incorporation. Additionally, because PRE, RDC, and PCS are determined

relative to the paramagnetic center [Solomon, 1955, Bloembergen and Morgan, 1961, Guéron, 1975, Bertini, *et al.*, 2002], lanthanide chelators that are amine- or carboxyl-reactive do not confer sufficient site-specificity to determine accurate PRE, RDC, and PCS. Survivin is a cancer drug target which is thought to lack a traditional hydrophobic drug pocket; the utility of site-specific lanthanide incorporation to elucidate lowly-populated states that Survivin adopts upon binding its protein partners such as histone-3 may reveal druggable pockets amenable to therapeutic intervention.

Small-molecule lanthanide chelators have been synthesized, however, the syntheses required numerous steps, were performed under organic, not aqueous conditions, and only yielded chelators that were thiol-reactive [Saha, *et al.*, 1993, Ge and Selvin, 2003, Ge, *et al.*, 2004, Häussinger, *et al.*, 2009]. Synthesis of a small molecule chelator amenable to click chemistry (described below) was demonstrated [Martin, *et al.*, 2010], however, the synthesis required many steps and utilized organic reagents; in addition, the chelator was clicked into a synthetic azide-containing peptide rather than an azide-containing protein target. To overcome these current limitations, we proposed to synthesize, using aqueous conditions, in two steps, a small-molecule lanthanide chelator amenable to click chemistry-mediated, site-specific incorporation into the target protein, Survivin.

1.6 Click Chemistry

The reaction between an azide and a terminal alkyne to generate a cycloadducted product was first described as a 1,3-dipolar cycloaddition in 1961 [Huisgen, 1961]. More recently, the 1,3-dipolar cycloaddition has been optimized as a

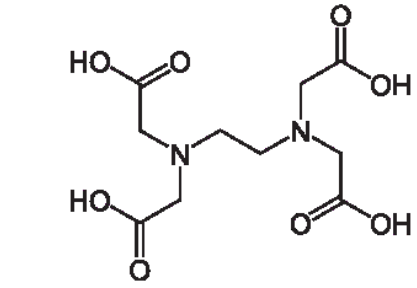

EDTA (ethylenediaminetetraacetic acid)

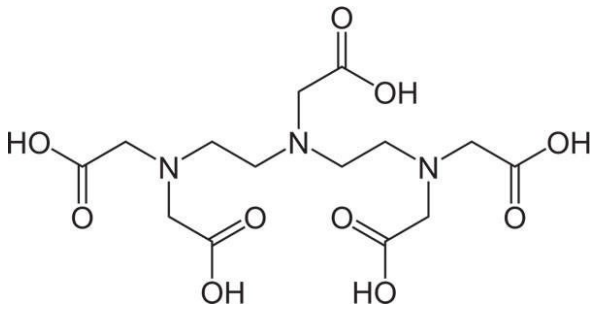

DTPA (diethylenetriaminepentaacetic acid)

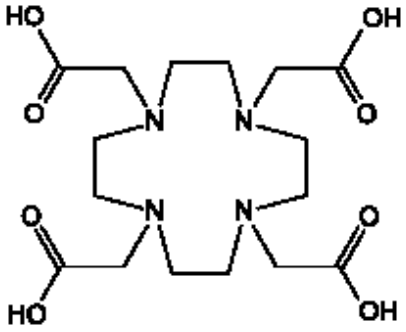

DOTA (1,4,7,10-tetraazacyclo-dodecane-1,4,7,10-tetraacetic acid)

Figure 1.1: Chemical structures of small-molecule lanthanide chelators ethylenediaminetetraacetic acid (EDTA), 1,4,7,10-tetraazacyclo-dodecane-1,4,7,10-tetraacetic acid (DOTA), and diethyelentriaminepentaacetic acid (DTPA).

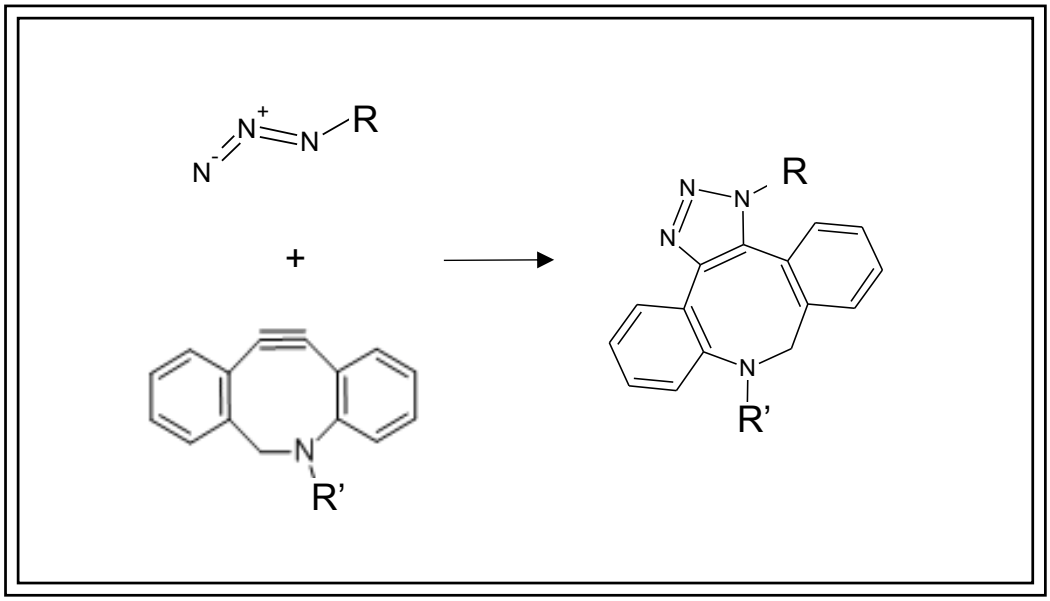

Figure 1.2: Schematic of a general copper-free click chemistry reaction between an azide-containing molecule and a cyclooctyne-containing molecule to generate a 1,4-disubstituted triazole-containing molecule.

"click chemistry" reaction [Kolb, *et al.*, 2001], because it utilizes relatively straightforward facile reaction conditions to generate single products under mild reaction conditions and in high yields using common reagents. One drawback to this approach, however, is that this click chemistry reaction between a terminal alkyne and an azide requires high amounts of copper to catalyze the formation of the triazole-containing cycloadduct.

Copper-mediated click chemistry has been performed *in vitro* to evaluate the *in vivo* activities of proteins of interest [Speers & Cravatt, 2004]. The millimolar copper concentration required, however, gave rise to relatively harsh experimental conditions that were not conducive to mimicking physiologically-relevant settings and, because cells contain no free copper, copper may initiate redox cycling, which may cause cell death [Kim, *et al.*, 2008]. Therefore, copper-free click chemistry reactions may be preferred over those requiring high copper concentrations [Jewett and Bertozzi, 2010], to evaluate proteins *in vitro* and *in vivo*.

Because of their ring strain and the energy contained within the carbon-carbon triple bond, cyclooctynes exhibit excellent reactivity towards azides to specifically form triazole cycloadducts in the absence of a copper catalyst [Gordon, *et al.*, 2012], as depicted in Figure 1.2. Due to their superior reactivity over terminal alkynes, cyclooctynes have become useful tools for completing copper-free click chemistry reactions under physiologically-relevant reaction conditions (Gordon, *et al.*, 2012). Consequently, copper-free click chemistry has been pursued to chelate a lanthanide site-specifically within the target protein (chapter 4).

One advantage of a click chemistry reaction is that the azide or alkyne moiety can be on the reporter molecule and its complementary reactive group can exist in a

specific site within a protein of interest. Through tRNA synthetase cloning and mutagenesis strategies, *Archaea* bacterial expression systems have been optimized to recognize and incorporate unnatural amino acids [Xie, *et al.*, 2007, Chin, *et al.*, 2002, Deiters and Schultz, 2005, Brustad *et al.*, 2008, Young and Schultz, 2010], such as the phenylalanine analog *para*-azidophenylalanine (paF). The unnatural amino acyl tRNA synthetase charges a tRNA with paF for site-specific incorporation into the protein at the amber stop codon [Chin, *et al.*, 2002]. The result is a protein with a reactive azide in a specific position within the protein, which can undergo click chemistry-mediated incorporation with an alkyne-containing reporter molecule. The protein can then be site-specifically labeled, using click chemistry, with a fluorescent and/or paramagnetic label. Site-specific incorporation may be determined using mass spectrometry approaches. The fluorescently- or paramagnetically-labeled protein can then be utilized in protein-protein interaction studies using fluorescence- and/or NMR-based approaches. Fluorescence-based analyses may include monitoring steady-state fluorescence intensity, fluorescence lifetime, and/or FRET; NMR-based analyses may include protein structure determination and analyzing the conformational changes the protein adopts as its protein binding partner is added.

1.7 Objectives of the Efforts Described in this Dissertation

Considering the advantages conferred upon lanthanide chelation to augment NMR-mediated protein structure determination, and the utility of fluorescence-based approaches to facilitate monitoring of protein-protein interactions, the central hypothesis of the efforts described in chapters 3 and 4 of this dissertation was that site-specific

labeling of the protein of interest, Survivin, with a fluorescent or paramagnetic tag may be used to monitor protein-protein interactions.

The central hypothesis of the efforts described in chapter 5 of this dissertation was that high-throughput screening using fluorescence polarization is a viable platform to identify candidate molecules of a specific non-enzymatic protein-peptide interaction, Survivin-histone-3.

1.8 Statement of Purpose

One strategy to bring therapies to the clinic is to use structure-aided design to synthesize a small molecule inhibitor of the protein target's function. This strategy may be particularly advantageous for inhibiting assembly of non-enzymatic proteins and/or architectural/scaffold proteins. To facilitate this, it is attractive to expand the utility of x-ray crystallography, NMR, or fluorescence-based structure determination methods. One strategy to achieve this is to incorporate a lanthanide into the protein of interest. Lanthanides have unique fluorescence and paramagnetic properties that can be harnessed to expand structure determination methods, which may improve efforts at structure-aided drug design. The efforts of this research aimed to merge site-directed mutagenesis and copper-free click chemistry to label the protein of interest (Survivin, in this case) with a fluorophore or lanthanide chelator, with the purpose of augmenting efforts at structure-aided drug design.

A strategy to identify small molecule leads that may be suitable for structure-aided drug design is to screen small molecule libraries containing candidate molecules that may have suitable pharmacological properties. In this regard, our research objective was to establish a fluorescence polarization-based platform to identify inhibitors of a specific protein-peptide interaction, namely the Survivin-histone-3 protein-peptide interaction.

1.9 Specific Aims

Working under the hypothesis that site-specific labeling of the Survivin protein with a fluorescent tag may be accomplished using copper-free click chemistry and unnatural amino acid incorporation, the specific aim of the experiments described in chapter 3 was to evaluate the utility of click chemistry to label the Survivin protein with a fluorophore in order to monitor protein-protein interactions of Survivin with its protein binding partners.

Working under the hypothesis that site-specific labeling of the Survivin protein with a paramagnetic tag may be accomplished using copper-free click chemistry and unnatural amino acid incorporation, the specific aim of the experiments described in chapter 4 was to synthesize a small molecule lanthanide chelator amenable to copper-free click chemistry in order to perform NMR-based structural analyses of Survivin with its protein binding partners.

Working under the hypothesis that high-throughput fluorescence polarization-based screening of chemical compound libraries may serve as a platform to identify candidate molecules of specific protein-protein interactions, the specific aim of the experiments described in chapter 5 was to design a fluorescence polarization assay to rapidly screen chemical libraries in order to identify candidate inhibitors of the Survivin-histone-3 protein-protein interaction.

Chapter 2. Materials and Methods

2.1 Chemicals

Europium trichloride ($EuCl_3$), lanthanum trichloride ($LaCl_3$), terbium trichloride ($TbCl_3$), ytterbium trichloride ($YbCl_3$), ethylenediaminetetraacetic acid (EDTA), diethylenetriaminepentaacetic acid (DTPA), and 1-ethyl-3-(3-dimethylamino-propyl)-carbodiimide (EDC) were procured from Sigma (St. Louis, MO); dibenzylcyclooctyne (DBCO) conjugated to fluorescein (DBCO488) and DBCO-amine were purchased from Click Chemistry Tools (Scottsdale, AZ). *Para*-azidophenylalanine (paF) (Bachem, Torrance, CA) was dissolved in 100% acetic acid prior to the addition of water to achieve 80% (v/v) acetic acid and 100 mM paF. All other reagents were of the highest grade commercially available.

2.2 Determination of Fluorescence Excitation and Emission Maxima or Steady-State Fluorescence Intensities

Excitation and emission maxima and/or steady-state fluorescence intensities of the following compounds were determined at room temperature (22f°C) using a quartz cuvette and a Fluoromax4 Fluoro-Hub spectrofluorometer (HORIBA Jobin Yvon, Edison, NJ), with the Origin FluorEssence™ software package (HORIBA Jobin Yvon):

A) 1 μM $Survivin_{1-120}$ labeled at the extreme C-terminus with DBCO488 (DBCO488-CtermpaF$surv_{1-120}$) in 50 mM Tris, pH 7.46 at 22˚C, 500 mM sodium chloride, 2 mM β-mercaptoethanol.

B) 10 mM DTPA, 40 mM terbium chloride, and 10 mM metallated DTPA in 100 mM MES, pH 5.5.

C) 193.5 μM DBCO-amine in 3.2% (v/v) DMSO in 100 mM MES, pH 5.5.

D) 10 mM clickable chelator in 100 mM MES, pH 5.5.

E) Fractions (3.5 mL) collected from the anion exchange chromatographic separation of the metallation reaction, using an excitation of 350 nm. Emission was monitored from 400-800 nm.

F) G10 Sephadex chromatography fractions (~4 mL) collected from the amide coupling reaction using two different experimental conditions. Terbium emission was monitored from 400-800 nm using an excitation of 350 nm. DBCO-amine emission was monitored from 300-800 nm using an excitation of 259 nm.

G) 100 nM carboxyfluorescein-labeled histone-3 (H3*) peptide in 100 mM potassium phosphate, pH 7.5. The excitation scan was from 300 to 500 nm and the emission scan was from 520 to 750 nm.

2.3 Synthetic Peptides

The following peptides were synthesized (Kansas State University, Jon Tomich laboratory); fam refers to carboxyfluorescein:

Histone-3 (abbreviated H3): Ac-ARTKQTARKS-$CONH_2$

Fluorescently-labeled Histone-3 (abbreviated H3*): Ac-ARTKQTARKS-K(fam)-$CONH_2$

Peptides were synthesized on an ABI Model 431 peptide synthesizer (Applied Biosystems, Foster City, CA) on a 0.1 mmol scale using solid phase peptide chemistry on 4-(2,4-dimethoxyphenyl-Fmoc-aminomethyl) phenoxyacetyl-norleucyl-cross-Linked Ethoxylate Acrylate Resin (Peptides International Inc., Louisville, KY) using Fmoc (N-(9-

fluorenyl)methoxycarbonyl)/tert-butyl chemistry [Kempe and Barany, 1996]. The carboxyamide is yielded at the C-terminus using this resin. Fmoc amino acids were obtained from Anaspec, Inc. (Fremont, CA). The peptides' N-termini were acetylated on the resin and subsequently cleaved using trifluoroacetic acid as previously described [Sukthankar, *et al.*, 2013]. Then, the released peptide product was washed with diethyl ether, re-dissolved in deionized, reverse osmosis-treated and distilled water, and then lyophilized. For the fluorescein incorporating variants, N-α-Fmoc-N-ε-(5-carboxyfluorescein)-L-lysine was manually coupled to the resin using HOBt/HBTU chemistry before automating the synthesis as before [Iwamoto, *et al.*, 1994]. Peptides were dried *in vacuo* and characterized on a Bruker Ultraflex III matrix-assisted laser desorption ionization time of flight mass spectrometer (MALDI TOF/TOF) (Bruker Daltonics, Billerica, MA) using 2,5-dihydroxybenzoic acid matrix (Sigma).

Variable masses of fluorescently-labeled histone 3 peptide (H3*) were reconstituted in 100 mM potassium phosphate, pH 7.5, containing 100 µg/mL bovine gamma globulin and 0.02% (w/v) sodium azide. Variable masses of unlabeled histone-3 peptide were reconstituted in 100 mM potassium phosphate, pH 7.5, devoid of bovine gamma globulin and sodium azide.

2.4 Synthesis of Survivin Protein Comprised of Amino Acids 1 – 120

Survivin$_{1\text{-}120}$ Cloning, Transformation, and Over-Expression

Full-length Survivin (amino acids 1 – 142) contains a hydrophobic C-terminal domain spanning amino acids 121 – 142 [Chantalat, *et al.*, 2000]; consequently, a Survivin construct comprised of amino acids 1 – 120 was generated as follows: the

cDNA of *Birc5*, the gene encoding full-length wild type human Survivin, was obtained from OriGene, in the pCMV6-XL4 vector (OriGene, Rockville, MD). An NdeI restriction site was cloned into the *Birc5* gene upstream of the 5' ATG nucleotide; a XhoI restriction site was cloned into the *Birc5* gene after Survivin amino acid 120. Using the NdeI and XhoI restriction sites, *Birc5* was cloned into the pET-15b vector (Novagen, Billerica, MA). The construct was confirmed by sequencing. The encoded His_6 tag and thrombin cleavage site (LVPRGS) immediately upstream of the Survivin gene's start site were utilized for protein purification. Plasmid containing the Survivin gene encoding amino acids 1-120 was transformed into BL21*DE3 *E. coli* competent cells according to manufacturer's specifications (Invitrogen). Transformed cells were plated on Luria-Bertani (LB) agar containing 100 µg/mL ampicillin and were grown overnight at 37°C. The next day, a single colony was picked to inoculate a starter culture (~70 mL) of LB broth containing 100 µg/mL ampicillin, which was then incubated overnight at 37°C with shaking at 225 revolutions per minute (rpm). The next day, the starter culture was transferred to Terrific Broth (TB) supplemented with 8 mL of 100% glycerol per liter and 100 µg/mL ampicillin, and incubated at 37°C with shaking at 225 rpm until an absorbance of 0.6-0.8 at 600 nm was achieved (~5 hours' incubation). The culture was induced with 1 mM IPTG and incubation resumed at 25°C at 160 rpm for 18-24 hours. After incubation, cells were collected by centrifugation at 6000xg for 10 minutes at 4°C; cell pellets were stored at -80°C until protein purification was performed.

Purification by Fast-Phase Liquid Chromatography - $Survivin_{1-120}$

Purification of $Survivin_{1-120}$ was conducted as for all $Survivin_{1-120}$ mutants (described in a subsequent section) with the following additional steps: after imidazole-

mediated elution of His_6-$Survivin_{1-120}$ from the nickel-NTA column, fractions containing His_6-$Survivin_{1-120}$ were pooled and dialyzed against 100 mM potassium phosphate, pH 7.5, with gentle stirring, at 2-8˚C, for a minimum of 2 hours per buffer exchange. Dialysis was performed until an imidazole concentration of 1 mM or lower was achieved, a concentration of imidazole that is thought not to interfere with thrombin enzyme activity (Novagen). After dialysis, thrombin cleavage was performed according to manufacturer's specifications (biotinylated thrombin from Novagen, NeutrAvidin from Thermo Fisher, Waltham, MA). Following thrombin cleavage, the sample, in 100 mM potassium phosphate, pH 7.5, was applied at a flow of 0.1-0.25 mL/min to an equilibrated HisTrap FF 5 mL nickel column (GE Healthcare) to separate the thrombin-cleaved $Survivin_{1-120}$ from uncleaved $Survivin_{1-120}$ and/or the His_6 tag. Cleaved $Survivin_{1-120}$, which no longer binds the nickel column, was collected in the column wash, in 9-mL fractions. Fractions exhibiting absorbance at 280 nm in the column wash were subjected to sodium dodecyl sulfate-polyacrylamide gel electrophoresis (SDS-PAGE) separation followed by staining with Coomassie, then concentrated.

$Survivin_{1-120}$ was concentrated using either 15-mL Amicon Ultra centrifugal filters (Ultracel 3000 MWCO, Millipore) spun with successive cycles at 6000xg for 10 minutes at 4˚C or with a 400-mL stirred cell concentrator at 75 pounds per square inch (psi) with a 3000 molecular weight cutoff (MWCO) filter, at 2-8˚C, according to manufacturer's specifications (EMD Millipore). $Survivin_{1-120}$ concentration was determined using a NanoDrop 1000 spectrophotometer (Thermo Fisher) controlled by ND-1000 software (version 3.8.1, Thermo Fisher). A molar extinction of 16500 $M^{-1}cm^{-1}$ (ProtParam Tools,

ExPASy, Swiss Institute of Bioinformatics) was used. Survivin$_{1-120}$ was stored at -80˚C until analysis.

Purification by Manual Column Application and Elution – Survivin$_{1-120}$

An approximately 100-mL HisPur™ nickel-NTA resin column was poured according to manufacturer's specifications (Thermo Fisher) and contained within an enclosed cold cabinet (2-8˚C). The column was equilibrated with loading buffer prior to the addition, by gravity, of the aforementioned supernatant from the ultracentrifugation step containing His$_6$-Survivin$_{1-120}$. The column was washed with loading buffer (50 mM Tris, pH 8.0 at 4°C, 500 mM sodium chloride, 2 mM β-mercaptoethanol) for approximately 20 column volumes, during which time fractions were not collected. After washing, elution of His$_6$-Survivin$_{1-120}$ was achieved using a gradient maker containing 500 mL loading buffer in chamber A and 500 mL loading buffer containing 400 mM imidazole in chamber B. The gradient was carried out with gentle stirring at 2-8°C, at a flow of 1.0 mL/min during which time approximately ~9-mL fractions were collected. Fractions exhibiting absorbance at 280 nm in the elution phase of the method were analyzed for Survivin presence by SDS-PAGE separation followed by Coomassie staining. Fractions containing Survivin were pooled and dialyzed, and thrombin cleavage, purification, and concentration were performed as for the Fast-Phase Liquid Chromatography-mediated purification.

2.5 SDS-PAGE, Coomassie Staining, Western Blotting, UV Illumination

FPLC fractions exhibiting absorbance at 280 and/or 500 nm were prepared for SDS-PAGE separation by combining 20:1 Laemmli Sample Buffer (Bio-Rad, Hercules,

CA):β-mercaptoethanol and sample in a 1:1 ratio, heating to 95°C for 5 minutes, and then spinning briefly prior to adding to 4-15% gel (Bio-Rad 456-1084) or homemade 15, 18, or 20% resolving gel with a 4% stacking gel. Running buffer comprised of 1x Tris/Glycine/SDS was prepared from a 10x stock Tris/Glycine/SDS Buffer (Bio-Rad).

For Coomassie analysis after SDS-PAGE separation, the gel was gently washed 3 times on a rotating platform at room temperature for 5 minutes per wash with MilliQ water, then stained with 0.05% (w/v) Coomassie R-250 (Thermo Fisher Scientific) in 4:5:1 methanol:water:acetic acid for 45-60 minutes with gentle agitation on a rotating platform at room temperature. Stain was decanted and the gel destained with 30% (v/v) methanol, 10% (v/v) acetic acid in water with gentle agitation on a rotating platform at room temperature.

For western blotting after SDS-PAGE separation, the gel was transferred onto a 0.2-μm nitrocellulose membrane (Bio-Rad) and electrophoresed for 60 minutes at 100 V prior to blocking with 5% (w/v) milk in 1x Tris-buffered saline (TBS) for 60 minutes with gentle rocking. Three 5-minute washes were performed in 1xTBS-T (TBS with 0.1% (v/v) Tween-20) at room temperature, with gentle rotation on a rotating platform. Subsequently, mouse α-human Survivin primary antibody (Catalog number 2802S, Cell Signaling, Danvers, MA) at 1:1000 dilution was applied in 5% (w/v) milk in 1xTBS-T and incubated at 2-8°C with gentle rocking for a minimum of an overnight. Three 5-minute washes were performed in 1xTBS-T at room temperature, with gentle rotation on a rotating platform. Then, horseradish peroxidase (HRP)-conjugated goat α-mouse secondary antibody (Thermo Fisher Scientific) was applied at 1:10000 dilution in 5% (w/v) milk in 1xTBS-T and incubated at room temperature with gentle rocking for 60

minutes. Subsequently, the blot was incubated in Enhanced Chemiluminescent (ECL) reagent (Pierce, Rockford, IL) for 5 minutes with gentle rocking, at room temperature, protected from light. Blots were exposed to radiography film (BlueBasic AutoRad Film, BioExpress, Kaysville, UT) and developed using a film processor (SRX-101A, Konica Minolta, Wayne, NJ).

For analysis of fluorescence after SDS-PAGE separation, the gel was transferred to an 8-watt, 0.4 Amp, 100-115V-60 Hertz Benchtop 3UV™ Transilluminator (UVP, Upland, CA) and exposed to an excitation wavelength of 254 nm.

2.6 Whole-peptide Mass Spectrometry

For protein mass measurement, 10 microliters of 0.4 mg/mL thrombin-cleaved Survivin$_{1\text{-}120}$ protein solution were desalted on a C8 reversed phase column (ZC-GU-C8SBW 320S guard column 1 cm x 0.32 mm, Micro-Tech Scientific, Vista, CA). After washing the column with 0.1% (v/v) formic acid for 20 minutes at a flow rate of 0.5 mL/min, the flow of the column was diverted to the stage of a Linear Trap Quadrupole – Fourier Transform (LTQ FT) mass spectrometer and the protein was eluted using a 0-70% (v/v) acetonitrile gradient in 0.1% (v/v) formic acid at a flow rate of 300 nL/min. The mass spectrometer was operated in the positive ion mode, to acquire in full mass scan in the m/z range of 400 to 2000 atomic mass units (amu). For mass measurement, the spectrum was deconvoluted using the Biomass deconvolution algorithm provided in the Xcalibur (Thermo Fisher Scientific) software set of applications.

2.7 Synthesis of paF-containing Survivin$_{1-120}$ Proteins

Mutagenesis of the Survivin Gene for the Synthesis of paF-containing Survivin$_{1-120}$ Proteins

The pET-15b-His$_6$-LVPRGS-*Birc5*$_{1-120}$ construct was used as the template to generate paF-containing Survivin$_{1-120}$ mutants as follows: primers for site-directed mutagenesis were designed according to the recommendations in the Stratagene site-directed mutagenesis protocol. The codon for the amber stop (*tag*) replaced the existing codon wherever paF was inserted as depicted in Figure 2.1, using primers shown in Table 2.1. Seven Survivin mutants were generated (Figure 2.1) by performing site-directed mutagenesis with pET-15b-His$_6$-LVPRGS-*Birc5*$_{1-120}$ as template. After polymerase chain reaction (PCR), DpnI digestion was performed and putative mutant plasmids were purified by gel extraction from an ethidium bromide-containing 0.8% (w/v) agarose gel in 1x Tris-acetate-EDTA (Sigma) or 1x Tris-borate-EDTA (Sigma). Putative mutant plasmids were transformed into XL1Blue competent cells (Invitrogen, Grand Island, NY) according to manufacturer's recommendations. Transformed cells were plated on LB agar containing 100 µg/mL ampicillin and grown overnight at 37°C. A single colony from each mutant was picked and grown in LB broth containing 100 µg/mL ampicillin overnight at 37°C with shaking at 225 rpm. Plasmid preparation was performed according to manufacturer's specifications (Qiagen, Valencia, CA). Aliquots of plasmids were sent for sequencing (ACGT, Wheeling, IL). Sequences were analyzed using Bio-

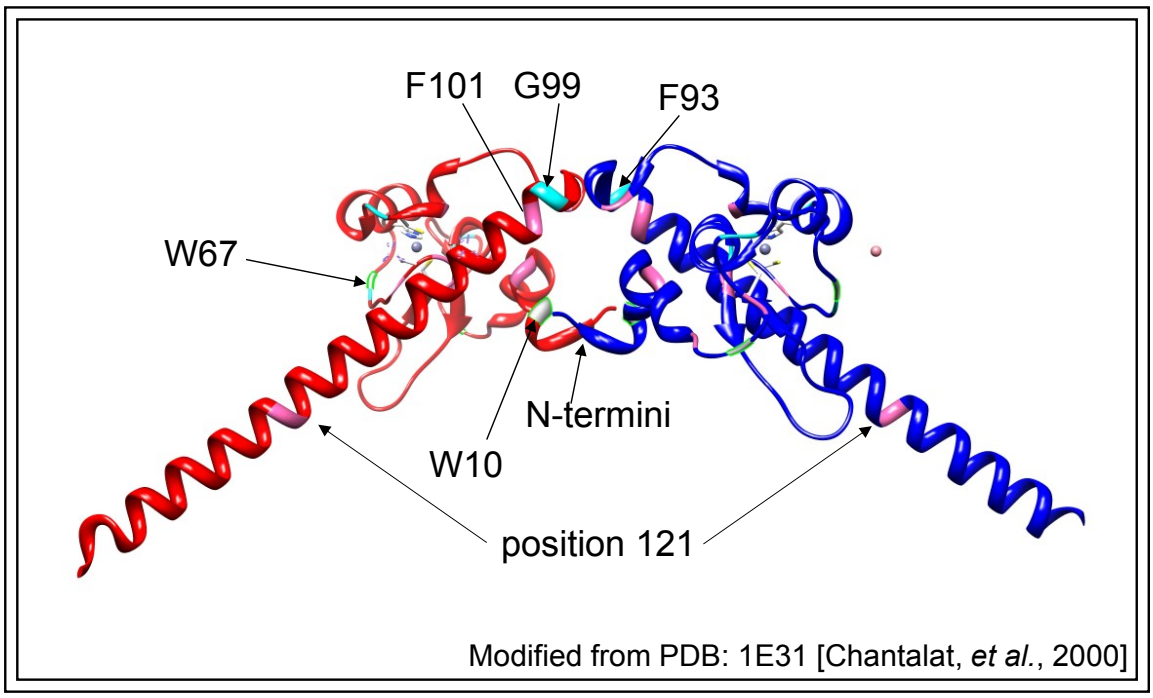

Figure 2.1: Full-length Survivin, amino acids 1-142, in its homodimeric conformation, modeled in Chimera [University of California – San Francisco], modified from the Protein Data Bank entry 1E31 [Chantalat, *et al.,* 2000]. Positions of paF insertion or substitution into the Survivin protein are depicted. paF insertions were at the extreme N- (position 0) and C-termini (position 121); paF substitutions were of tryptophans 10 and 67, phenylalanines 93 and 101, and glycine 99.

paF at N-terminus	F	5'-ggc agc cat atg tag atg ggt gcc cc-3'
	R	5'-gg ggc acc cat cta cat atg gct gcc-3'
W10paF	F	5'-g ccc cct gcc tag cag ccc ttt ctc-3'
	R	5'-gag aaa ggg ctg cta ggc agg ggg c-3'
W67paF	F	5'-g ctg gaa ggc tag gag cca gat gac g-3'
	R	5'-c gtc atc tgg ctc cta gcc ttc cag c-3'
F93paF	F	5'-ctt tct gtc aag aag cag tag gaa gaa tta acc ctt gg-3'
	R	5'-cc aag ggt taa ttc ttc cta ctg ctt ctt gac aga aag-3'
G99paF	F	5'-cag ttt gaa gaa tta acc ctt tag gaa ttt ttg aaa ctg gac aga g-3'
	R	5'-c tct gtc cag ttt caa aaa ttc cta aag ggt taa ttc ttc aaa ctg-3'
F101paF	F	5'-tta acc ctt ggt gaa tag ttg aaa ctg gac aga gaa-3'
	R	5'-ttc tct gtc cag ttt caa cta ttc acc aag ggt taa-3'
paF at C-terminus	F	5'-acc aac aat aag tag gga tcc ggc tgc taa c-3'
	R	5'-g tta gca gcc gga tcc cta ctt att gtt ggt-3'

Table 2.1: Primer sequences for site-directed mutagenesis of the Survivin gene encoding amino acids 1-120, to insert (at the extreme N- and C- termini) or substitute (at positions 10, 67, 93, 99, and 101) paF at the amber stop codon (*tag*) into pET-15b-His_6-LVPRGS-$Birc5_{1\text{-}120}$. F: Forward primer sequence; R: Reverse primer sequence.

Edit Sequence Alignment Editor (version 7.1.3.0, Ibis Biosciences, Carlsbad, CA). The remaining plasmid stocks were stored at -20°C.

Unnatural tRNA Synthetase Plasmid Preparation

The plasmid containing the *Methanococcus jannaschii* (also referred to as *Methanocaldococcus jannaschii)* tRNA synthetase that recognizes paF (Ryu and Schultz, 2006) was procured from Peter Schultz's laboratory and transformed into Top10 cells (Invitrogen) according to manufacturer's specifications (Invitrogen). Transformed cells were plated on LB agar containing 20 µg/mL chloramphenicol and grown overnight at 37°C. A single colony was picked and grown in LB broth containing 20 µg/mL chloramphenicol overnight at 37°C with shaking at 225 rpm. Plasmid preparation was performed according to manufacturer's specifications (Qiagen) and DNA concentration determined. Plasmid was sent for sequencing (ACGT). Sequences were analyzed using BioEdit; the remaining plasmid stock was stored at -20°C.

Preparation of Competent Cells Encoding Unnatural tRNA Synthetase

To incorporate the unnatural amino acid paF into the amber stop codon during translation of the Survivin mRNA, the plasmid that encodes the amber stop codon tRNA and the unnatural amino acyl tRNA synthetase that recognizes the unnatural amino acid, is transformed into competent cells. Subsequently, the plasmid encoding the Survivin gene containing the amber stop is transformed into these competent cells that encode the amber suppressor tRNA and unnatural amino acyl tRNA synthetase.

Although DH10B *E. coli* were originally used to incorporate the unnatural amino acyl tRNA synthetase plasmid into the host chromosome, DH10B cells express the unnatural tRNA synthetase gene under a constitutive promoter. Compared to BL21*DE3 *E. coli* cells, DH10B *E. coli* confers inferior protein yield. Although BL21*DE3 *E. coli* cells may confer improved yield compared to DH10B cells, BL21*DE3 *E. coli* can aberrantly recognize and insert arginine into the amber stop codon, yielding protein that contains arginine in place of the unnatural amino acid paF, which may result in improperly folded protein and/or protein that cannot participate in a copper-free click chemistry reaction.

Methanococcus jannaschii tRNA and tRNA synthetase-containing plasmid was transformed into BL21*DE3 *E. coli* competent cells (Invitrogen) for the preparation of amber suppressor tRNA and tRNA synthetase-containing competent cells according to the Sambrook and Russell protocol for the preparation of *E. coli* competent cells using calcium chloride (Sambrook & Russell, Molecular Cloning, 3rd Edition, volume 1, protocol 25). Competent cells were stored at -80°C.

Transformation and Over-Expression - Survivin$_{1\text{-}120}$ Mutants

Plasmids encoding mutant Survivin proteins containing paF were transformed into BL21*DE3 *E. coli* competent cells containing the amber suppressor tRNA and unnatural amino acyl tRNA synthetase using the same transformation protocol as commercially-available BL21*DE3 *E. coli* competent cells (Invitrogen). Transformed cells were plated on LB agar containing 100 µg/mL ampicillin and 20 µg/mL chloramphenicol and were grown overnight at 37°C. The next day, a single colony was picked to inoculate a 70-mL starter culture of LB broth containing 100 µg/mL

ampicillin and 20 μg/mL chloramphenicol, which was then incubated overnight at 37°C with shaking at 225 rpm. The next day, the starter culture was transferred to 1L of LB broth containing 100 μg/mL ampicillin and 20 μg/mL chloramphenicol and incubated at 37°C with shaking at 225 rpm until an absorbance of 0.6-0.8 at 600 nm was achieved (~5 hours' incubation). The culture was simultaneously induced with 1 mM IPTG, protected from UV exposure using aluminum foil to reduce azide activation, and 100 μM paF was added. Incubation resumed at 25°C at 160 rpm for 18-24 hours, protected from light. After incubation, cells were collected by centrifugation at 6000xg for 10 minutes at 4°C, protected from light. Cell pellets were stored at -80°C until protein purification was performed. A negative control sample was executed identically in the absence of paF to evaluate the fidelity with which paF is incorporated at the amber stop codon.

Purification - Survivin$_{1\text{-}120}$ Mutants

Cell pellets were placed on ice, protected from light, and gently stirred until thawed in the presence of lysis buffer (50 mM Tris, pH 8.0 at 4°C, 500 mM sodium chloride, 2 mM β-mercaptoethanol, and 1 mM phenylmethylsulfonyl fluoride (PMSF)) at 5 mL lysis buffer per gram cell pellet; lysis was achieved by sonication (Ultrasonic Processor) and cellular debris removed by ultracentrifugation at 100,000xg for 60 minutes at 4°C in an Optima L-100 XP Ultracentrifuge and 70 Ti rotor (Beckman Coulter). The supernatant was retained and protected from light for subsequent chromatographic purification.

An ÄKTA Purifier 100 / 10 FPLC controlled by UNICORN software (version 5.20 General Electric Healthcare, Piscataway, NJ), was used for protein purification in an enclosed cold cabinet (2-8˚C). Protein was shielded from light throughout the purification. For all chromatographic steps, columns were equilibrated with a sufficient volume of loading buffer required to achieve stable baseline, as monitored by absorbance in the UNICORN program. The aforementioned supernatant was filtered through an Acrodisc® 32 mm syringe filter with 0.2 µm Supor® non-pyrogenic membrane (Pall Corporation, Cornwall, United Kingdom) prior to applying the filtrate to an equilibrated HisTrap FF 5 mL nickel column, used in conjunction with loading buffer. The protein was loaded at 0.1 – 0.25 mL/min. Unbound protein was removed by washing the column with 20-30 column volumes of loading buffer. Elution of His_6-tagged mutant $Survivin_{1-120}$ was achieved using 0-100% loading buffer containing 400 mM imidazole; the gradient was carried out over 10 column volumes during which time 9-mL fractions were collected. Fractions exhibiting absorbance at 280 nm in the elution phase of the method were separated by SDS-PAGE then analyzed for Survivin presence by Coomassie staining and western blotting.

Mutant $Survivin_{1-120}$ proteins were concentrated and the concentrations determined as described above. Mutant $Survivin_{1-120}$ proteins were stored at -80˚C until analysis.

2.8 Copper-free Small Molecule Click Chemistry

Absorbance scans of 100 mM paF in 80% (v/v) acetic acid, 1 mM DBCO488 in 100% DMSO, and 1 µM DBCO488-labeled $Survivin_{1-120}$ at the extreme N-terminus

(DBCO488-NtermpaF-Survivin$_{1\text{-}120}$) in loading buffer were carried out at slow speed (200 nm/min), at room temperature, using a quartz cuvette and the appropriate blanking solutions from 800-200 nm in a Cary50 Bio UV-Vis Spectrophotometer (Varian, Agilent Technologies, Santa Clara, CA), under control of Varian UV software, version 3.00(303) (Agilent Technologies).

After determining the absorbance maxima of 100 mM paF in 80% (v/v) acetic acid and 1 mM DBCO488 in 100% DMSO, copper-free click chemistry reactions to generate a cycloadducted product (Figure 2.2) were performed using paF (azide) and DBCO488 (alkyne) as indicated in Table 2.2. Copper-free click chemistry reactions were also performed using the small molecule unnatural amino acid paF and the clickable chelator (DBCO-DTPA:Tb) as indicated in Table 2.2, in a 200 µL total final volume, with 100 mM MES, pH 5.5, as diluent. Reactions were gently rocked, protected from light with aluminum foil, for 24 hours at room temperature. Reactions were allowed to proceed to completion prior to analyzing 50-µL aliquots of each reaction by high-performance liquid chromatography (HPLC).

HPLC Separation of Copper-free Click Chemistry Reactions of Small Molecules paF and DBCO488 or DBCO-DTPA:Tb

A Shimadzu HPLC with Shimadzu SPD-M20A diode array detector and CLASS VP software (LabSolutions Lite, version 5.52, Shimadzu, Kansas City, MO) and Supelco 15 cm x 4.6 mm x 5 µm Supelcosil-LC18 column (Sigma) were used.

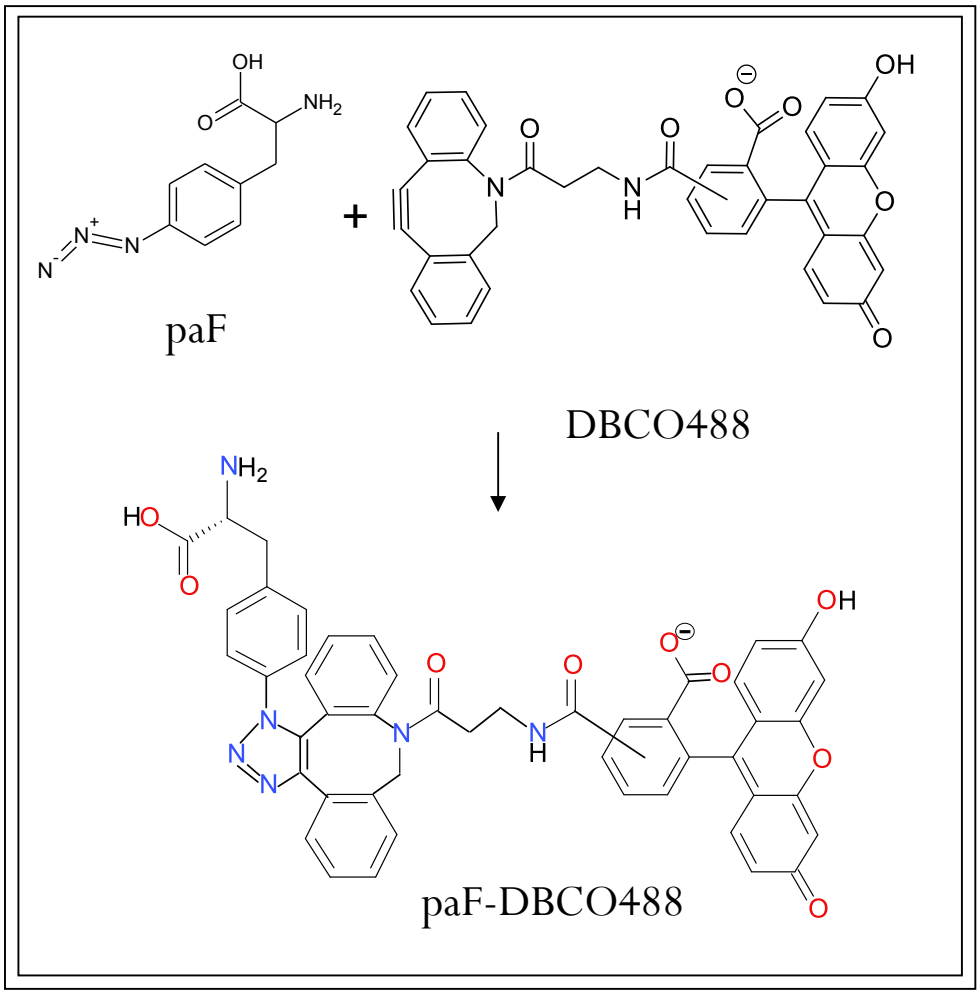

Figure 2.2: Schematic representation of the small molecule copper-free click chemistry reaction of *para*-azidophenylalanine (paF, azide) and DBCO488 (fluorescent, alkyne) to generate the triazole-containing fluorescent paF-DBCO488 cycloadduct (one product shown).

Molar stoichiometry of alkyne:azide	Final concentration (μM)
1:1	500, 500
10:1	500, 50
1:10	500, 5000

Table 2.2: Click chemistry reaction conditions between *para*-azidophenylalanine (azide) and DBCO488 (alkyne) in 100 μL or between *para*-azidophenylalanine (azide) and clickable chelator (alkyne) in a 200 μL total final volume. Left panel: molar stoichiometries of alkyne and azide. Right panel: final concentration of alkyne (left value) and azide (right value) in reaction.

paF and DBCO488

Mobile phases to separate copper-free click chemistry reactions between DBCO488 and paF consisted of A: 0.1% (v/v) trifluoroacetic acid (TFA) in water, B: 100% acetonitrile (ACN). The flow was 1.5 mL/min; the gradient was 10-90% B from 1-9 minutes, 90% B from 9-15 minutes, 90-0% B from 15-16 minutes, 0% B from 16 to 22 minutes. During each HPLC separation of the click chemistry reactions, 1-mL fractions were collected. To confirm the identity of the HPLC peaks that correspond to the cycloadducted product paF-DBCO488, fractions that exhibited absorbance at 280 and 310 nm (absorbance maxima for paF) and 454 (absorbance maximum for DBCO488 in DMSO) were collected and dried under gentle nitrogen sparge then reconstituted in 40% TFA in water (0.1% (v/v)): 60% acetonitrile (100%) for small-molecule mass spectrometry.

paF and DBCO-DTPA:Tb

Mobile phases to separate copper-free click chemistry reactions between DBCO-DTPA:Tb and paF consisted of A: 0.1% (v/v) TFA in water, B: 100% ACN. Flow was 0.75 mL/min; the gradient was 0-1 min, 0% B, 1-10 min, 0-100% B, 10-16 min, 100% B, 16-17 min, 100-0% B, 17-22 min, 0% B. 1-mL fractions that exhibited absorbance and retention times of the clickable chelator (DBCO-DTPA:Tb) and the clicked clickable chelator (the product of the click chemistry reaction between the clickable chelator (DBCO-DTPA:Tb) and paF) were collected.

Small-molecule Mass Spectrometry of paF-DBCO488 Cycloadduct

An Acquity Ultra Performance Liquid Chromatograph (Waters, Milford, MA) controlled by MassLynx (version 4.1, Waters) was used with mobile phases A: 0.1% (v/v) formic acid and B: 0.1% (v/v) formic acid in 100% ACN, with a linear gradient from 0-100% over 20 minutes, using a 2.1 x 100 mm, 1.7 μm Acquity UPLC BEH C18 column (Waters).

A QTOFMS (SYNAPT G1 HDMS, Waters) was operated in positive ion mode with electrospray ionization. The source and desolvation temperatures were set at 120°C and 350°C, respectively. Nitrogen was applied as the cone gas (10 L/hr) and desolvation gas (700 L/hr). TOFMS was calibrated with sodium formate and monitored by the intermittent injection of lock mass leucine enkeophalin in real time, generating a reference ion at m/z 556.2771. The capillary voltage and cone voltage were set at 3.5 kV and 35V, respectively.

2.9 Copper-free Click Chemistry with Azide-containing Survivin

A copper-free click chemistry reaction between Survivin$_{1\text{-}120}$ labeled at the extreme N-terminus with paF (NtermpaF-surv$_{1\text{-}120}$) and DBCO488 was performed by combining approximately 1 mg of NtermpaF-surv$_{1\text{-}120}$ with 1.015 mg DBCO488 in 100% DMSO, to yield an estimated molar stoichiometry of 1:26.9; the resulting DMSO concentration was 2%. The reaction was gently rocked at 2-8°C, in loading buffer, protected from light with aluminum foil, for 24 hours until reaction was applied to an equilibrated HiLoad 26/60 Superdex 200 prep grade size-exclusion column (GE Healthcare). The reaction was allowed to proceed to completion.

A copper-free click chemistry reaction between Survivin$_{1-120}$ labeled at the extreme C-terminus with paF (CtermpaFsurv$_{1-120}$) and DBCO488 was performed by combining approximately 0.5 mg of CtermpaFsurv$_{1-120}$ with 0.564 mg DBCO488 in 100% DMSO (100%) to yield an estimated molar stoichiometry of 1:29.9; the resulting DMSO concentration was 2%. The reaction was gently rocked at 2-8°C in loading buffer, protected from light with aluminum foil, for 24 hours until reaction was applied to an equilibrated HiLoad 26/60 Superdex 200 prep grade size-exclusion column (GE Healthcare). The reaction was allowed to proceed to completion.

Size-exclusion Chromatography

An aliquot of the copper-free click chemistry reaction mix containing DBCO488 and NtermpaF-surv$_{1-120}$ in loading buffer was applied to a HiLoad 26/60 Superdex 200 prep grade size-exclusion column (GE Healthcare) equilibrated with loading buffer, at a rate of 0.1 – 0.25 mL/min. An ÄKTA Purifier 100 / 10 FPLC was used. One and a half column volumes (495 mL) of loading buffer were passed over the size-exclusion column during which time 9-mL fractions were collected. Absorbance was monitored at 280 and 500 nm (the absorbance maximum of DBCO488-labeled Survivin$_{1-120}$). Fractions exhibiting absorbance at 280 and 500 nm were separated by SDS-PAGE and analyzed by Coomassie, western blotting, and UV gel illumination.

2.10 Time-Domain Fluorescence Lifetime Determination

Time-correlated single-photon counting (TCSPC) experiments utilized a 451 nm NanoLED (HORIBA Jobin Yvon) excitation source and emission monitoring at 520 nm.

The Prompt (instrument response) was established by preparing a 1:10 dilution of precisely 1 drop (~100 µL) of 34% (w/v) LUDOX (Sigma) into 3 mL MilliQ H_2O. Excitation Source Repetition Rate was 1 MHz. Bandpass was 1.1 nm, Alpha Value ≤2.0%, and Sync Delay 30 ns. Measurement Range was 200 ns. The RT Preset was 0 seconds; the Peak Preset was 10000 counts. Lifetime determinations were performed on 1 µM DBCO488 and on 1 µM uncleaved CtermpaF-DBCO488-$surv_{1\text{-}120}$ in loading buffer. Data were processed using DataStation Analysis Software (HORIBA Jobin Yvon).

2.11 Metallation of Diethylenetriaminepentaacetic acid (DTPA)

Dissolution of 10 mM DTPA in 100 mM MES, pH 5.5, was achieved by incubation at 75˚C for 5-10 minutes. Metallation of DTPA with terbium was achieved by incubating 40 mM $TbCl_3$ and 10 mM DTPA at 75˚C for 8.25 hours in 100 mM MES, pH 5.5. Samples were cooled to room temperature prior to fluorescence analysis using an excitation of 350 nm.

1D NMR Analysis of Metallated DTPA

1D NMR analysis of the following was performed at 298K on a 600 MHz Bruker (Billerica, MA) NMR magnet:

10 mM DTPA in 100 mM ammonium acetate, pH 5.5, containing 10% (v/v) D_2O

40 mM $TbCl_3$ in 100 mM ammonium acetate, pH 5.5, containing 10% (v/v) D_2O

10 mM DTPA, 40 mM $TbCl_3$ in 100 mM ammonium acetate, pH 5.5, containing 10% (v/v) D_2O before and after metallation incubation

Anion Exchange Purification of Metallated DTPA

Separation of metallated DTPA (hereafter denoted DTPA:Tb) from excess terbium trichloride was achieved using anion exchange chromatography. The metallation incubation reaction (4 mL) was filtered through an Acrodisc® 32 mm syringe filter with 0.2 µm Supor® non-pyrogenic membrane. An ÄKTA Purifier 100 / 10 FPLC was used in conjunction with a HiTrap Q FF 5 mL (GE Healthcare) anion exchange column, equilibrated with at least five column volumes (25 mL) of 100 mM MES, pH 5.5, prior to addition of the filtered metallation reaction. After application of the metallation reaction (4 mL), the SuperLoop® injector column was protected from light with aluminum foil. Three column volumes (15 mL) of 100 mM MES, pH 5.5, were applied to the HiTrap Q FF anion exchange column, during which time 3.5-mL fractions were collected. Elution of metallated DTPA was achieved using 0-100% loading buffer containing 1 M sodium chloride; the gradient was carried out over 8 column volumes during which time 3.5-mL fractions were collected. The Frac-920 carousel fraction collector and fraction collection tubes were protected from light with aluminum foil for the duration of the purification.

2.12 Amide Coupling to Synthesize Clickable Chelator

Amide coupling was performed as follows: DTPA:Tb from anion exchange chromatography separation was estimated to be 10 mM based on the initial concentration of DTPA used in the metallation experiment (10 mM) and the 1D NMR data that suggested the reaction went to completion; DBCO-amine in 8.33% (v/v) DMSO in 100 mM MES, pH 5.5, was added to achieve a final concentration of 50 mM

DBCO-amine. Amide coupling reagent 1-ethyl-3-(3-dimethylamino-propyl)-carbodiimide (EDC) was added to 50 mM to facilitate the amide coupling reaction. The amide coupling reaction was performed at room temperature, protected from light with aluminum foil, with gentle rocking, for 120 minutes, prior to applying approximately 1000 µL of the reaction mix to an equilibrated G10 Sephadex size-exclusion column.

Size-Exclusion Column Chromatography Separation of Amide Coupling Reaction

A 3.5-mL Sephadex G10 column was poured according to manufacturer's specifications (GE Healthcare) into a 10 cm x 1 cm glass Econo-column low-pressure chromatography column with a cross-sectional area of 0.79 cm^2 with translucent polypropylene end fittings (Bio-Rad) and low-pressure tubing (Bio-Rad). The column was shielded from light with aluminum foil. Separation of the product (the clickable chelator (DBCO-DTPA:Tb)) and reactants (DBCO-amine and metallated DTPA (DTPA:Tb)) from the amide coupling reaction mix was achieved by addition of 12-14 column volumes (42 – 49 mL) of 100 mM MES, pH 5.5, during which time approximately 4 mL fractions were collected, protected from light with aluminum foil, at room temperature.

2.13 Fluorescence Anisotropy or Polarization

Cuvette Fluorometer

Fluorescence anisotropy experiments were initiated using the Fluoromax4 Fluoro-Hub. The experimental setup for preliminary binding assays utilized a 3-mL

quartz cuvette, 100 nM fluorescently-labeled histone-3 peptide (H3*) of sequence Ac-ARTKQTARKS-K(fam)-$CONH_2$, and variable concentration of purified uncleaved or thrombin-cleaved $Survivin_{1-120}$ in 100 mM potassium phosphate, pH 7.5, 100 µg/mL bovine gamma globulin (BGG), 0.02% (w/v) sodium azide. Different maximum concentrations of cleaved and uncleaved Survivin were obtained during protein purifications of cleaved and uncleaved Survivin. These different maximum Survivin concentrations were used in serial dilutions of Survivin for fluorescence anisotropy experiments. For the experiment evaluating thrombin-cleaved $Survivin_{1-120}$, the following final concentrations (µM) were used: 0, 0.16, 0.36, 0.66, 1.32, 2.63, 5.26, 10.53, and 21.05. For the experiment evaluating uncleaved His_6-$Survivin_{1-120}$, the following final concentrations (µM) were used: 0, 0.02, 0.04, 0.07, 0.14, 0.28, 0.56, 1.13, 2.25, 4.5, 9.0, 18.0, and 36.0. $Survivin_{1-120}$ and 100 nM H3* (total final volume of 2.5 mL) were incubated for 30 minutes at 37°C with gentle stirring, protected from light, then read at 37°C in a pre-warmed cuvette holder using an excitation of 493 nm monitoring emission at 522 nm. Instrument output was in percent anisotropy (%r) or percent polarization (%P).

Plate Fluorometer

Determination of Dissociation Constant

To determine the dissociation constant of carboxyfluorescein-labeled histone-3 peptide (H3*) for $Survivin_{1-120}$, a black, flat-bottom 96-well plate (Costar, Corning, Tewksbury, MA), 1 µM H3*, and 0 – 152 µM uncleaved $Survivin_{1-120}$ in 100 mM potassium phosphate, pH 7.5, were used. Samples were analyzed in triplicate.

Uncleaved His_6-$Survivin_{1-120}$ and 1 μM H3* (total final volume of 100 μL) were incubated for 30 minutes at 37°C, protected from light, with occasional gentle mixing, then read at 37°C in a pre-warmed BioTek Synergy 2 (BioTek, Winooski, VT) plate reader using Gen5 software, version 1.11.5 (BioTek), using the tungsten-halogen lamp. Excitation and emission wavelengths were 485 and 528 nm, respectively.

For all plate fluorometer experiments, instrument output was in parallel fluorescence intensity and perpendicular fluorescence intensity; data were processed using Excel. Fluorescence polarization values (P) (in fluorescence polarization units) were determined using the following equation:

$$P = \frac{((I_{VVsample} - I_{VVblank}) - (I_{VHsample} - I_{VHblank}))}{((I_{VVsample} - I_{VVblank}) + (I_{VHsample} - I_{VHblank}))}$$

Where I_{VV} is the parallel fluorescence intensity (excitation and emission polarizers are both oriented vertically) and I_{VH} is the perpendicular fluorescence intensity (excitation polarizer is oriented vertically and emission polarizer is oriented horizontally).

Evaluation of Binding Specificity

To evaluate specificity of the His_6-$Survivin_{1-120}$:H3* binding interaction, unlabeled histone 3 (H3) peptide was titrated into wells containing 30 μM His_6-$Survivin_{1-120}$ and 1 μM H3* in 100 mM potassium phosphate, pH 7.5. The assay was performed one time and included samples in triplicate. His_6-$Survivin_{1-120}$ and H3* (total final volume of 100 μL) were incubated for 30 minutes at 37°C, with occasional gentle mixing, then read at

37°C in a pre-warmed plate reader. Then, unlabeled histone-3 peptide was added to each well and the plate incubated at 37°C for 5 minutes, after which time the plate was read. Excitation and emission wavelengths were 485 and 528 nm, respectively.

Chapter 3: Utility of Copper-Free Click Chemistry to Site-Specifically Fluorescently Label the Survivin Protein for Protein-Protein Interaction Studies

3.1 Introduction

Steady-state fluorescence intensity measurements, FRET, and fluorescence lifetime have been successfully used to evaluate protein dynamics [Beechem and Brand, 1985, Lim, *et al.*, 1995, Kuppens, *et al.*, 2003, Poupart, *et al.*, 2006, Hou, *et al.*, 2007, Serrano, *et al.*, 2012, Lemos and Hungerford, 2013]. Information about the fluorophore environment such as changes in viscosity, polarity, pH, and/or solvation, shape and size of molecules examined, and molecular interactions may be gleaned from fluorescence lifetime determination [reviewed in Berezin and Achilefu, 2010]. Although fluorescence analyses may be performed using endogenous tryptophans in the protein of interest [Allen and McLendon, 2006], site-specific introduction of an exogenous fluorophore into the protein of interest may be preferable in many cases. Site-specific incorporation confers the ability to probe a specific region of the protein of interest where a tryptophan may not exist. In addition, relative to endogenous fluorophores, the exogenous fluorophore may exhibit excitation and emission wavelengths disparate from many naturally-occurring fluorophores, allowing for selective monitoring of the fluorescence signal. Typically, exogenous fluorophores have a higher quantum yield, a higher molar extinction coefficient, a broader Stokes shift, narrower emission bands (narrow full-width at half maximum emission peak), and longer fluorescence lifetimes. Fluorescein and the lanthanide terbium are examples of fluorophores that meet many of these criteria [Brannon and Magde, 1978, Ge, *et al.*, 2004, Rajapaske, *et al.*, 2009], making them ideal probes for evaluating *in vitro* protein-protein interactions.

Survivin binds one of its partners, histone-3, via the involvement of specific amino acids within Survivin's baculoviral IAP repeat (BIR) domain [Jeyaprakash, *et al.*, 2011]. Because the structure of the Survivin-histone-3 complex has been solved [Jeyaprakash, *et al.*, 2011], Survivin was chosen to provide proof-of-concept for the fluorescence-based analyses described herein. Consequently, we hypothesized that site-specific labeling of the Survivin protein with a fluorescent tag may be accomplished using copper-free click chemistry and unnatural amino acid incorporation. The aim, thus, was to evaluate the utility of click chemistry to site-specifically label the Survivin protein with a fluorophore using copper-free click chemistry in order to monitor protein-protein interactions of Survivin with its protein binding partners by steady-state fluorescence, FRET, and fluorescence lifetime analysis. Specifically, a FRET pair amenable to these analyses is proposed in a subsequent section.

3.2 Results and Discussion

Rationale for Selecting Positions for *Para*-azidophenylalanine Insertion

In order to glean information about specific amino acids involved in a particular protein-protein interaction, the specific placement of the fluorophore within the protein of interest should be considered. An additional factor is physical accessibility of the introduced unnatural amino acid (paF) with regard to the click chemistry reaction to introduce the fluorophore. The impact of the paF and the azide on secondary and tertiary structure(s) of the protein should be considered as well. To try to address each of these considerations, several mutants were made. In two separate mutants, phenylalanines at positions 93 and 101 were mutated to paF as conservative amino

acid substitutions to evaluate the impact of the azide on Survivin protein structure, function, and partner binding interactions. In three separate mutants, tryptophans in positions 10 and 67 and glycine in position 99 were mutated to paF due to the fact that amino acids 10, 67, and 99 reside within suvivin's baculoviral IAP repeat (BIR) domain, which is involved in binding protein partners along Survivin's apoptotic and mitotic pathways. Finally, paF was inserted at Survivin's extreme N- (position 0) and C-termini (position 121), in two separate mutants, to evaluate the consequences of paF insertion at locations disparate from Survivin's BIR domain. Click chemistry-mediated incorporation of a fluorophore with paF in each of these positions confers the opportunity to obtain information about Survivin protein binding interactions relative to each of these positions.

Para-azidophenylalanine-containing Survivin$_{1\text{-}120}$ Protein Purification

All seven mutant Survivin plasmid sequences encoding the amber stop codon where paF was inserted were correct. As shown in Figure 3.1, western blotting of all seven paF-containing Survivin$_{1\text{-}120}$ mutants yielded band density at the molecular weight corresponding to the Survivin$_{1\text{-}120}$ dimer. The N-terminal paF-containing Survivin mutant was selected for initial copper-free click chemistry with DBCO488.

Copper-free Click Chemistry Reactions with Small Molecules

To analyze HPLC separation of the triazole-containing cycloadducted click

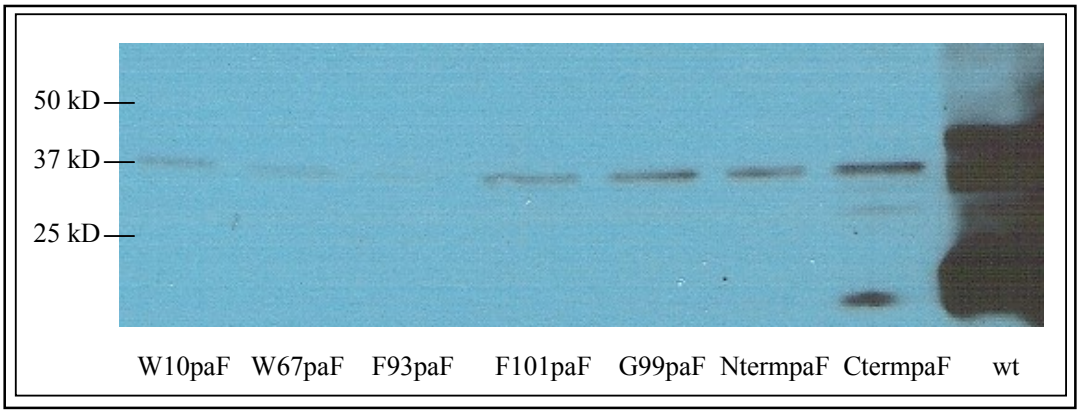

Figure 3.1: Western blot of paF-containing His_6-$Survivin_{1-120}$ mutant proteins W10paF, W67paF, F93paF, F101paF, G99paF, NtermpaF, and CtermpaF(dimers ~32 kD, monomers at ~16 kD), with $Survivin_{1-120}$ control.

chemistry product, an HPLC method for a triazole-containing small molecule ketoconazole (data not shown), was employed. Subsequently, the small molecules paF and DBCO488 were individually evaluated by HPLC. The small molecule paF was used in preliminary attempts at performing copper-free click chemistry with DBCO488 prior to utilizing paF-containing $Survivin_{1\text{-}120}$ protein, due to the limited availability of the latter. The copper-free click chemistry reactions using small molecules paF and DBCO488, described in the Materials and Methods chapter, were evaluated by HPLC. As shown in Figure 3.2, 100 mM paF in 80% (v/v) acetic acid exhibited absorbance at 280 and 310 nm and eluted from the column at precisely 4 minutes. As shown in Figure 3.3, 354 μM DBCO488 in 100% DMSO exhibited absorbance at 454 nm and eluted at 7 minutes (Figure 3.4). These results established the absorbance maxima that correlated with paF and DBCO488, which were subsequently used as a starting point for analyzing small molecule click chemistry reaction success by HPLC. As shown in Figures 3.5, 3.6, and 3.7, HPLC analysis of the 1:1, 10:1, and 1:10 alkyne:azide copper-free click chemistry reactions, respectively, yielded the following: paF generated a peak at the expected retention time (4 minutes) and with absorbance at 280 and 310 nm. DBCO488 generated a peak at the expected retention time (7 minutes) and with absorbance at 454 nm. The paF-DBCO488 cycloadducted product generated a single peak that exhibited absorbance of paF and DBCO488 (280, 310, and 454 nm). In other words, a single peak in the HPLC spectrum exhibited absorbance at the same unique wavelengths of paF and DBCO488 (280, 310, and 454 nm). This suggested that the new peak contains paF, which absorbs at 280 and 310 nm, and DBCO488, which absorbs at 454 nm. In addition, the paF-DBCO488 cyclo-

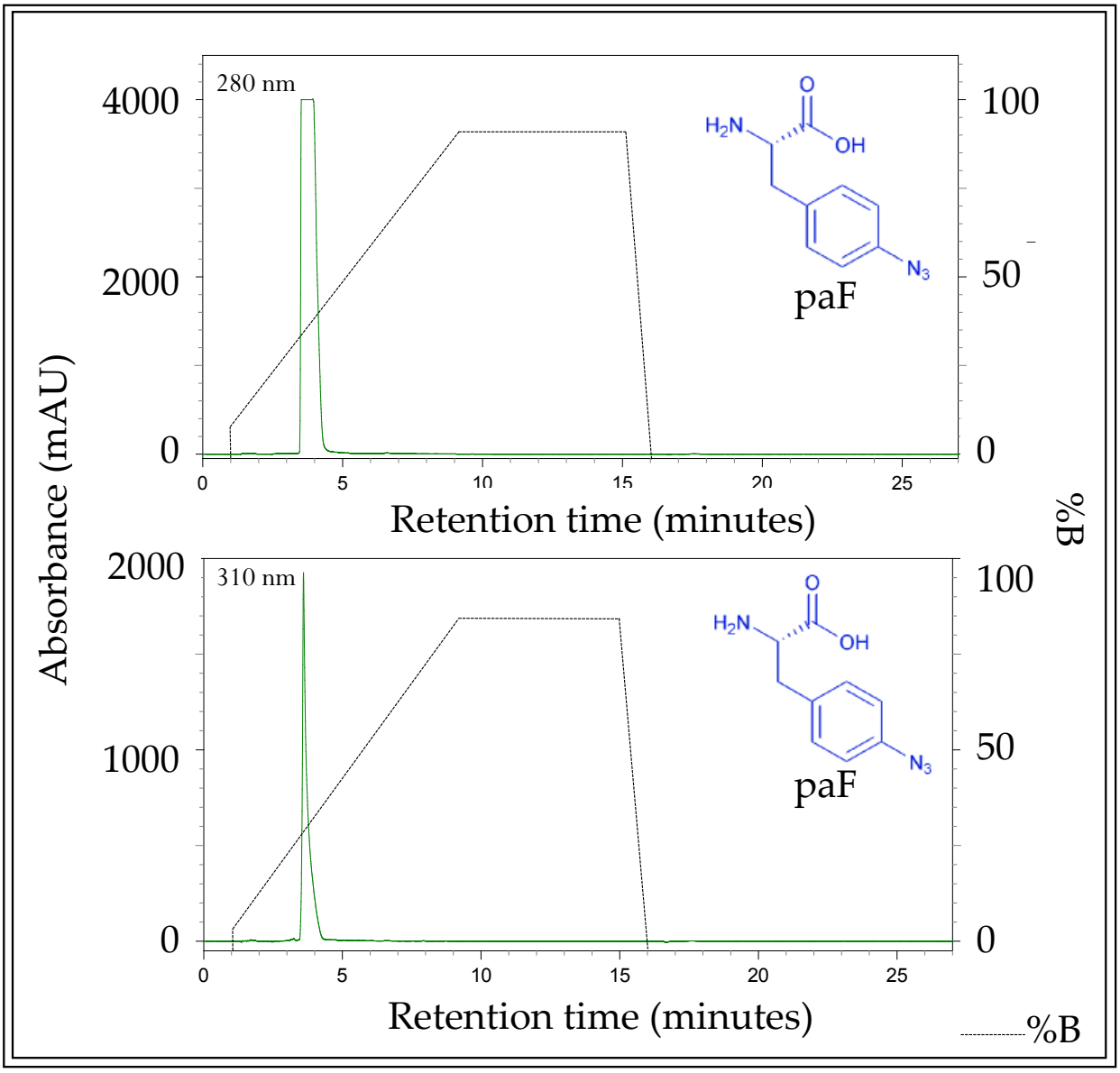

Figure 3.2: HPLC separation of 50 µL of 100 mM *para*-azidophenylalanine (paF) in 80% (v/v) acetic acid. Absorbance (milli Absorbance Units (mAU)) is depicted on the left y-axis, retention time (minutes) on the x-axis, and %B (light gray trace) on the right y-axis.

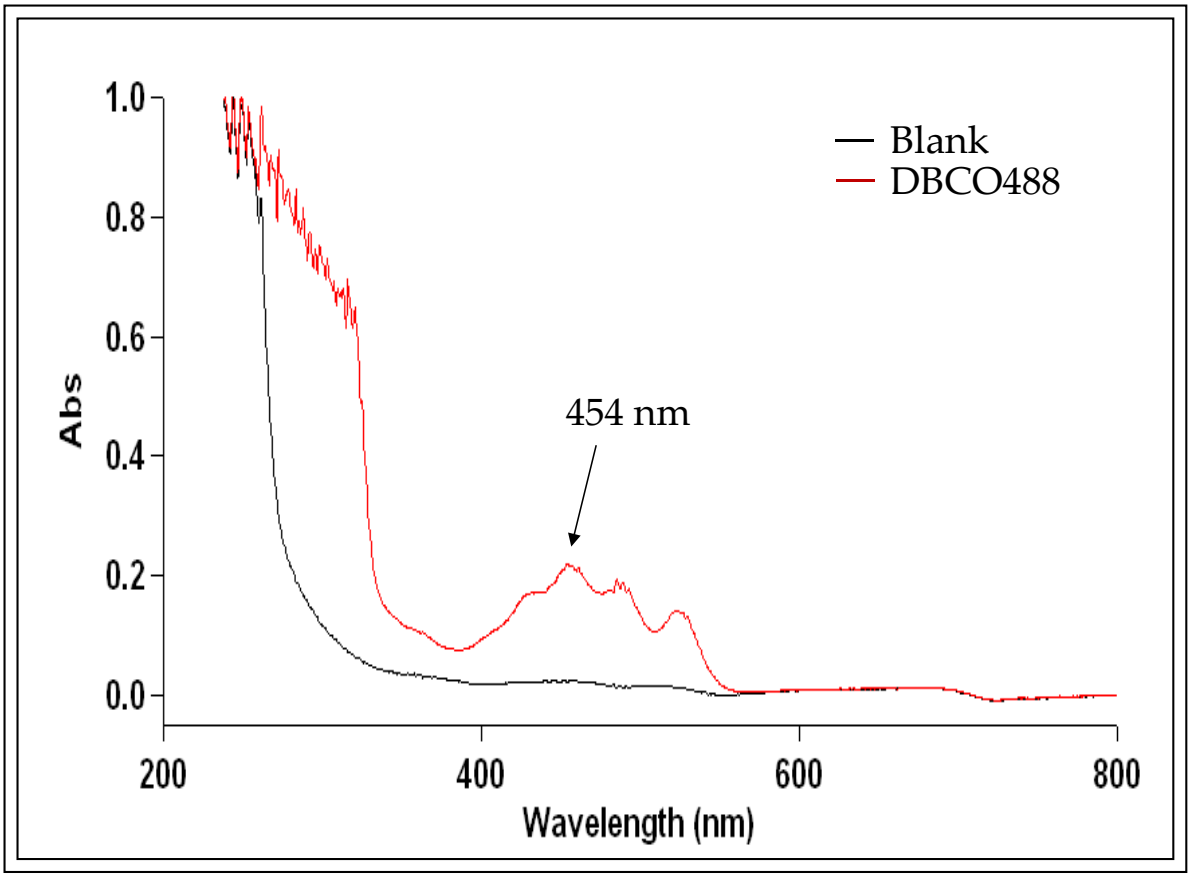

Figure 3.3: Absorbance scan of 50 µL of 354 µM DBCO488 (DBCO488 trace) in 100% DMSO relative to DMSO (Blank trace). Absorbance (Abs) is on the y-axis and wavelength (nm) on the x-axis.

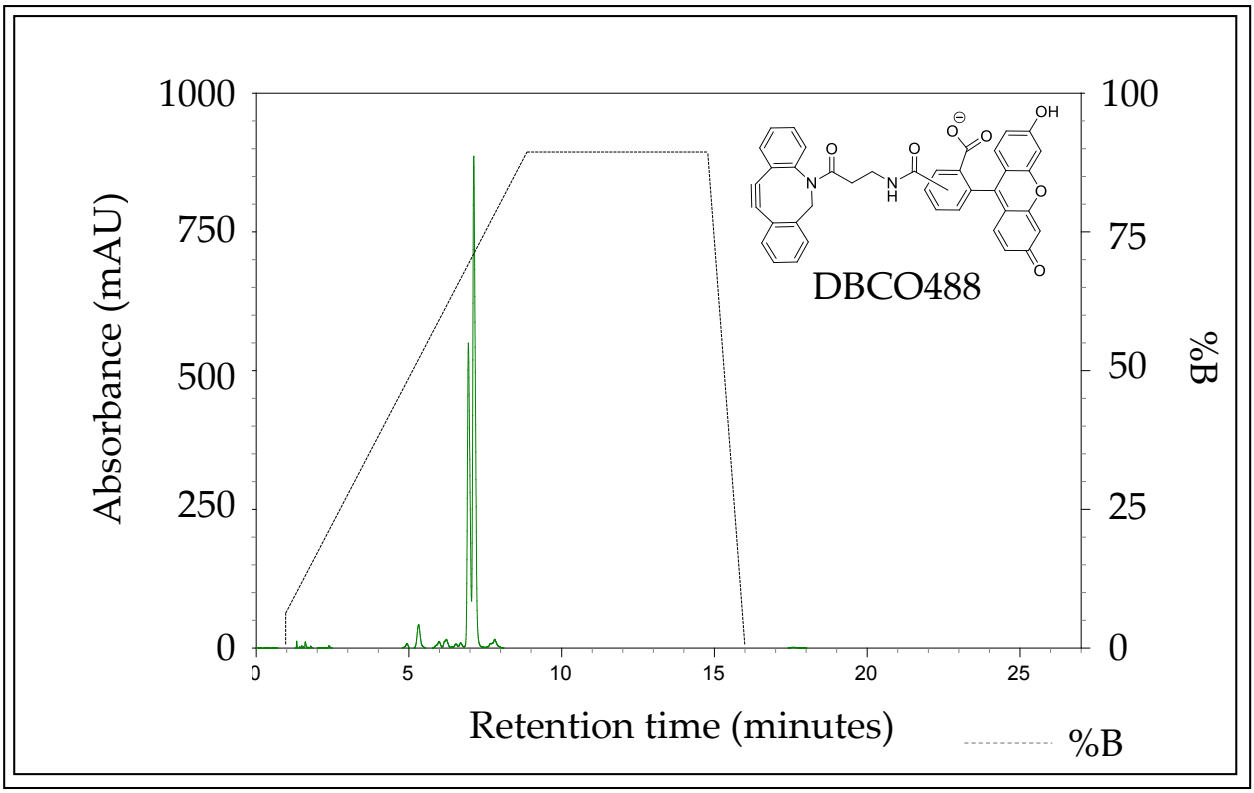

Figure 3.4: HPLC separation of 50 µL of 1 mM DBCO488 in 100% DMSO. Absorbance (mAU) is depicted on the left y-axis, retention time (minutes) on the x-axis, and %B (light gray trace) on the right y-axis. Absorbance was monitored at 454 nm.

adducted product eluted at 6 minutes, as shown in Figures 3.5, 3.6, and 3.7 for the 1:1 alkyne:azide, 10:1 alkyne:azide, and 1:10 alkyne:azide reactions, respectively. This unique retention time of the paF-DBCO488 is expected as the addition of the paF to the DBCO488 makes DBCO488 slightly more hydrophilic. The unique retention times and absorbance character of the reactants and products suggested that these molar stoichiometries generated the desired paF-DBCO488 cycloadduct. Interestingly, the presence of two DBCO488 peaks in Figure 3.6 may suggest that stereoisomers of DBCO488 are present. Multiple DBCO488 conformers may be present that exhibit differential retention on the C18 column matrix. This suggestion is corroborated by evaluating the rendering of the chemical structure provided by the DBCO488 supplier (Click Chemistry Tools), where the representation of the covalent bond joining the amide bond to the fluorescein moiety is drawn to the center of the phenyl ring, not to one specific carbon on the phenyl ring. Interestingly, under conditions of excess alkyne, the copper-free click chemistry reaction appears to yield two product peaks (Figure 3.6, at 6.05 and 6.2 minutes), which may suggest that the parent conformers are equally able to react with paF when excess alkyne is present. Notably, the mass of alkyne was kept constant in all reactions, using variable azide to yield the different molar stoichiometries tested.

To confirm the identity of the HPLC peaks that correspond to the cycloadducted product paF-DBCO488, small molecule mass spectrometry of the putative paF-DBCO488 cycloadducted product from the HPLC-mediated separation of the 1:1 alkyne:azide click chemistry reaction (fraction 6 minutes) was performed. As shown in Figure 3.8, mass spectrometry analysis of an aliquot of the 6-minute HPLC fraction

showed a single, sharp peak that corresponded to the theoretical mass of the cycloadduct, 841.26 Da.

Collectively, these results suggest that the copper-free click chemistry reactions were successful using the small molecules paF and DBCO488. Thus, the next step was to attempt copper-free click chemistry with the azide-containing protein NtermpaFsurv$_{1\text{-}120}$ and the fluorescent cyclooctyne, DBCO488.

Copper-free Click Chemistry Reaction with Azide-containing Survivin$_{1\text{-}120}$

As was shown in Figure 3.3, 354 μM DBCO488 in 100% DMSO yielded an absorbance maximum of 454 nm. As shown in Figure 3.9, however, DBCO488 bound to NtermpaFSurvivin$_{1\text{-}120}$ exhibited an absorbance maximum of 500.5 nm. This shift is due to solvatochromism, i.e. the property of a compound's change in absorbance character depending on the solvent in which it is dissolved. Therefore, size exclusion analyses monitored absorbance at 280 and 500 nm.

As shown in Figure 3.10, size-exclusion chromatography results indicated that NtermpaF-DBCO488-Survivin$_{1\text{-}120}$ size exclusion chromatography fractions possessed dual absorbance at 280 nm and 500 nm. This result suggested that the protein and fluorophore co-eluted. Because unbound DBCO488 would have eluted much later in the size exclusion column compared to protein, due to its small size when unbound to protein, the FPLC A280 and A500 traces' overlap suggests that Survivin$_{1\text{-}120}$ protein and DBCO488 bound each other. This suggested that the copper-free click chemistry reaction between DBCO488 and paF-containing Survivin$_{1\text{-}120}$ was successful. Thus, the next step was to separate select fractions by SDS-PAGE, then analyze them by UV ill-

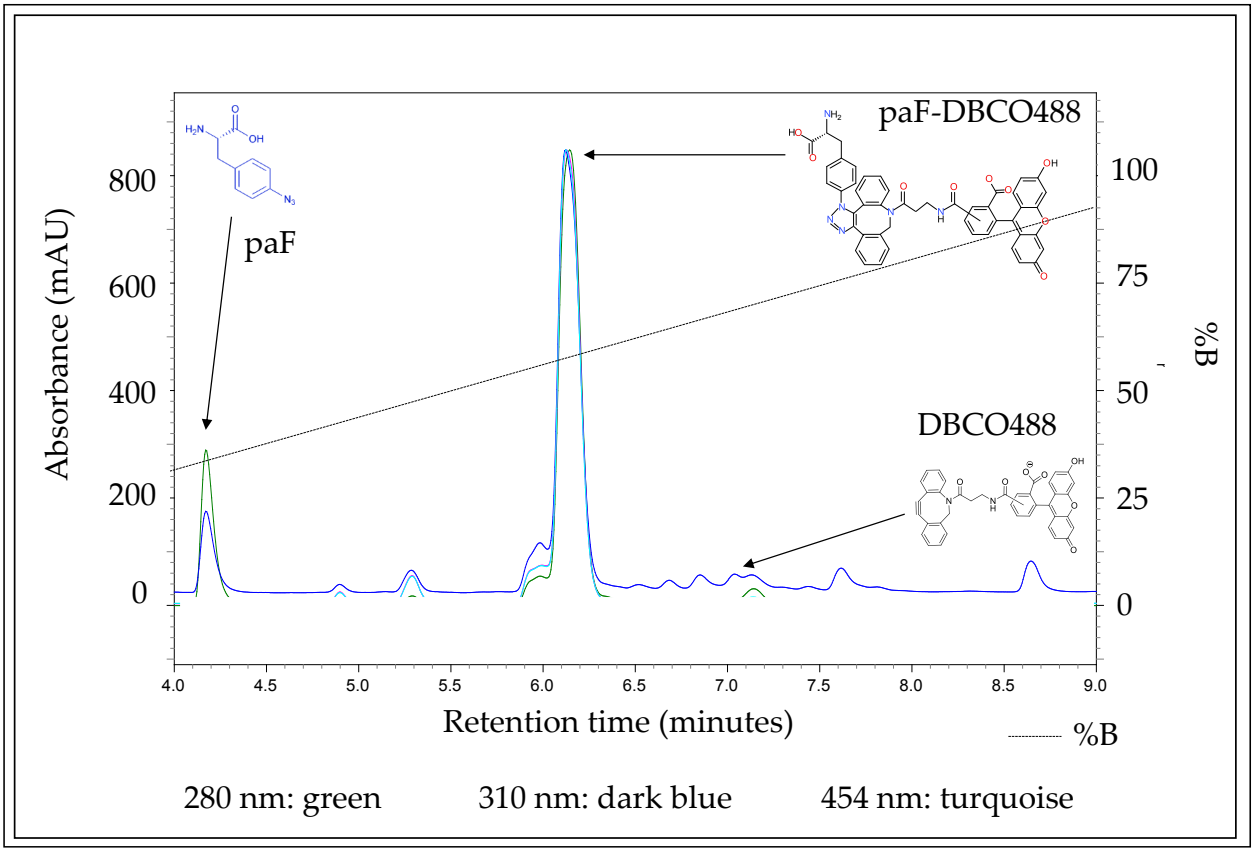

Figure 3.5: HPLC separation of 50 µL of 1:1 alkyne:azide copper-free click chemistry reaction of reactants *para*-azidophenylalanine (paF) and DBCO488 in loading buffer, and product, paF-DBCO488. Absorbance (mAU) is depicted on the left y-axis, retention time (minutes) on the x-axis, and %B (light gray trace) on the right y-axis.

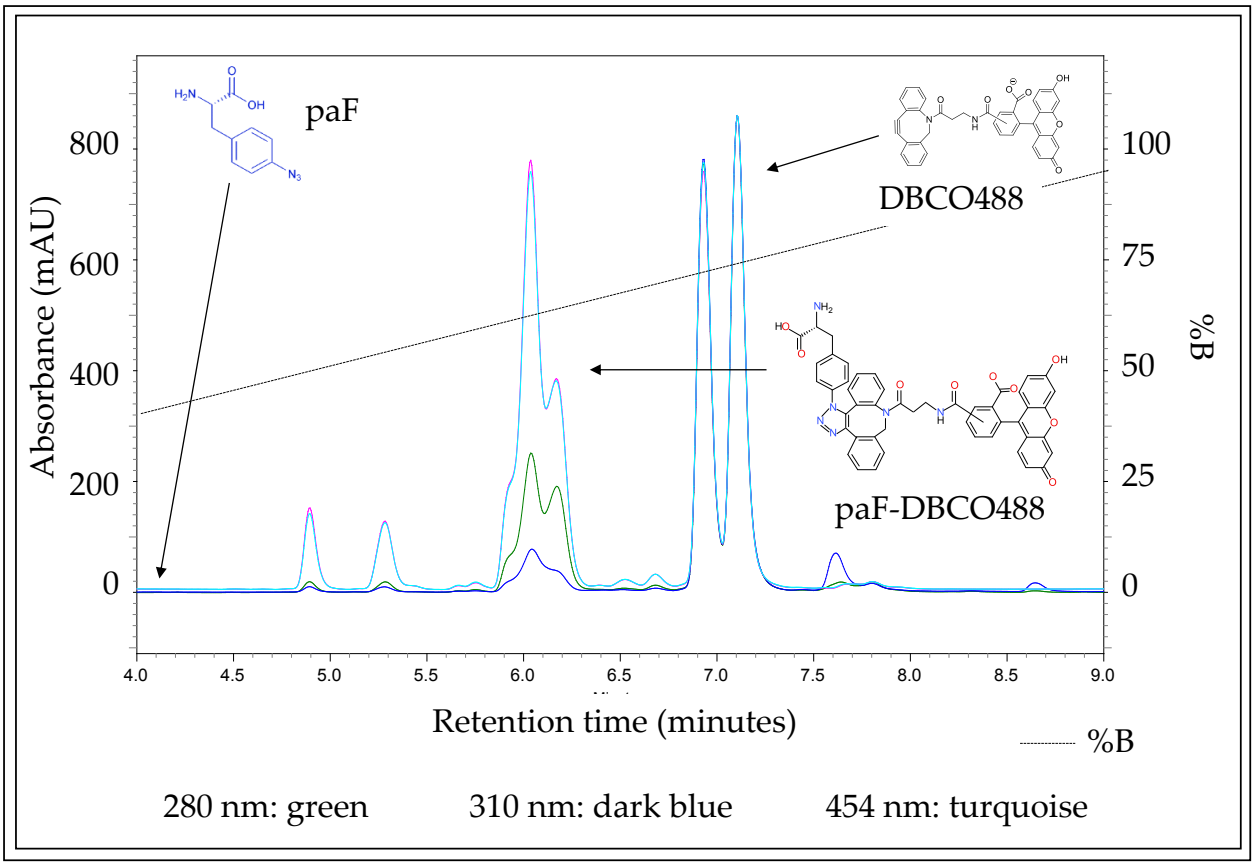

Figure 3.6: HPLC separation of 50 µL of 10:1 alkyne:azide copper-free click chemistry reaction of reactants *para*-azidophenylalanine (paF) and DBCO488 in loading buffer, and product, paF-DBCO488. Absorbance (mAU) is depicted on the left y-axis, retention time (minutes) on the x-axis, and %B (light gray trace) on the right y-axis.

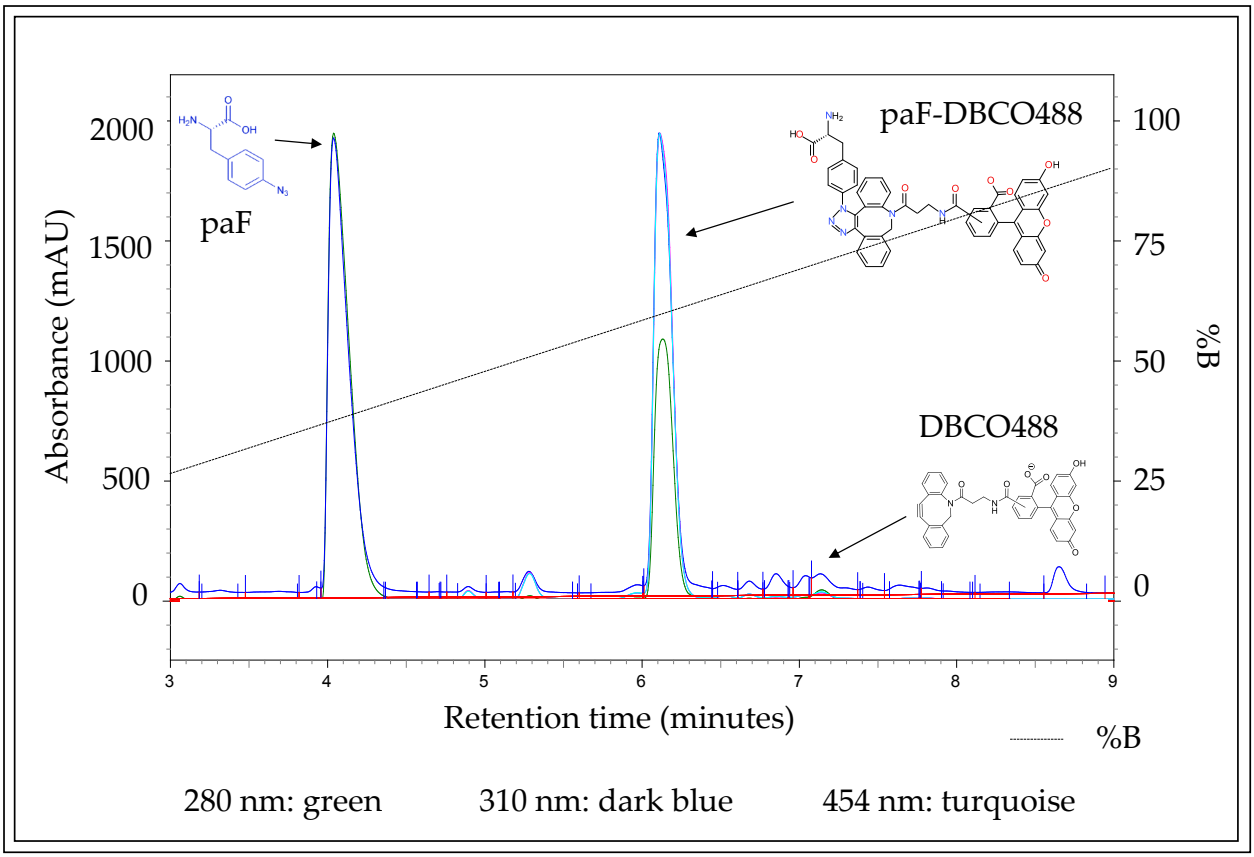

Figure 3.7: HPLC separation of 50 µL of 1:10 alkyne:azide copper-free click chemistry reaction of reactants *para*-azidophenylalanine (paF) and DBCO488 in loading buffer, and product, paF-DBCO488. Absorbance (mAU) is depicted on the left y-axis, retention time (minutes) on the x-axis, and %B (light gray trace) on the right y-axis.

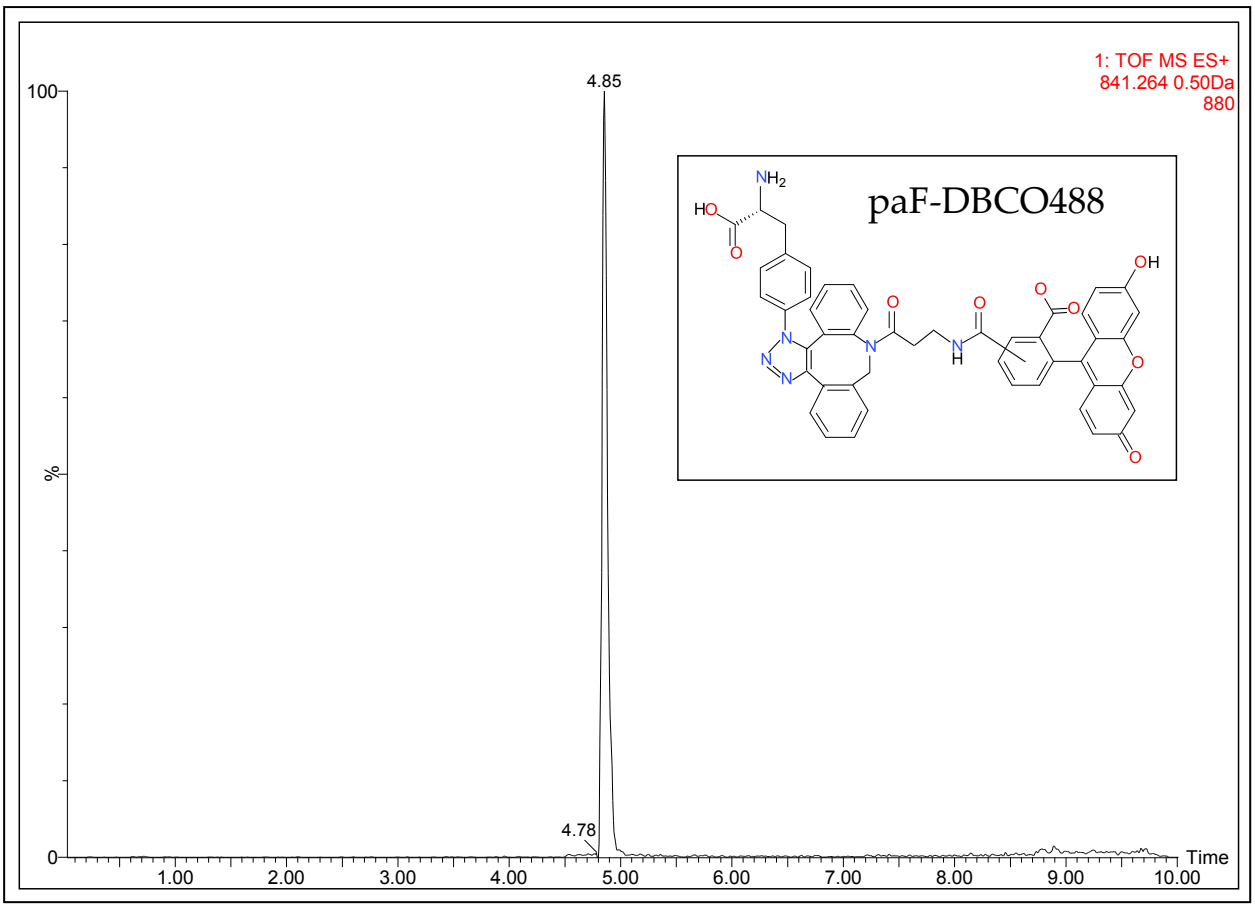

Figure 3.8: TOF electrospray mass spectrometry in positive ion mode detection of cycloadducted product, paF-DBCO488, inset, of the copper-free click chemistry reaction of *para*-azidophenylalanine and DBCO488. Expected monoisotopic mass: 840.26 Da. The y-axis depicts the percent relative abundance; the x-axis depicts the retention time in minutes.

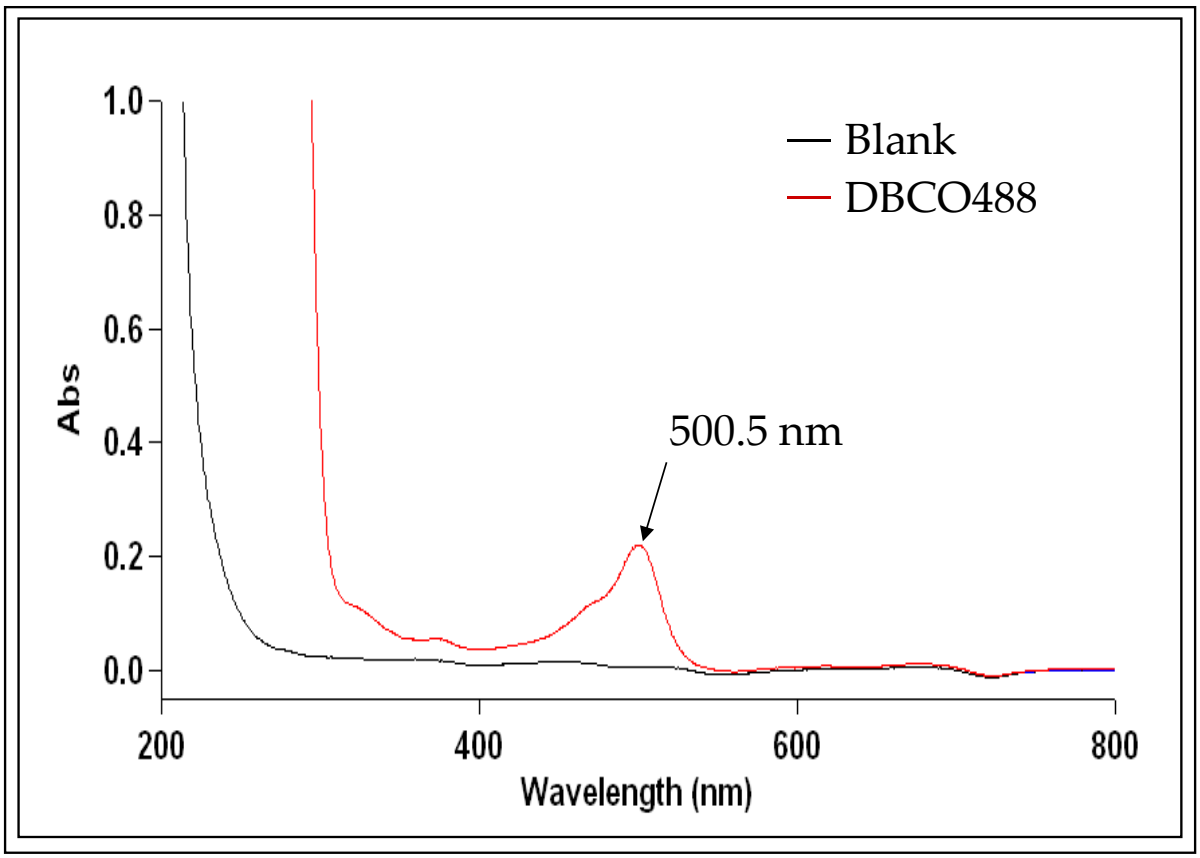

Figure 3.9: Absorbance scan of NtermpaF-DBCO488-Survivin$_{1\text{-}120}$ (DBCO488 trace) in loading buffer (Blank trace). Absorbance (Abs) is on the y-axis and wavelength (nm) on the x-axis.

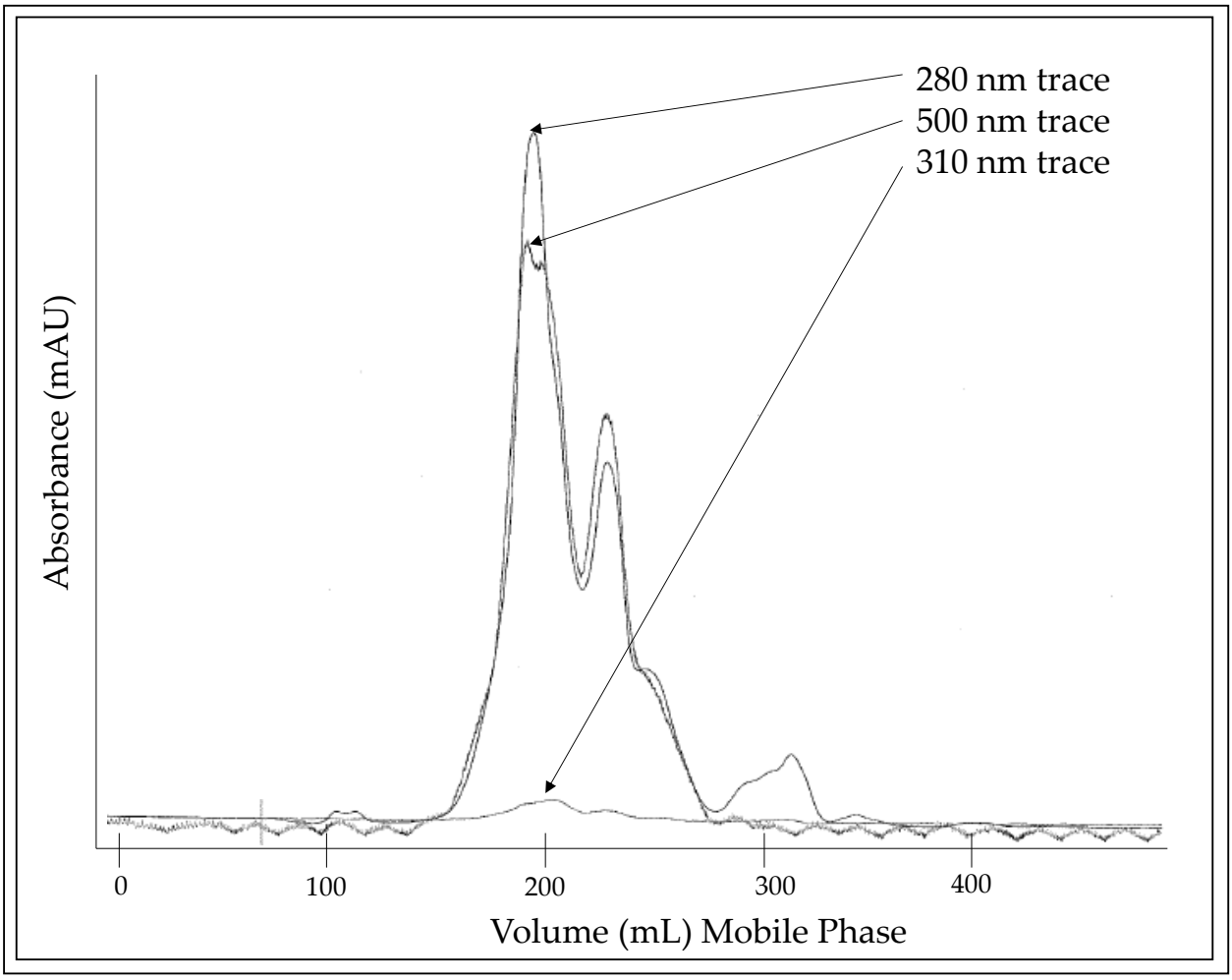

Figure 3.10: Chromatograph of NtermpaF-DBCO488-Survivin$_{1\text{-}120}$ separated by HiLoad 26/60 Superdex 200 preparative-grade size-exclusion column. The y-axis depicts absorbance (mAU) and the x-axis indicates the volume (mL) of mobile phase passed over the column. The 280, 500, and 310 nm traces are as indicated.

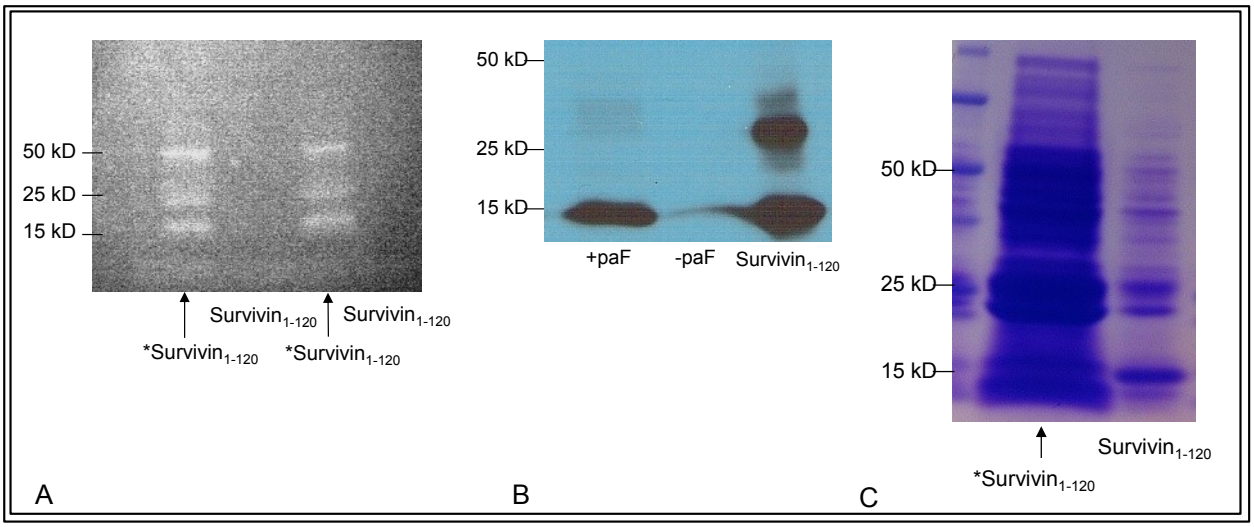

Figure 3.11: A: Fluorescence of SDS-PAGE-resolved fractions containing NtermpaF-DBCO488-Survivin$_{1\text{-}120}$ (denoted *Survivin$_{1\text{-}120}$) or Survivin$_{1\text{-}120}$. B: Western blot of SDS-PAGE-resolved NtermpaF-DBCO488-Survivin$_{1\text{-}120}$ with and without paF (denoted +paF and –paF, respectively) included in the overexpression medium, or Survivin$_{1\text{-}120}$. C: Coomassie stained gel of SDS-PAGE-resolved NtermpaF-DBCO488-Survivin$_{1\text{-}120}$ (denoted *Survivin$_{1\text{-}120}$) or Survivin$_{1\text{-}120}$.

umination, Coomassie staining, and western blotting to evaluate click chemistry reaction success.

As shown in Figure 3.11A, SDS-PAGE separation followed by UV gel illumination to monitor fluorescence revealed discrete fluorescent bands. This suggested that DBCO488 had been specifically incorporated into a protein that can oligomerize; $Survivin_{1-120}$ molecular weights are 15 kD (monomer), ~30 kD (dimer), and ~45 kD (trimer). Therefore, the fluorescence result suggests that DBCO488 bound a protein that exhibited nearly identical molecular weights of $Survivin_{1-120}$ monomer, dimer, and trimer.

As shown in Figure 3.11B, western blot analysis of $Survivin_{1-120}$ yielded substantial band density at 15 kD in the +paF and $Survivin_{1-120}$ lanes. In the wild type $Survivin_{1-120}$ control (Figure 3.11B), band density is evident at ~15 and ~30 kD, corresponding to Survivin monomer and dimer, respectively. Band density that would correspond to Survivin trimer (~45 kD) is not present in the $Survivin_{1-120}$ control. These results suggest that $Survivin_{1-120}$ does not adopt a trimeric association or that the conformational antibody does not recognize and bind Survivin in its trimeric conformation. These results may also mean that the modification yields a trimeric aggregate, in addition to the monomer and dimer. The immunogen used for Survivin antibody generation is a synthetic peptide that corresponds to the amino terminal of the Survivin protein (Cell Signaling product information, catalog number 2802S). Our results suggest that this antibody can recognize and bind the N-terminus of $Survivin_{1-120}$ when it adopts both its monomeric and dimeric conformations. A Coomassie stain of pure $Survivin_{1-120}$ indicated the presence of protein at ~15 kD (Figure 5.1); a Coomassie

stain and western blotting of pure DBCO-labeled NtermpaFSurvivin$_{1\text{-}120}$ could be used to determine the presence of dimeric and/or trimeric Survivin$_{1\text{-}120}$ or contaminants.

As shown in Figure 3.11 panels A and B, the western blot band density at 15 kD in the +paF lane overlaps the fluorescent band near 15 kD in the NtermpaF-DBCO488-Survivin$_{1\text{-}120}$ lane. This suggests that the fluorescence at 15 kD corresponds to fluorophore incorporation into Survivin$_{1\text{-}120}$. The presence of multiple fluorescent bands in the NtermpaF-DBCO488-Survivin$_{1\text{-}120}$ lanes suggest that the fluorophore was incorporated into protein that is present at ~15, ~30, and ~45 kD. Interestingly, however, band density in the western blot +paF lane is only present at ~15 kD. That very faint band density in the NtermpaF-DBCO488-Survivin$_{1\text{-}120}$ lane was detected at ~30 and virtually none was detected at ~45 kD by western blotting suggests that protein is present at these positions. Given that the antibody recognizes the amino terminal of Survivin, it is possible that the fluorophore at the extreme N-terminus of the protein may interfere with antibody recognition and binding of the dimeric conformation of the NtermpaF-DBCO488-Survivin$_{1\text{-}120}$ construct. Although highly unlikely, an alternative possibility is that the protein present at ~30 and ~45 kD by fluorescence is not Survivin.

As shown in Figure 3.11 panel C, Coomassie-staining of these same samples yields many bands, which suggest that the preparation is quite impure. While this is undesirable regarding sample purity and further purification was necessary (and subsequently achieved (Figure 3.12)), this is still a promising result when the fluorescence and Coomassie outcomes are considered simultaneously. The Coomassie result suggests that many proteins are present within the lane. The fluorescence result, however, indicates that fluorescence is only associated with three

discrete bands. This result suggests that only some of the proteins present in the lane impart a signal by fluorescence. The conclusion based on this result is that the fluorophore was specifically incorporated into only some proteins in the lane. If the fluorophore was non-specifically incorporated into all of the proteins present in the lane, as indicated by the Coomassie, then the fluorescence signal would also have been smeared and would have correlated with the entire height of the lane. Taken together, we believe that these results demonstrate the ability to introduce a fluorophore site-specifically into the protein of interest using click chemistry.

To address BL21*DE3 *E. coli* expressing the unnatural amino acyl tRNA synthetase to insert arginine at the amber stop codon, over-expression, purification, and western blot analysis of the –paF negative control was performed. Western blot analysis (Figure 3.11B) revealed a faint band at ~15 kD, which suggested that only a small fraction of Survivin translation resulted in putative arginine incorporation at the amber stop codon. A repeat of this analysis with optimal concentrations of loaded protein would clarify whether or not the faint band in the –paF lane was inadvertent contamination from the neighboring Survivin$_{1\text{-}120}$ control lane.

After we demonstrated the ability to fluorescently label the N-terminal paF-containing Survivin$_{1\text{-}120}$ protein, we subsequently performed copper-free click chemistry on the C-terminal paF-containing Survivin$_{1\text{-}120}$ protein. The labeled Survivin protein was purified using size-exclusion chromatography, as shown in Figure 3.12. Distinct band density is evident at 15 kD, the expected size of uncleaved Survivin$_{1\text{-}120}$ protein. The C-terminally-labeled protein did not appear to aggregate, as suggested by the presence of

a single band at 15 kD. This purified protein was utilized in the fluorescence lifetime determination.

DBCO488-labeled Survivin$_{1\text{-}120}$ Excitation and Emission Maxima

Survivin$_{1\text{-}120}$ with the DBCO488 fluorophore adducted to the extreme C-terminus (CtermpaF-DBCO488-Survivin$_{1\text{-}120}$) (1 μM) yielded an emission maximum of 520 nm using the Nano-LED excitation wavelength of 451 nm in 50 mM Tris, pH 7.46 at 22˚C, 500 mM sodium chloride, 2 mM β-mercaptoethanol. Emission was monitored at 520 nm for the time-correlated single photon counting (TCSPC) analyses.

TCSPC Analyses of Fluorescently-Labeled Survivin Protein

The pKa of the fluorescent moiety of DBCO488, fluorescein, is 6.4, so at pH 7.01, the pH of this experiment, fluorescein fluctuates between neutral and negatively-charged, unprotonated, species. As shown in Figure 3.13, time-correlated single-photon counting analysis of 1 μM CtermpaF-DBCO488-Survivin$_{1\text{-}120}$ in 50 mM Tris, pH 7.01 at 37˚C, 500 mM sodium chloride, 2 mM β-mercaptoethanol yielded a single-exponent decay curve, random residuals, and an acceptable chi-squared <1.2, of 1.078. The calculated fluorescence lifetimes equaled 1.39 and 4.03 ns, which exactly recapitulated literature precedent for unprotonated fluorescein [Magde, *et al.*, 1999]. These data suggested that DBCO488-labeled at the C-terminus of Survivin$_{1\text{-}120}$ protein exhibited the expected fluorescein fluorescence lifetimes.

3.3 Conclusions

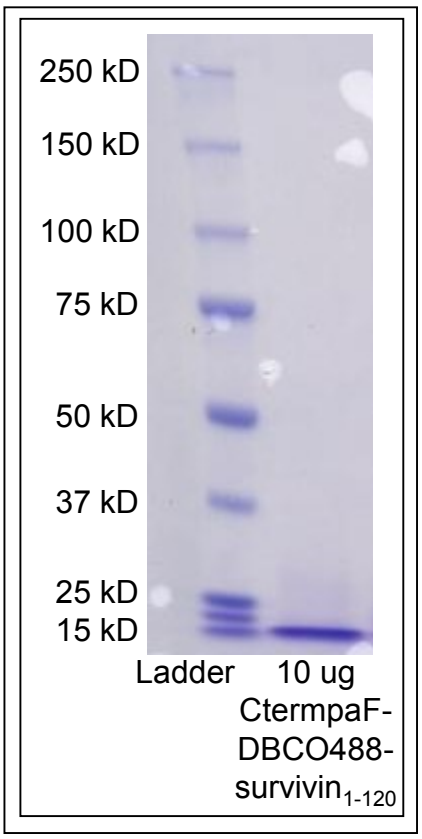

Figure 3.12: SDS-PAGE followed by Coomassie analysis of purified uncleaved CtermpaF-DBCO488-Survivin$_{1-120}$.

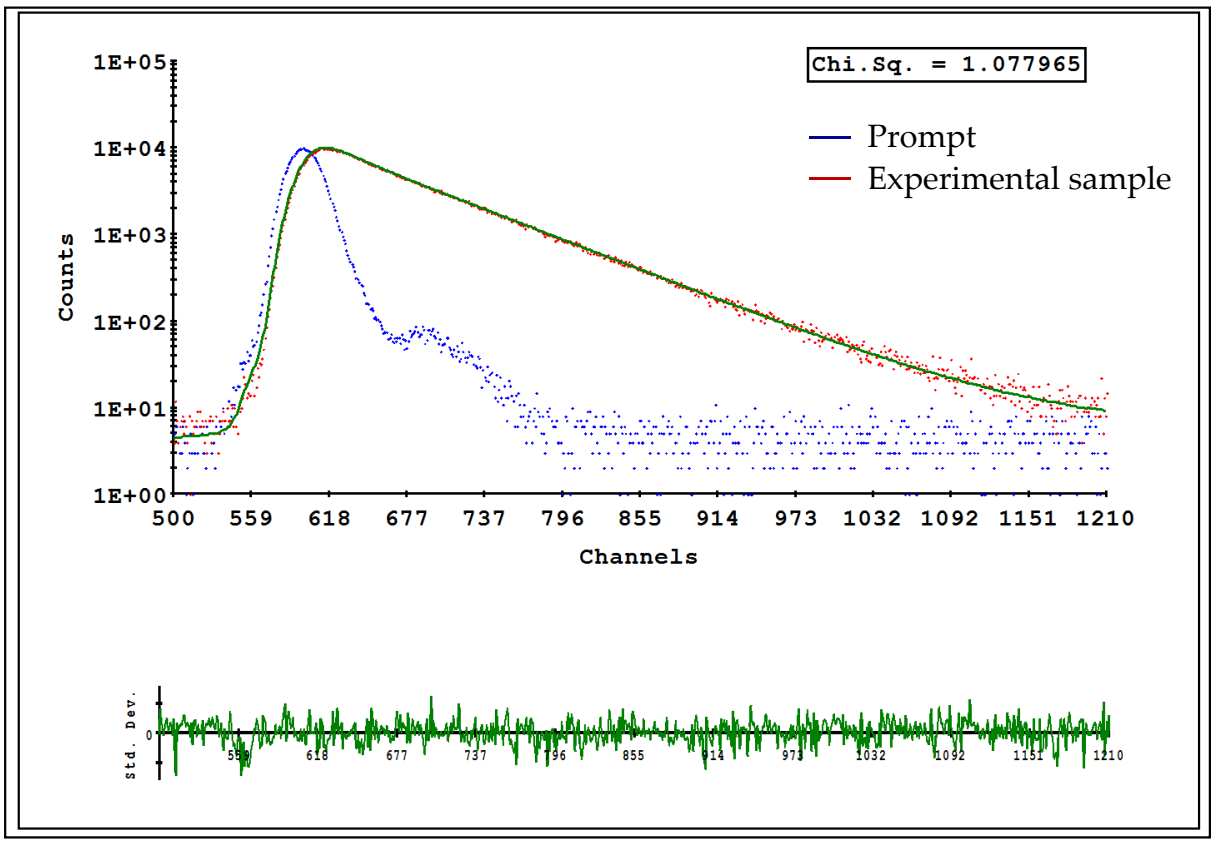

Figure 3.13: Time-correlated single photon counting data of 1 μM CtermpaF-DBCO488-Survivin$_{1\text{-}120}$ (Experimental sample trace – red dots with green curve) in 50 mM Tris, pH 7.01 at 37˚C, 500 mM sodium chloride, 2 mM β-mercaptoethanol, compared to the instrument response (Prompt trace – blue dots) to determine fluorescence lifetime of DBCO488-labeled Survivin$_{1\text{-}120}$ protein. The residuals plot (green trace) is depicted below. Counts: counts per second of emitted photons. Channels: 0.055 ns/channel.

Utility of Copper-Free Click Chemistry *In Vitro*

The objective of these analyses was to site-specifically label Survivin$_{1\text{-}120}$ with a fluorophore using click chemistry for analysis of protein-protein interactions. Data obtained using HPLC and MS suggested that copper-free click chemistry reactions between small molecules paF and DBCO488 are promising, thereby providing precedent that the reaction might also work with azide-containing Survivin and other proteins. Data obtained using Coomassie, western blot, fluorescence, and size exclusion chromatography suggested that the copper-free click chemistry reaction between DBCO488 and paF-containing Survivin$_{1\text{-}120}$ was successful. This suggested that further examination of the fluorescently-labeled Survivin$_{1\text{-}120}$ protein, including characterizing the steady-state fluorescence and determining the fluorescence lifetime, was merited. The results obtained supported the hypothesis that copper-free click chemistry may be used to site-specifically label azide-containing target proteins with fluorophores.

Because of the sensitivity and versatility of the fluorescence-based approaches, including steady-state fluorescence intensity, FRET, and fluorescence lifetime analysis, improved technologies are needed to fully harness the utility of these methods. Endogenous fluorophores such as tryptophan may be used in certain fluorescence analyses, but advantages may be conferred by using exogenous fluorophores. Relative to tryptophan, the common fluorophore fluorescein exhibits a higher quantum yield, higher molar extinction coefficient, and excitation and emission maxima disparate from endogenous fluorophores. The lanthanide terbium also possesses some of these optimal fluorescence characteristics, in addition to a much longer fluorescence lifetime.

For these reasons, exogenous fluorophores have gained appeal for performing steady-state fluorescence intensity, FRET, and fluorescence lifetime analysis in studying proteins and protein-protein interactions. Importantly, it may not be possible to incorporate exogenous fluorophores using the protein target's endogenous cysteines. Therefore, an alternative approach using copper-free click chemistry may be utilized to site-specifically incorporate an exogenous fluorophore.

Site-directed mutagenesis, click chemistry, and fluorescence techniques, used together, provide the ability to investigate the consequences of partner binding on a specific region of the protein of interest. The ability to site-specifically introduce a fluorescent label into a protein of interest offers the possibility of identifying specific amino acids that are germane to a particular protein-protein interaction. Click chemistry enables the introduction of these probes that can be monitored while a binding partner is titrated. Steady-state fluorescence, FRET, and fluorescence lifetime analyses can provide insight into the consequences of partner binding, however, because the local environmental factors can impact fluorescence intensity, emission maxima, and fluorescence lifetime, data should be interpreted accordingly. These environmental factors are described in the following sections.

Utility of Steady-State Fluorescence Intensity Determination to Study Protein-Protein Interactions

Steady-state fluorescence intensity is a quantitative output that yields information about the fluorophore environment. Factors that can affect fluorescence intensity

include solvent quenching, buffer constituents, fluorophore concentration, and shielding/obstruction by protein partner binding.

In the context of analyzing the consequences of protein partner binding, steady-state fluorescence intensity can give information about protein folding and the degree to which a protein is in an unfolded or folded conformation. When tryptophan is buried within a protein, tryptophan exhibits an emission maximum at 330 nm [reviewed in Ghisaidoobe and Chung, 2014]. When tryptophan is accessible to solvent, the emission is shifted to 340 – 350 nm [reviewed in Ghisaidoobe and Chung, 2014]. Endogenous tryptophan fluorescence intensity may be quenched in an unfolded protein, but may increase as the protein folds, shielding tryptophans from solvent quenching, however, the polarity of the solvent may alter this trend [reviewed in Ghisaidoobe and Chung, 2014]. Additional considerations concern the quantum yield, as follows.

The efficiency with which a molecule absorbs then emits a photon, the quantum yield (Φ), is expressed as the percent of emitted photons divided by the total number of absorbed photons [reviewed in Lakowicz, 1999]. Fluorescence quenching results from non-radiative decay of the energy of the photon to the system, thereby decreasing fluorescence intensity [reviewed in Lakowicz, 1999], a phenomenon called “collisional quenching”. Sources of collisional quenching include interactions of the emitted photon with the solvent or with a neighboring small molecule or protein within the experimental system. Quenching may be affected by choosing a different solvent [reviewed in Lakowicz, 1999]. Photobleaching, or photochemical destruction of the fluorophore, may be reduced by decreasing the time that the sample is exposed to the incident beam [reviewed in Lakowicz, 1999]. The fluorophore concentration may be increased to

compensate for photobleaching [reviewed in Lakowicz, 1999]. Another strategy is to reduce the frequency (and thus the photon energy) of the incident beam [reviewed in Lakowicz, 1999]. Finally, robust fluorophores less susceptible to photobleaching may also be utilized [reviewed in Lakowicz, 1999].

Utility of Fluorescence Lifetime Analyses for Monitoring Protein-Protein Interactions

Fluorescein is one of the fluorescent moieties comprising the DBCO488 molecule. Fluorescein and other fluorophores may exhibit different fluorescence lifetimes based on protonation state [Martin and Lindqvist, 1975, Magde, 1999]. Fluorescein's pKa is 6.4 and when protonated, fluorescein exhibits a fluorescence lifetime of 3 ns; unprotonated, the fluorescence lifetime is 4 ns [Magde, 1999]. Fluorescein fluorescence lifetime has therefore been used as a pH indicator [Hammer, *et al.*, 2005]. In addition to protonation state, changes in solvent shielding may alter fluorescence lifetime. Static and dynamic fluorescence quenching can decrease fluorescence lifetime because the fluorophore is prevented from achieving its excited state or returns to its lower energy state more readily than when quenching does not occur [Alcala, *et al.*, 1987], respectively. If the fluorophore is shielded from quenching, the fluorescence lifetime may be longer than if the fluorophore is accessible to the quenching solvent [Alcala, *et al.*, 1987]. Fluorophore shielding may result from protein partner binding near the fluorophore. Therefore, changes in fluorophore lifetime can provide insights into protein partner binding. Importantly, if the purpose of the experiment is to obtain information about the protein binding interface, the location of

the fluorophore within the protein of interest should be known, i.e., site-specific. Survivin binds many partners including caspase-9 to inhibit apoptosis. Inhibiting Survivin binding to caspase-9 may facilitate cancer cell apoptosis. Identifying druggable binding interfaces of the Survivin-caspase-9 interaction may be achieved using the fluorescence-based approaches described herein. Subsequently, the portion of the labeled Survivin found to interact with caspase-9 could be mimicked with a synthetic peptide and implemented in a high-throughput fluorescence polarization screening assay (chapters 1 and 5) to identify candidate small molecule inhibitors of the Survivin-caspase-9 protein-protein interaction.

Although the DBCO488-labeled Survivin$_{1\text{-}120}$ construct recapitulated literature precedent for unprotonated fluorescein fluorescence lifetime (4.03 ns), the only conclusion that can be drawn from this single experiment is that the fluorescein moiety behaves, in this context, like free, unprotonated fluorescein with regard to fluorescence lifetime. There are limitations to the interpretation of fluorescence lifetimes. Although fluorescence lifetime can yield protein conformation information, lifetime measurements, alone, may provide only limited information given the complexity of the experimental setup and output interpretation. A series of experiments are required for proper interpretation of the observed fluorescence lifetime. In the context of fluorescein-labeled Survivin$_{1\text{-}120}$ binding histone-3, several interpretations may be possible. Mixed populations of 3.0 and 4.0 ns lifetimes may be observed as a result of solvent accessibility or shielding. Mixed populations may also arise because the side chain of histidine exhibits a pKa of 6.0, which is near that of fluorescein. It is possible that protons may be exchanged between the fluorescein moiety of DBCO488 and Survivin's

histidine 80. Because a single fluorescence lifetime output has multiple interpretations, lifetime data interpretations are usually made in concert with outputs from other fluorescence-based approaches. Steady-state fluorescence intensity, for example, gives information on the quantity of photons emitted and FRET analyses give information about donor-acceptor distance. Consequently, in order to fully appreciate the consequences of titrating protein binding partner into protein of interest, the three methods together yield the most comprehensive information about the fluorophore environment.

Fluorophore Limitations

Fluorescein

Fluorescence lifetime measurements, in tandem with additional fluorescence-based experiments, have been proposed to evaluate protein-protein interactions. The fluorophore utilized in this chapter (dibenzylcyclooctyne-488, Click Chemistry Tools) was a fluorescein derivative amenable to copper-free click chemistry-mediated incorporation into the protein of interest. DBCO488 was also chosen because it is relatively small and lacks a long, flexible linker region between the DBCO- moiety and the fluorescein moiety. Fluorescein has been widely used for fluorescence analyses because it elicits a quantum yield near unity, 94% [Brannon and Magde, 1978]. It also can yield two different fluorescence lifetimes depending on whether or not the carboxylic acid is protonated and has found utility as a pH indicator [Magde, *et al.*, 1999]. In the context of pH determination, that fluorescein exhibits different lifetimes based on protonation state is a benefit. In the context of protein-protein interactions,

that fluorescein can exhibit multiple lifetimes based on protonation state may confound data interpretation. Therefore, it is important to consider the sources of protonation state changes in experimental design and to interpret the data accordingly.

DBCO-Containing Fluorophores for TCSPC Analyses

A variety of commercially-available DBCO-containing fluorophores exist that may be site-specifically incorporated into the protein of interest including DBCO-carboxyrhodamine, DBCO-sulforhodamine, DBCO-Cy3, DBCO-Cy5, and DBCO-Cy7 (Click Chemistry Tools). Currently, however, there is a dearth of clickable fluorophores amenable to our analyses because we possess the 293, 335, and 451 nm Nano-LEDs, which is a specialized incident beam for performing time-correlated single-photon counting fluorescence lifetime determinations. DBCO-rhodamine has an excitation profile that overlaps 451 nm, however, 451 nm excitation would elicit only about 25% of the fluorescence intensity compared to maximal excitation wavelength. In addition, the long, flexible linker region between the DBCO- moiety and the fluorophore may stymie data interpretation regarding the fluorophore environment and effects of solvent quenching, as it may rotate more freely in solution than a fluorophore devoid of a long, flexible linker.

With few exceptions, the emitted photon exits the molecule with a unique, specific, and unchanging emission wavelength [Kasha, 1950]. That a molecule elicits a consistent emission profile may be beneficial for monitoring that molecule during processes such as chemical synthesis or in cases where excitation of an exogenous fluorophore overlaps that of an endogenous fluorophore, but the

fluorophores exhibit different emission maxima. Therefore, one possible alternative to the commercially-available DBCO-containing fluorophores may be to utilize the fluorescence character of the dibenzylcyclooctyne moiety (described in more detail in chapter 4). Briefly, upon excitation at 259 nm, DBCO-amine yielded a unique fluorescence emission with a peak at 383 nm as well as a broad emission band at 740 nm. It is possible that emission at 740 nm of this inflexible fluorescent moiety could be monitored in fluorescence lifetime determinations.

Solvatochromism

Solvatochromism, or a shift in a molecule's absorbance maximum based on solvent polarity, should be considered when moving from control stock solution analysis to *in situ* analyses. DBCO488 exhibited an absorbance maximum of 454 nm in 100% DMSO and 500.5 nm when adducted to the $Survivin_{1\text{-}120}$ protein in 50 mM Tris, pH 8.0, 500 mM sodium chloride, 2 mM β-mercaptoethanol. This bathochromic shift, a shift to a longer wavelength with increasing solvent polarity (positive solvatochromism), may occur with other fluorophores that may be utilized for the studies described in this chapter. Negative solvatochromism (hypsochromism), or a shift to a shorter wavelength with increasing solvent polarity, is also possible. In some cases, maxima may shift several hundred nanometers [Brooker, *et al.*, 1951, Morley, *et al.*, 1997]. Therefore, it may be necessary to determine the absorbance maxima of the fluorophore in different solvent contexts to ascertain that the analytical conditions are most reflective of the experimental conditions.

Proposed Approach to Utilize Endogenous Tryptophan Fluorescence in FRET with the Lanthanide Terbium

The lanthanide terbium has a moderate extinction coefficient but imparts substantial fluorescence emission intensity at wavelengths separate from endogenous fluorophores. Interestingly, terbium excitation maximum is 350 nm, which is near the emission maximum of tryptophan. One possible FRET experiment would include exciting the endogenous tryptophan in the target protein in the presence of terbium-labeled partner.

In summary, using site-directed mutagenesis coupled with copper-free click chemistry, we have demonstrated the ability to insert a fluorescent tag into the Survivin$_{1-120}$ protein and purify the labeled protein. We recapitulated literature precedent regarding unprotonated fluorescein fluorescence lifetime in labeled Survivin$_{1-120}$ protein. These approaches poise us for performing fluorescence analyses on Survivin$_{1-120}$ with Survivin's binding partners.

Chapter 4: Two-Step Aqueous Synthesis of a Clickable Lanthanide Chelator

4.1 Introduction

Lanthanides, rare earth metal elements, are novel tools for fluorescence-based [Nitz, *et al.*, 2004, Hagan and Zuchner, 2011], x-ray crystallographic [Hiruma, *et al.*, 2013], and NMR [Su, *et al.*, 2006, Otting, 2008, Hiruma, *et al.*, 2013] applications. Lanthanides have broad Stokes shifts [Horrocks, 1993], long fluorescence lifetimes [Hemmila, 2005], narrow emission bands (narrow full-width at half maximum (FWHM)) [Lakowicz, 1999], are relatively insensitive to photobleaching [Pandya, 2006], and have excitation and emission maxima disparate from tryptophan, phenylalanine, and tyrosine [Brittain, *et al.*, 1976, Horrocks, 1993]. In the context of x-ray crystallography, lanthanides are used for anomalous dispersion experiments [Purdy, *et al.*, 2002]. Lanthanides' unique paramagnetic properties may be utilized in NMR applications [Iwahara and Clore, 2006, Clore and Iwahara, 2009, Madl, *et al.*, 2009]. These approaches can be used to evaluate protein dynamics and protein-peptide interactions, but incorporation of a suitable lanthanide chelator is required to fully harness lanthanides' unique properties.

Numerous strategies for the incorporation of lanthanide chelators have been employed including genetic or thiol-reactive insertion [Franz, *et al.*, 2003, Hiruma, *et al.*, 2013] of a lanthanide binding tag (LBT) [Nitz, *et al.*, 2004]. The LBT's cumbersome size may interfere with proper folding of the target protein, prompting efforts to pursue small molecule lanthanide chelators. Small molecule lanthanide chelators such as ethylenediaminetetraacetic acid (EDTA) and its derivatives 1,4,7,10-tetraazacyclo-dodecane-1,4,7,10-tetraacetic acid (DOTA) and diethylenetriaminepentaacetic acid (DTPA) exhibit attomolar lanthanide binding affinity [Cacheris, *et al.*, 1987] and have

been used for decades for their superior luminescence intensities [Brittain, *et al.*, 1976, Horrocks, 1993] and, more recently, for NMR experiments [Almeida, *et al.*, 2011]. These small molecule lanthanide chelators and their analogs have been derived to react with a protein's available cysteines [Su, *et al.*, 2008, Häussinger, *et al.*, 2009, Almeida, *et al.*, 2011, Zhang, *et al.*, 2011]. Where only one reactive cysteine is present, this can generate peak shifts of substantial magnitude and facilitate deconvolution of NMR spectra to yield structural information [Otting, 2008]. In most cases, however, the protein of interest contains multiple cysteines and/or they are critically involved in disulfide bond formation or other secondary structure stabilizing events, thereby precluding site-directed mutagenesis-mediated insertion or substitution of cysteine for site-specific insertion of a lanthanide chelator.

Synthesis of small-molecule lanthanide chelators has been demonstrated, however, the syntheses published to date require numerous steps, are performed under organic, not aqueous conditions, and yield chelators that are thiol-reactive [Saha, *et al.*, 1993, Ge and Selvin, 2003, Ge, *et al.*, 2004, Häussinger, *et al.*, 2009]. Synthesis of a small molecule chelator amenable to click chemistry was demonstrated [Martin, *et al.*, 2010], however, the synthesis required many steps and utilized organic reagents; in addition, the chelator was clicked into a synthetic azide-containing peptide rather than an azide-containing protein target.

To yield site-specific labeling of a protein of interest with a fluorescent or paramagnetic tag, I hypothesized that cyclooctyne-mediated copper-free click chemistry [Jewett and Bertozzi, 2010, Gordon, *et al*., 2012] may be coupled with incorporation of an unnatural amino acid such as paF [Chin, *et al.,* 2002] to yield a protein labeled with a

lanthanide chelator. Therefore, I sought to synthesize a small-molecule lanthanide chelator amenable to copper-free click chemistry-mediated incorporation into the target, paF-containing protein, using aqueous conditions. *Consequently, the unprecedented two-step aqueous synthesis of a lanthanide chelator amenable to site-specific incorporation is herein described using dibenzylcyclooctyne-amine (DBCO-amine) and the small molecule lanthanide chelator diethylenetriaminepentaacetic acid (DTPA)* (Figure 4.1).

As its name implies, DTPA contains 5 carboxylic acid moieties (Figure 4.1, panel A). Briefly, lanthanide was first chelated with DTPA to confer reaction specificity at DTPA's central carboxylic acid prior to amide coupling with DBCO-amine. Terbium, a paramagnetic lanthanide, was chosen for its unparalleled ability to induce pseudocontact shifts, large paramagnetic relaxation enhancements (PREs) [Otting, 2008], attomolar DTPA binding affinity [Cacheris, *et al.*, 1987], and ability to elicit substantial fluorescence intensity [Horrocks, 1993, Lakowicz, 1999]. The lanthanide, because of its attomolar affinity, remains chelated throughout synthesis and purification. The entire synthetic route is described in more detail, in the following section.

Metallation of DTPA (molecule A, Figure 4.1) with terbium was performed to generate metallated DTPA (complex B), which conferred amide coupling reaction specificity at DTPA's central carboxylic acid. Metallated DTPA was then reacted with the cyclooctyne-containing molecule dibenzylcyclooctyne-amine (DBCO-amine (C)), which was applied to an amide coupling reaction to synthesize the clickable chelator (D). Finally, in a copper-free click chemistry reaction, the clickable chelator (D) reacted with the unnatural amino acid paF (E), to generate the clicked clickable chelator (F).

The entire synthesis was performed in aqueous buffers under relatively mild conditions (~2-75˚C), with common reagents and commercially-available separation matrices (GE Healthcare). Successful completion of the efforts described herein provides a new tool for expanding NMR and x-ray crystallography approaches to study relatively larger proteins and protein dynamics of complexes heretofore not facile. Fluorescence and HPLC data indicated that the chelator synthesis was successful.

4.2 Results and Discussion

Metallation of DTPA

The first step in the 2-step aqueous synthesis of the clickable lanthanide chelator was metallation of the chelator with terbium. As shown in Figure 4.2, prior to metallation incubation, 350 nm excitation of 100 mM MES, pH 5.5, or 10 mM DTPA in 100 mM MES, pH 5.5, did not yield emissions between 400 and 800 nm save for the water Raman (702 nm). Under the same experimental conditions, 40 mM terbium trichloride in 100 mM MES, pH 5.5, yielded four sharp emission peaks at 489, 544, 584, and 621 nm, each of which exhibited substantial fluorescence intensity; the water Raman was evident at 702 nm. Ten millimolar DTPA with 40 mM terbium trichloride in 100 mM MES, pH 5.5, yielded four sharp emission peaks at 489, 544, 584, and 621 nm, each of which exhibited greater fluorescence intensity than did 40 mM terbium trichloride, alone; the water Raman was evident at 702 nm.

These fluorescence data demonstrated that DTPA chelated terbium and imparted substantial fluorescence emission at specific wavelengths: 489, 544, 584, and 621 nm. Because 1) DTPA was devoid of pi electrons and did not impart substantial

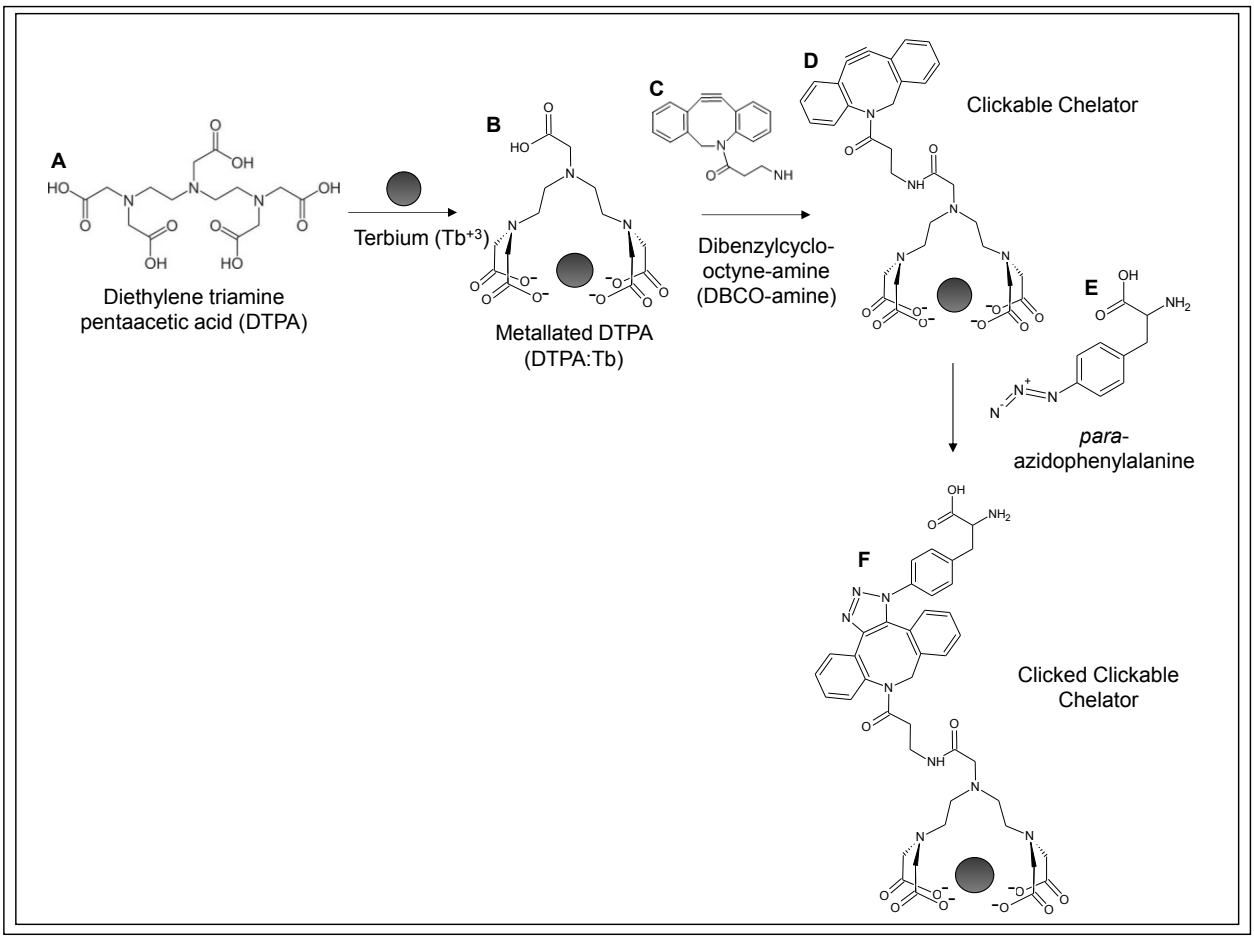

Figure 4.1: Synthetic route of Clickable Chelator and Clicked Clickable Chelator. Metallation of DTPA (A) with terbium (Tb^{+3}) to form metallated DTPA (DTPA:Tb) (B). Amide coupling of metallated DTPA (DTPA:Tb) (B) to dibenzylcyclooctyne-amine (DBCO-amine) (C) to synthesize the clickable chelator (D). Copper-free click chemistry reaction between the clickable chelator (D) and *para*-azidophenylalanine (paF) (E) to generate the clicked clickable chelator (F). Single product shown.

fluorescence emission and 2) terbium imparted emissions at 489, 544, 584, and 621 nm, demonstrated that the observed emission of metallated DTPA (DTPA:Tb) resulted from terbium fluorescence, not from DTPA. Increased fluorescence intensity of the metallated DTPA relative to terbium, alone, indicated that DTPA chelates terbium.

Based on efforts of Häussinger and coworkers [2009], it was thought that incubation at 75˚C would be required to facilitate metallation of terbium with DTPA. We observed, however, that metallation incubation at 75˚C for 8.25 hours failed to increase the intensity of the fluorescence emissions for 10 mM DTPA with 40 mM terbium trichloride in 100 mM MES, pH 5.5. This suggested that metallation of DTPA with terbium may be achieved with the thermal energy required to dissolve 10 mM DTPA in 100 mM MES, pH 5.5.

Compared to 10 mM DTPA in 100 mM ammonium acetate, pH 5.5 and 40 mM terbium in 100 mM ammonium acetate, pH 5.5, 1D NMR analysis of DTPA:Tb yielded broadened DTPA peaks, indicating complex formation or metal coordination of terbium with DTPA (Figure 4.3). A new peak at ~14.0 ppm most likely corresponded to a coordinated water molecule. As with the fluorescence results, the 1D NMR +/- incubation spectra were nearly identical, suggesting that metallation of terbium trichloride by DTPA was achieved using incubation at 75˚C (the temperature used to dissolve 10 mM DTPA (chapter 2)), for 8.25 hours, although incubation did not appear to be mandatory to metallate DTPA with terbium. In addition, these data suggested that, in the presence of a 4-fold molar excess of terbium, the reaction went to completion. Consequently, all 10 mM DTPA was metallated with terbium.

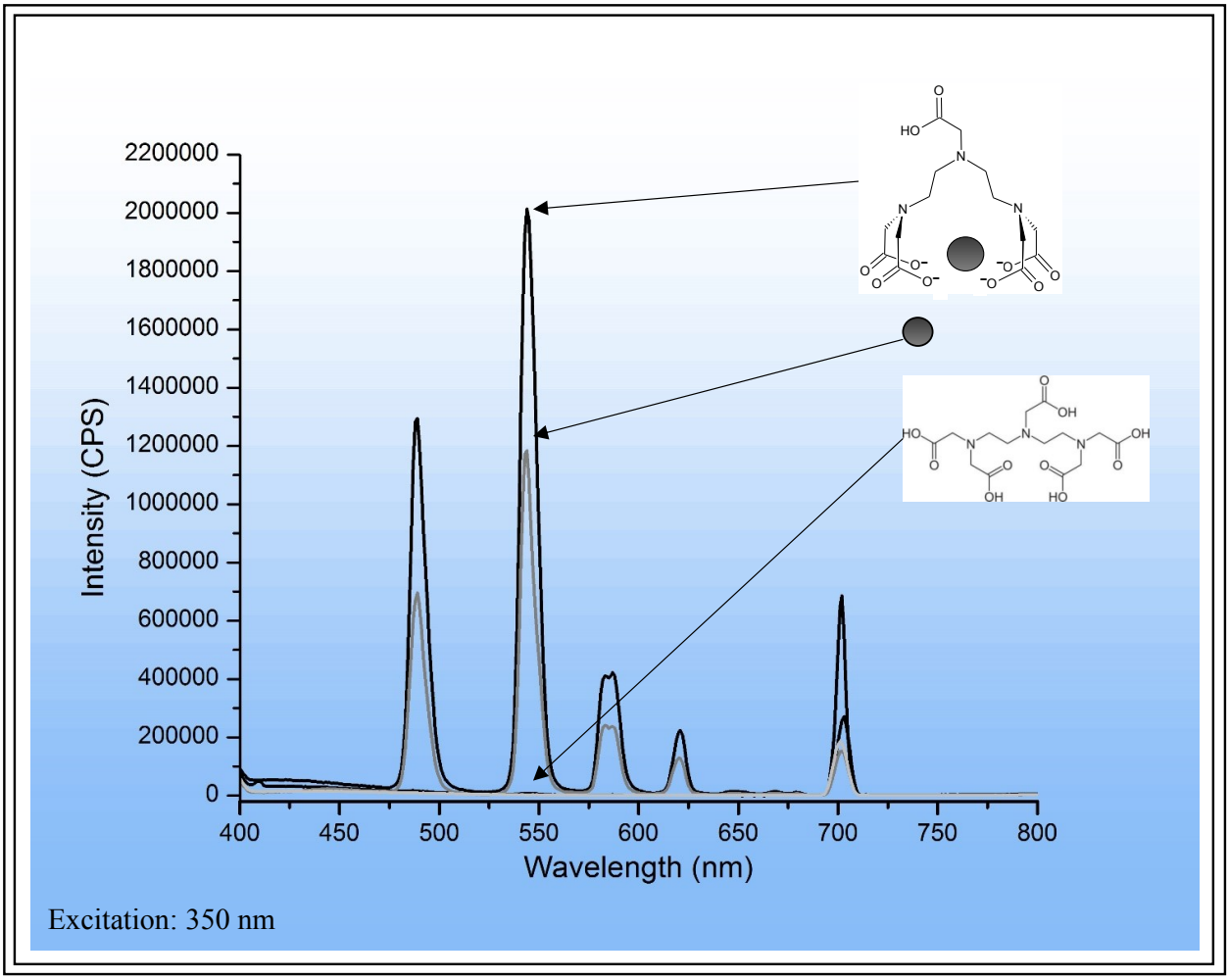

Figure 4.2: Spectrum of fluorescence intensity (counts per second (cps)) of emission of 100 mM MES, pH 5.5 (blue trace), 10 mM DTPA in 100 mM MES, pH 5.5 (black trace), 40 mM terbium (Tb) in 100 mM MES, pH 5.5 (green trace), and metallated DTPA (DTPA:Tb) (red trace) in 100 mM MES, pH 5.5 upon excitation at 350 nm. Peaks at 489, 544, 584, and 621 nm correspond to terbium. The peak at 702 nm corresponds to the water Raman.

The fluorescence and 1D NMR data corroborated the conclusions that DTPA chelated terbium, the reaction went to completion, incubation was not required if DTPA dissolution was achieved with heat, and DTPA:Tb imparted unique and substantial fluorescence emission peaks at specific wavelengths 489, 544, 584, and 621 nm.

Metallated DTPA Purified by Anion Exchange Chromatography

Anion exchange chromatography was used to separate excess, positively-charged terbium from negatively charged metallated DTPA. Excess unmetallated positively-charged terbium eluted in the column void volume. Because the metallation incubation included 4-fold molar excess of terbium, the fluorescence intensity associated with free, excess terbium should be greater than that of metallated DTPA. As expected, substantial fluorescence intensity at 489, 544, 584, and 621 nm was observed in anion exchange fractions 1-4 (Figure 4.4), which corresponded to the excess unchelated terbium present in the DTPA metallation incubation.

Metallated DTPA contained a single carboxylic acid that associated with the column matrix's positive charge. Addition of sodium chloride displaced metallated DTPA from the column resin; consequently, fluorescence emission corresponding to the terbium in metallated DTPA is expected in fractions from the sodium chloride gradient. As expected, elution with sodium chloride elicited fluorescence intensity at emission

Figure 4.3: 1D NMR analysis of 10 mM DTPA in 100 mM ammonium acetate, pH 5.5, and 10 mM DTPA with 40 mM terbium trichloride, with and without incubation, in 100 mM ammonium acetate, pH 5.5.

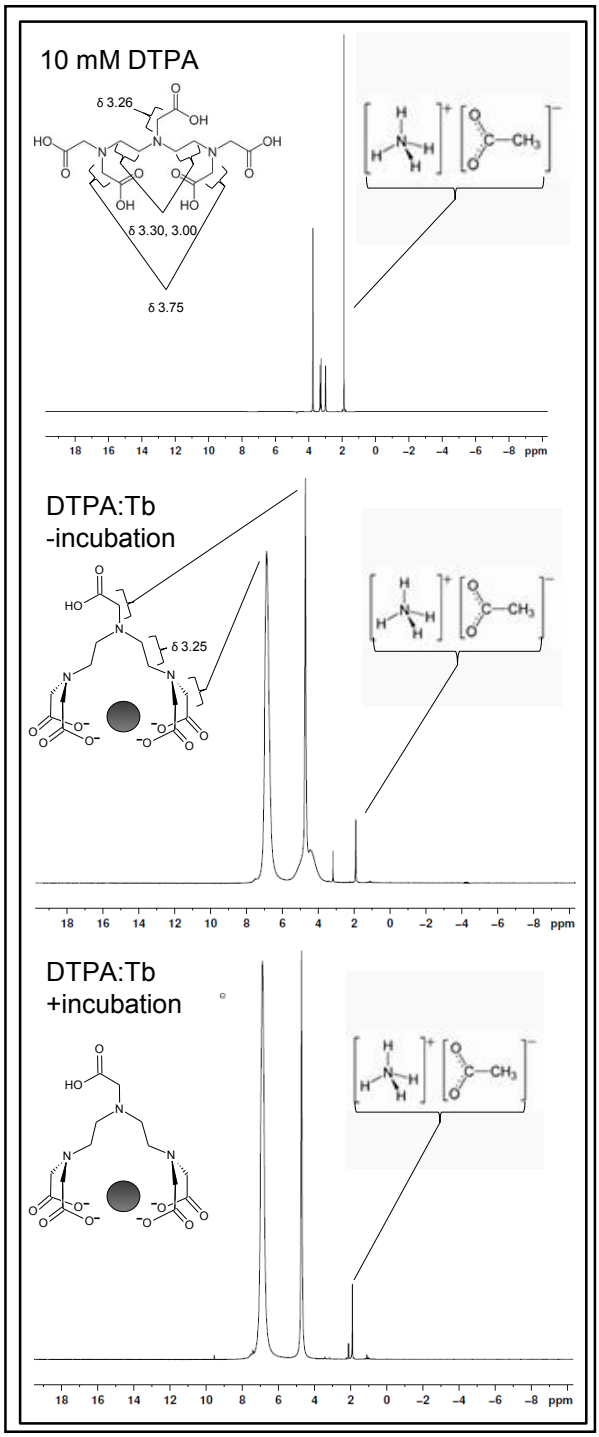

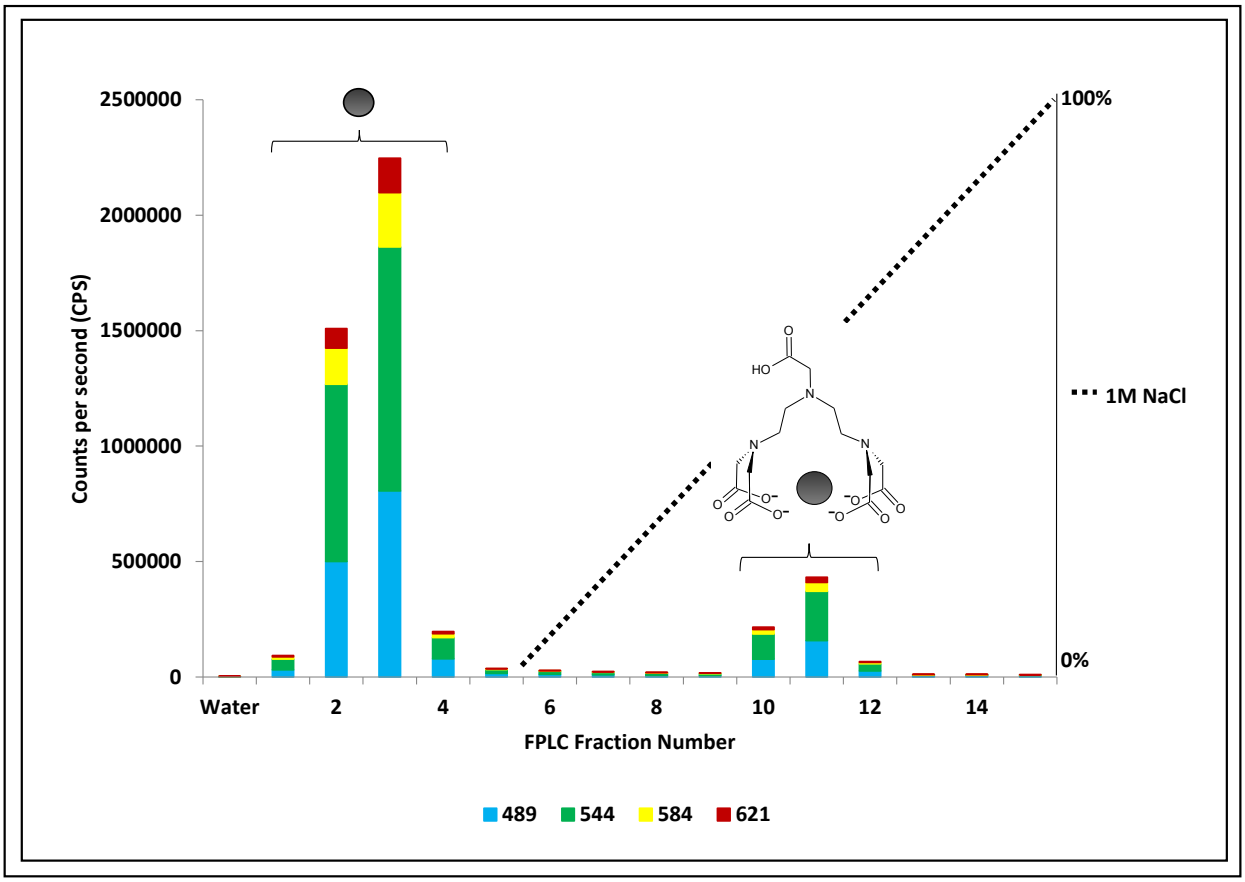

Figure 4.4: Cumulative fluorescence intensity in counts per second (cps) (left y-axis) of emissions at 489, 544, 584, and 621 nm of 3.5-mL fractions collected during anion exchange chromatography separation of metallation reaction. Excitation was at 350 nm. The x-axis depicts the anion exchange fraction number; the right y-axis depicts the 1M sodium chloride (NaCl) gradient (black dashed line).

wavelengths 489, 544, 584, and 621 nm in fractions 10, 11, and 12, which corresponded to terbium-metallated DTPA. In addition, the cumulative fluorescence intensity of the free, excess terbium (Fractions 1-4) was greater than that of metallated DTPA (Fractions 10-12). These results indicated that metallated DTPA may be separated from excess terbium. Fraction 11 was used for amide coupling.

DBCO-amine Fluorescence Excitation and Emission Maxima

As shown in Figure 4.5, fluorescence excitation and emission maxima were determined on 193.5 μM DBCO-amine in 3.2% (v/v) DMSO in 100 mM MES, pH 5.5. A moderately sharp emission peak, with maximum at 383 nm and a broad emission band with a maximum at 740 nm was observed. The excitation maximum was 259 nm. The water Raman was evident at 519 nm. Based on the aromatic character of the dibenzylcyclooctyne moiety, this was most likely the region of the molecule, not the free amine, which imparted the observed fluorescence.

Fluorescence of G10 Fractions

The second step in the 2-step aqueous synthesis of the clickable lanthanide chelator was amide coupling. Reactants for amide coupling, metallated DTPA and DBCO-amine, which were 548 and 276 Da, respectively, were retained within the G10 Sephadex matrix. In contrast, the amide coupling reaction product, the clickable chelator, at 802 Da, was excluded from the matrix and eluted in the void volume. Because metallated DTPA, DBCO-amine, and the clickable chelator each imparted

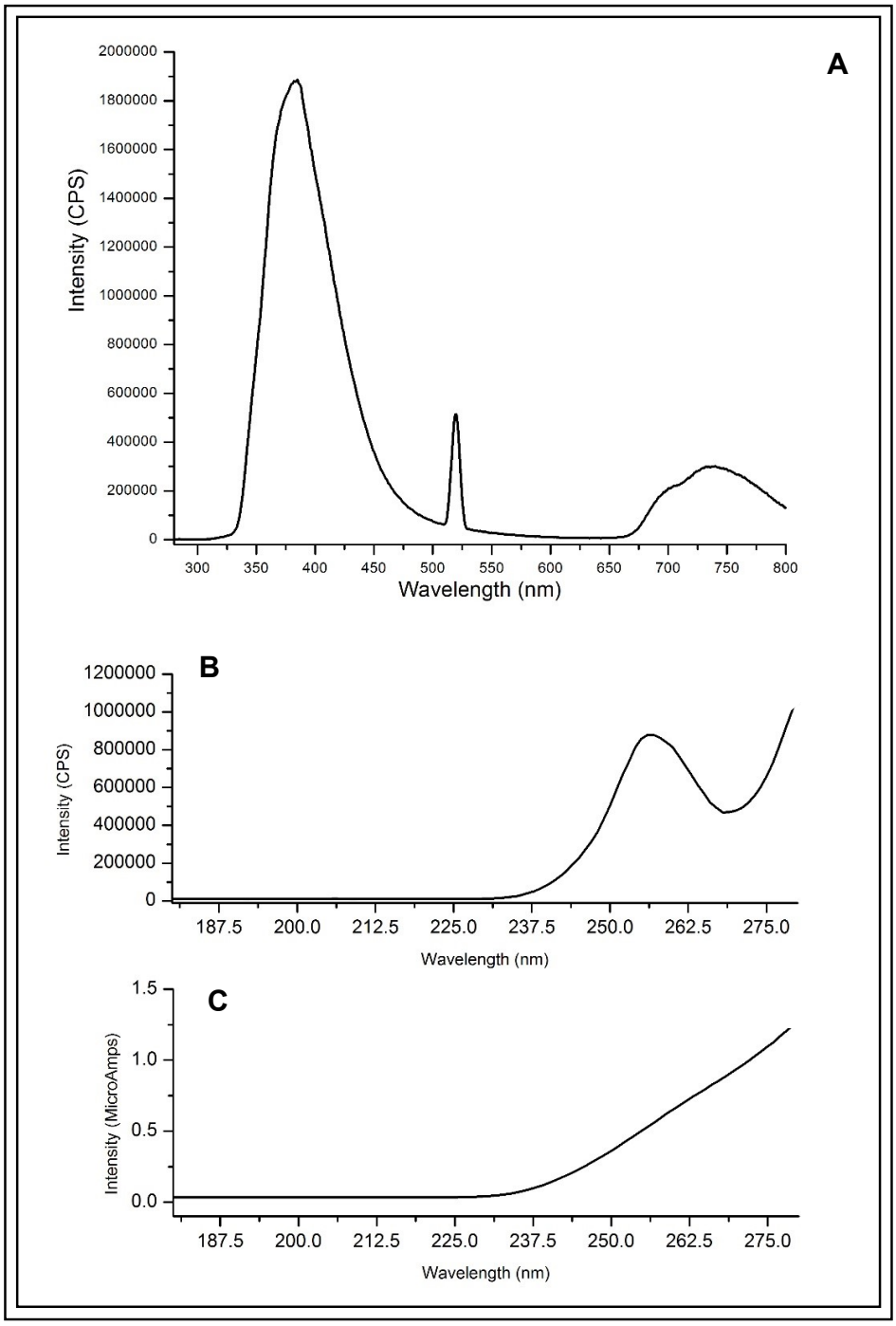

Figure 4.5: Spectra of fluorescence emission (Panel A) and excitation (Panel B) scans of 193.5 µM DBCO-amine in 3.2% (v/v) DMSO in 100 mM MES, pH 5.5, with Panel C depicting the excitation reference scan. The water Raman is evident at 519 nm in the emission scan (Panel A). The emission and excitation maxima were determined to be 383 and 259 nm, respectively. Wavelength (nm) is depicted on each x-axis; intensity in counts per second (cps) is depicted on panels A and B y-axes while intensity in MicroAmps is depicted on Panel C y-axis.

unique and substantial fluorescence signatures, fluorescence analysis of the fractions collected from G10 Sephadex would indicate the presence of these molecules in each fraction.

Upon excitation at 350 nm, the first collected fraction from the G10 Sephadex column yielded emission peaks at 489, 544, 584, and 621 nm (Figure 4.6). Because terbium emits at 489, 544, 584, and 621 nm, the fluorescence intensity of G10 Fraction 1 is imparted by terbium. In addition, G10 Fraction 1 exhibited substantial fluorescence intensity at an emission of 429 nm. Based on the structure of the dibenzylcyclooctyne moiety and the fluorescence character of DBCO-amine alone (Figure 4.5), the fluorescence emission at 429 nm most likely corresponded to the DBCO- moiety. No other collected G10 Sephadex fractions exhibited dual emissions from terbium and DBCO although several subsequent fractions exhibited fluorescence associated with excess DBCO present in the amide coupling reaction (data not shown). That a single fraction 1) possessed fluorescence character that corresponded to DBCO- and to metallated DTPA and 2) eluted in the void volume demonstrated that both DBCO- and metallated DTPA were present in one entity that is larger than 700 Da. Therefore, this data indicated that synthesis of the clickable chelator was successful.

HPLC Analysis of G10 Fraction 1 Yields Single Peak

HPLC analysis of G10 Fraction 1 yielded a single, sharp peak with a retention time of approximately 7 minutes (Figure 4.7). This fraction may be collected for small-molecule mass spectrometry to determine the nature of the molecule(s) that yielded the single HPLC peak. If the mass spectrometry data indicate that one product is present,

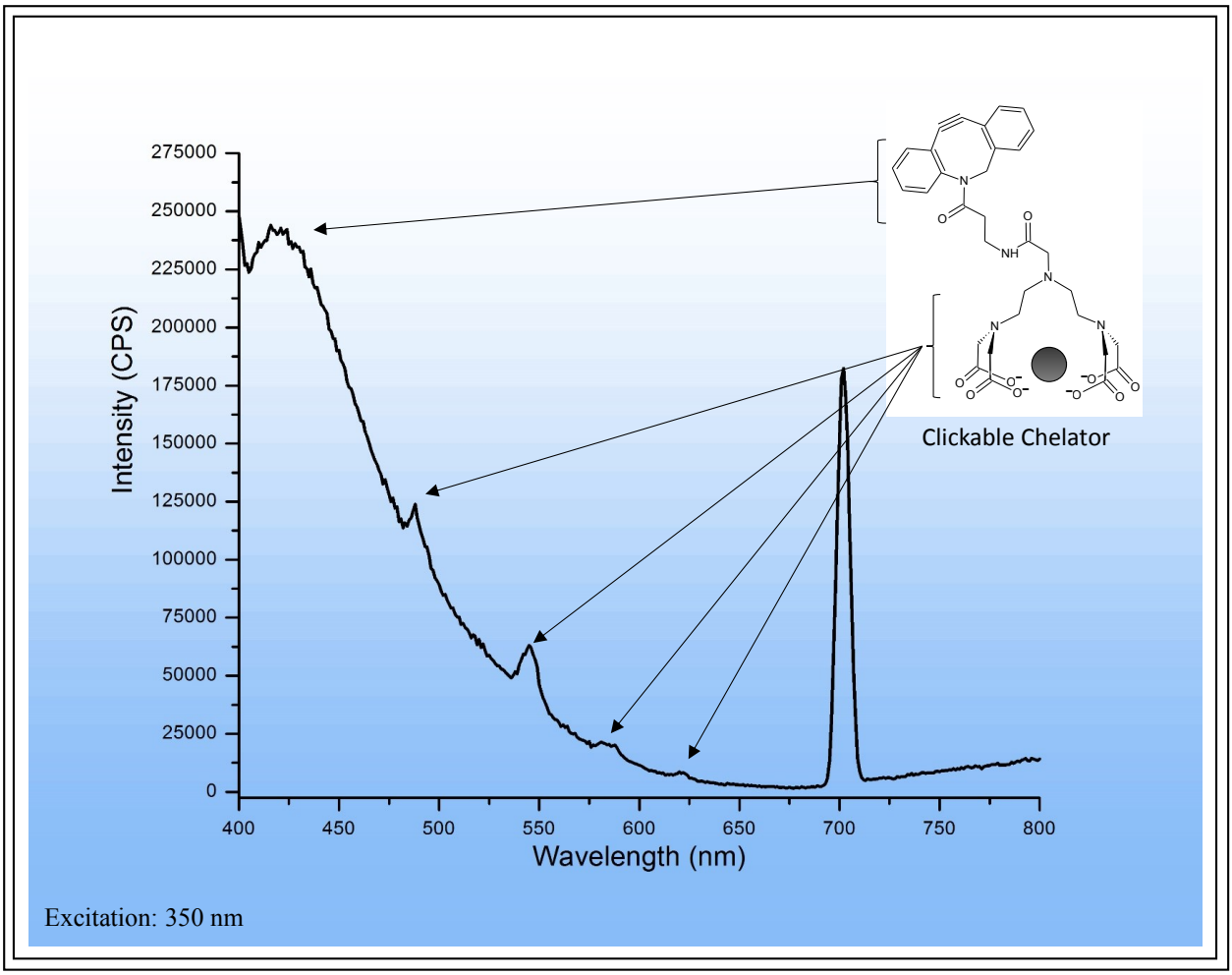

Figure 4.6: Emission scan of Fraction 1 collected from G10 Sephadex separation. Arrows correspond to emission wavelengths 429, 489, 544, 584, and 621 nm. The water Raman was evident at 702 nm. Excitation was at 350 nm. The x-axis depicts wavelength (nm) and the y-axis the fluorescence intensity (cps).

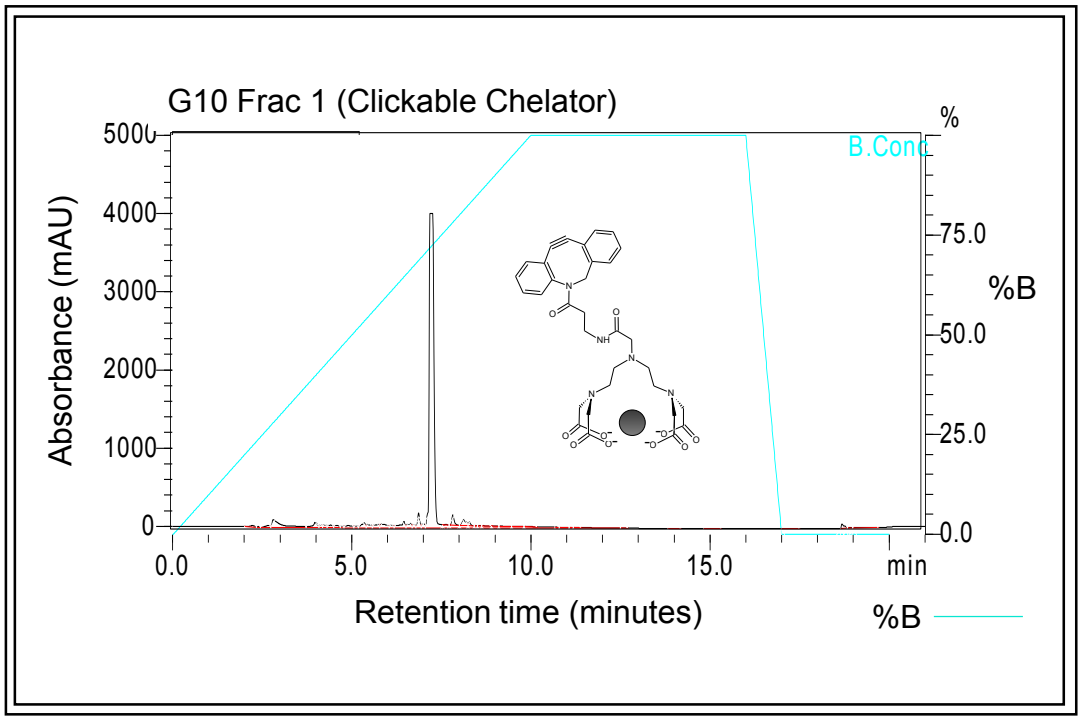

Figure 4.7: HPLC analysis of Fraction 1 collected from G10 Sephadex purification of the amide coupling reaction. Absorbance (mAU) is depicted on the left y-axis, retention time (minutes) on the x-axis, and %B (light blue trace) on the right y-axis.

these data suggest that the amide coupling yielded a single product that eluted in the void volume of the G10 Sephadex matrix.

Fluorescence Analysis of Clickable Chelator Yields Distinct Maxima

Excitation maximum of the clickable chelator was 322 nm; the emission maximum was 429 nm. An excitation wavelength of 322 nm did not yield discernible terbium fluorescence peaks and likely corresponded to fluorescence associated with the dibenzylcyclooctyne- moiety in the clickable chelator. Excitation of the clickable chelator at 350 nm yielded terbium-associated emission peaks at the predicted wavelengths of 489, 544, 584, and 621 nm. These data demonstrated that the clickable chelator possessed unique fluorescence properties, which originated from its dual DBCO- and terbium constituents.

Copper-free Click Chemistry Reaction with Clickable Lanthanide Chelator

Para-azidophenylalanine (azide) eluted from a C18 stationary phase in a single peak at 5.5 minutes (Figure 4.8); clickable chelator (alkyne) eluted in a single peak at 7 minutes. HPLC separation of an aliquot of the 10:1 alkyne:azide yielded two sharp peaks, the first at 6 minutes, which corresponded to the copper-free click chemistry reaction product, the clicked clickable chelator, and the second at 7 minutes, which corresponded to the excess alkyne, the clickable chelator. The peak at 6 minutes exhibits a retention time unique from that of the reactants paF (5.5 minutes) and the clickable chelator (7 minutes). This result indicated that the copper-free click chemistry reaction yielded a product with a unique retention time.

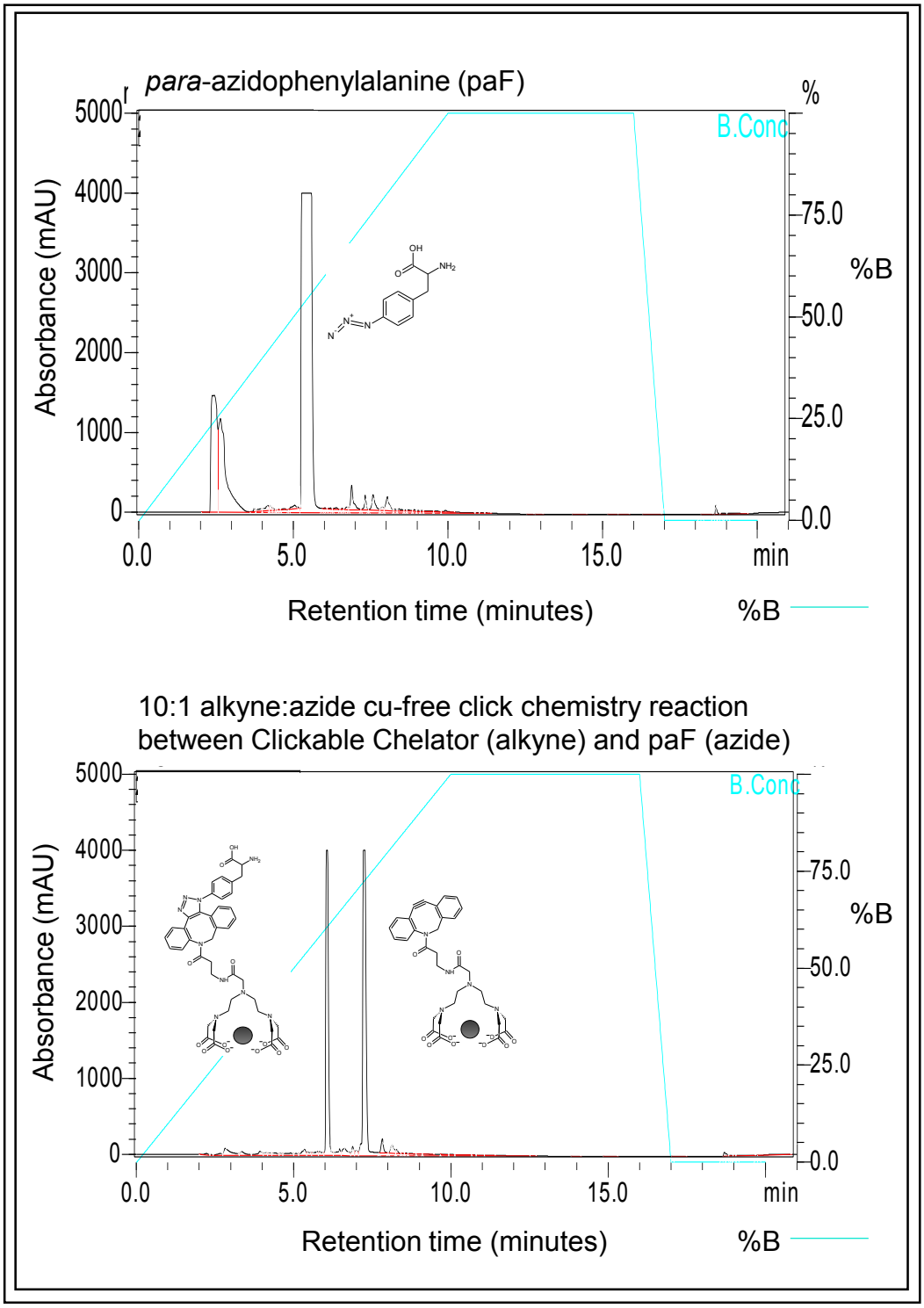

Figure 4.8: HPLC analysis of the reactant paF and the 10:1 alkyne: azide copper-free (cu-free) click chemistry reaction between paF (azide) and the clickable chelator to generate a clicked clickable chelator. Absorbance (mAU) is depicted on the left y-axis, retention time (minutes) on the x-axis, and %B (light blue trace) on the right y-axis.

Mass Spectrometry of Clickable Chelator

Select HPLC fractions from the copper-free click chemistry reactions were analyzed by MALDI mass spectrometry, however, the presence of additional peaks in the experimental and control spectra stymied data interpretation. Additional small-molecule mass spectrometry analyses of the clickable chelator and the clicked clickable chelator would ascertain peak assignments, and are discussed in more detail in chapter 6.

4.3 Conclusions

Lanthanide incorporation is a promising strategy to expand the utility of structural biology approaches NMR and x-ray crystallography, offering the ability to evaluate protein dynamics, conformational changes, and interactions of larger proteins than have previously been studied. The requirement for site-specific incorporation, however, coupled with the need for aqueous synthesis of a small-molecule chelator, has limited lanthanide use with these approaches. A new approach for site-specific lanthanide incorporation is articulated herein whereby a 2-step aqueous synthesis of a small molecule lanthanide chelator amenable to copper-free click chemistry is described using diethylenetriaminepentaacetic acid, terbium trichloride, and dibenzylcyclooctyne-amine.

Metallation of DTPA

The first step in the synthesis of a small-molecule lanthanide chelator amenable to copper-free click chemistry-mediated site-specific incorporation into the protein of interest was to metallate the chelator with the lanthanide of interest. For these studies,

diethylenetriaminepentaacetic acid (DTPA) and the lanthanide terbium were chosen. Metallation of DTPA with terbium was achieved first using 100 mM ammonium acetate, pH 5.5, using conditions that had already been utilized for similar objectives [Häussinger, *et al.*, 2009]. Subsequently, metallation of DTPA with terbium was achieved using a buffer devoid of free amines, 100 mM MES, pH 5.5. Notably, the use of buffers containing free amines, such as ammonium acetate, should be avoided for the metallation incubation, as the free amines in the buffer may react with the carboxylic acid of the chelator during the amide coupling reaction. Although it is possible to perform buffer exchange between the metalation and amide coupling steps, the use of an appropriate buffer for the metallation incubation should be considered for efficiency. While buffer exchange may be facilitated during anion exchange separation of the metallation reaction, the use of one buffer for metallation and anion exchange separation also prevents the need to optimize buffer exchange.

Metallation of DTPA with terbium was performed at a 1:4 molar stoichiometry of DTPA:$TbCl_3$ and metallated DTPA was purified from excess terbium using anion exchange chromatography. We thereby demonstrated the ability to metallate DTPA with terbium; it is expected that metallation of other chelators with a variety of other lanthanides may also be achieved.

Clickable Chelator Synthesized

Metallation of DTPA with terbium electrostatically engaged DTPA's peripheral four carboxylic acids with terbium's positive charge, leaving the central carboxylic acid of DTPA available to react with a cyclooctyne-containing molecule, dibenzyl-

cyclooctyne-amine (DBCO-amine), for synthesis of the clickable chelator by amide coupling. A room temperature, 120-minute amide coupling reaction of DTPA metallated with terbium was performed with an estimated 5-fold molar excess of DBCO-amine in the presence of the amide coupling reagent 1-ethyl-3-(3-dimethylamino-propyl)-carbodiimide (EDC). Separation of reactants DTPA:Tb and DBCO-amine and the product, DBCO-DTPA:Tb, was achieved by size-exclusion chromatography. Subsequently, fluorescence and HPLC analyses of the size-exclusion chromatography fractions demonstrated that the synthesis yielded a single product that elicited fluorescence emission corresponding to both the dibenzylcyclooctyne moiety and terbium. The next step was to perform a copper-free click chemistry reaction between the small molecules paF and DBCO-DTPA:Tb.

Copper-free Click Chemistry Reaction

In order to evaluate whether or not the clickable chelator contained a cyclooctyne amenable to copper-free click chemistry, a reaction was performed between the clickable chelator and the small molecule unnatural amino acid paF. HPLC analysis of the click chemistry reaction yielded a distinct, single peak with a slightly earlier retention time compared to the peak that corresponded to the clickable chelator. This result suggested that the copper-free click chemistry reaction yielded a new product; because of the reactivity of the azide and cyclooctyne molecules, the most likely conclusion from these data was that the cyclooctyne was present in the clickable chelator and it reacted with the unnatural amino acid paF. The next step is to administer the DBCO-DTPA:Tb (the clickable chelator) to paF-containing Survivin protein. Once that is accomplished,

^{15}N-backbone-labeled paF-containing Survivin protein will be generated; the clickable chelator will be added in a copper-free click chemistry reaction. After purification of the labeled Survivin protein, NMR analyses will be performed on Survivin with its binding partners.

In summary, the synthesis of a small-molecule lanthanide chelator amenable to copper-free click chemistry-mediated incorporation into a protein of interest is herein described using relatively mild reaction conditions and common reagents, with aqueous buffers, and two very straightforward purification steps that require common, commercially-available matrices and buffers. This is the first description of a 2-step synthesis of a small-molecule lanthanide chelator amenable to copper-free click chemistry-mediated incorporation into the protein of interest, using aqueous conditions. The synthesis yields a small-molecule lanthanide chelator that may be utilized in a variety of NMR- and fluorescence-based experiments that monitor protein-protein interactions.

Chapter 5: A High-Throughput Fluorescence Polarization Small-Molecule Screening Assay for Identification of Inhibitors of the Survivin-Histone-3 Protein-Peptide Interaction

5.1 Introduction

Efforts are ongoing to identify novel lead compounds that may serve as structural scaffolds which may be further altered chemically to produce drugs that exhibit a therapeutic effect on a relevant target. Hence, an abundance of high-throughput screening (HTS) platforms have been optimized for the identification of promising lead candidate compounds for use as therapies in many different diseases.

High-throughput screening can be conducted using a variety of chemical compound libraries. The Prestwick Chemical Library® [www.prestwick.com] is comprised of 1280 small molecules drugs approved by the Food and Drug Administration (FDA) and European Medicines Agency (EMA). The Prestwick Chemical Library® compounds exhibit high pharmacological and chemical diversity; their safety, bioavailability, and pharmacokinetic profiles in humans are known. The ZINC (ZINC is not commercial) library [Irwin and Shoichet, 2005] contains 727,842 commercially-available small molecules. ZINC is a virtual library produced for facile computational screening.

Each library is designed to facilitate the most efficient transition from *in vitro* screening to clinical utility. Thus, parameters such as oral bioavailability, compliance with Lipinski's rules, solubility, and safety, when available, are considered.

One drawback to utilization of these chemical compound libraries is the vast size and consequent large expense incurred testing thousands of compounds without any initial information about how the compound(s) may bind the target protein. Another drawback is that it may be difficult or cost-prohibitive to purify sufficient quantities of

target protein to screen hundreds or thousands of compounds, then follow-up with the requisite secondary analyses.

In silico analyses can generate structural predictions about how small molecules might bind putative protein targets. Such predictions may include hydrogen bonding interactions, electrostatics, and bond distance information, all of which can be used to determine whether or not the small molecule binding interaction observed *in silico* may have a likelihood of translating to an *in vitro* experimental observation. One such *in silico* approach, developed by Karanicolas and coworkers, can model the structure of the protein target in the presence of a protein binding partner with different small molecule candidate inhibitors [Karanicolas and Kuhlman, 2009, Karanicolas, *et al.*, 2011, Sievers, *et al.*, 2011, Johnson and Karanicolas, 2013]. This computational approach has the potential to identify promising candidates that may yield optimal *in silico* to *in vitro* translation; these select candidates can then be analyzed within the fluorescence polarization assay described below. This “rational screening” approach may decrease the time and expense involved in identifying candidate inhibitors because only select candidates identified from the computational screen are analyzed by fluorescence polarization.

The ratio of vertically- and horizontally-polarized fluorescence intensity yields the fluorescence polarization value (chapter 1). To identify candidate inhibitors of a specific protein-protein interaction, protein and fluorescently-labeled peptide are combined at fixed concentrations, then fluorescence anisotropy or polarization is measured. Small molecule inhibitors will disrupt the protein-peptide binding interaction, eliciting a decrease in the observed fluorescence anisotropy or polarization signal. Promising

small molecule candidate inibitors that elicit decreased fluorescence anisotropy or polarization are then screened for autofluorescence and quenching [Gribbon and Sewing, 2003], two factors that may alter the fluorescence polarization or anisotropy signal independent of disruption of the protein-protein interaction, leading to false positives or false negatives. Candidate molecules that are not false positives or negatives may then be tested further to determine IC_{50} for the protein-peptide interaction. Candidates may then be subjected to additional screening such as two-dimensional heteronuclear single quantum coherence (2D-HSQC) chemical shift perturbation NMR or x-ray co-crystallography, which may give information about the ability of the small molecule to displace the peptide from the target protein.

Fluorescence polarization may be most useful when the protein target is non-enzymatic and/or participates in many intracellular pathways. The platform is amenable to high-throughput analysis in 96- or 384-well plate formats, and can accommodate relatively small (100-200 µL for 96-well format, for example) assay volumes, facilitates analysis of specific- and non-specific binding, is performed in solution rather than via attachment of the target protein or peptide to a rigid substratum or antibody, utilizes relatively common instrumentation (fluorescence plate reader with adjustable excitation and emission polarizers), and can be adapted to evaluate false positives and false negatives. Depending on the fluorophore and fluorometer utilized, the method can be relatively sensitive. Taken together, these advantages can facilitate relatively straightforward and rapid identification of candidate protein-protein interaction inhibitors.

In previous studies, the HTS FP platform has been used to identify inhibitors of the X-linked Inhibitor of Apoptosis protein (XIAP) [Liu, *et al.*, 2000, Nikolovska-Coleska,

et al., 2004, Nikolovska-Coleska, *et al.*, 2008] and for identifying small molecule Smac/DIABLO mimics [Glover, *et al.*, 2003]. HTS assays have been sought for the identification of inhibitors of Survivin's protein-protein interactions, due to its important role in cancer cell survival and cell division. However, finding the appropriate protein-protein interaction to target among Survivin's many protein partners has been challenging.

Survivin binding histone-3 is a critical event in facilitating chromosomal passenger complex-mediated chromosomal segregation [reviewed in Carmena, *et al.*, 2012]. Therefore, inhibiting Survivin-histone-3 binding may disrupt chromosomal passenger complex assembly, resulting in G2/M arrest and cell death, an important outcome in cancer cells. An efficacious, selective inhibitor of Survivin protein-protein interactions has thus far eluded researchers and *no fluorescence polarization-based Survivin inhibitor screening assays have been established*. We hypothesize that high-throughput screening of candidate Survivin-histone-3 protein-peptide inhibitors may be accomplished using the fluorescence polarization platform. Successful completion of the work described herein will produce a validated assay to identify potential Survivin-histone-3 protein-peptide inhibitors.

5.2 Results and Discussion

Survivin$_{1\text{-}120}$ was over-expressed, purified, cleaved with thrombin, and analyzed by Coomassie, silver stain, and whole-peptide mass spectrometry. Uncleaved and thrombin-cleaved Survivin$_{1\text{-}120}$ yielded a sharp, dense, single band at the molecular weights that corresponds to uncleaved (~15 kD) and thrombin-cleaved Survivin$_{1\text{-}120}$ (14

kD) (Figure 5.1). Coomassie and silver stain results were corroborated by whole-peptide mass spectrometry, which yielded a sharp peak near the theoretical mass of thrombin-cleaved Survivin$_{1\text{-}120}$ (14095.9 Da) at 14094.4 Da (Figure 5.2). These data suggest that cleavage and purification of Survivin$_{1\text{-}120}$ was successful.

Histone-3 Peptide Binds Thrombin-Cleaved Survivin$_{1\text{-}120}$

As shown in Figure 5.3, excitation and emission maxima of carboxyfluorescein-labeled histone-3* (H3*) were determined to be 493 and 522 nm, respectively.

In order to determine if H3* bound thrombin-cleaved Survivin$_{1\text{-}120}$, 100 nM H3* was titrated with increasing amounts of thrombin-cleaved Survivin$_{1\text{-}120}$. As shown in Figure 5.4, increasing amounts of thrombin-cleaved Survivin$_{1\text{-}120}$ yielded a higher percent fluorescence polarization and percent fluorescence anisotropy. H3* binding appeared to approach saturation as the concentration of thrombin-cleaved Survivin$_{1\text{-}120}$ reached 20 μM. The experimental design was such that the amount of bovine gamma globulin (BGG) was constant in each experiment, to maintain viscosity of the experimental sample, thus, this result suggested that H3* bound thrombin-cleaved Survivin$_{1\text{-}120}$, not BGG.

In order to determine if H3* bound uncleaved Survivin$_{1\text{-}120}$, 100 nM H3* was titrated with increasing amounts of uncleaved Survivin$_{1\text{-}120}$. As shown in Figure 5.5, increased thrombin-cleaved Survivin$_{1\text{-}120}$ yielded a higher percent fluorescence polarization and percent fluorescence anisotropy. H3* binding did not approach saturation as the concentration of thrombin-cleaved Survivin$_{1\text{-}120}$ reached

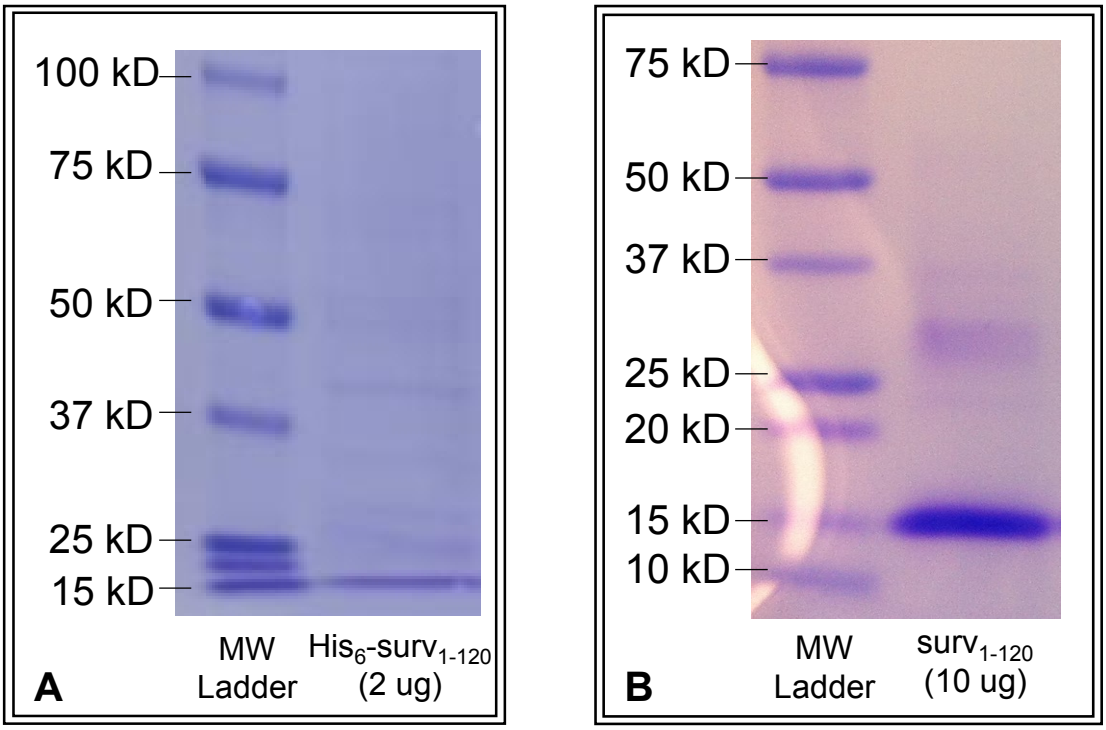

Figure 5.1: SDS-PAGE separation followed by Coomassie staining of Survivin$_{1-120}$ (~15 kD) before (Panel A) and after (Panel B) thrombin cleavage and purification.

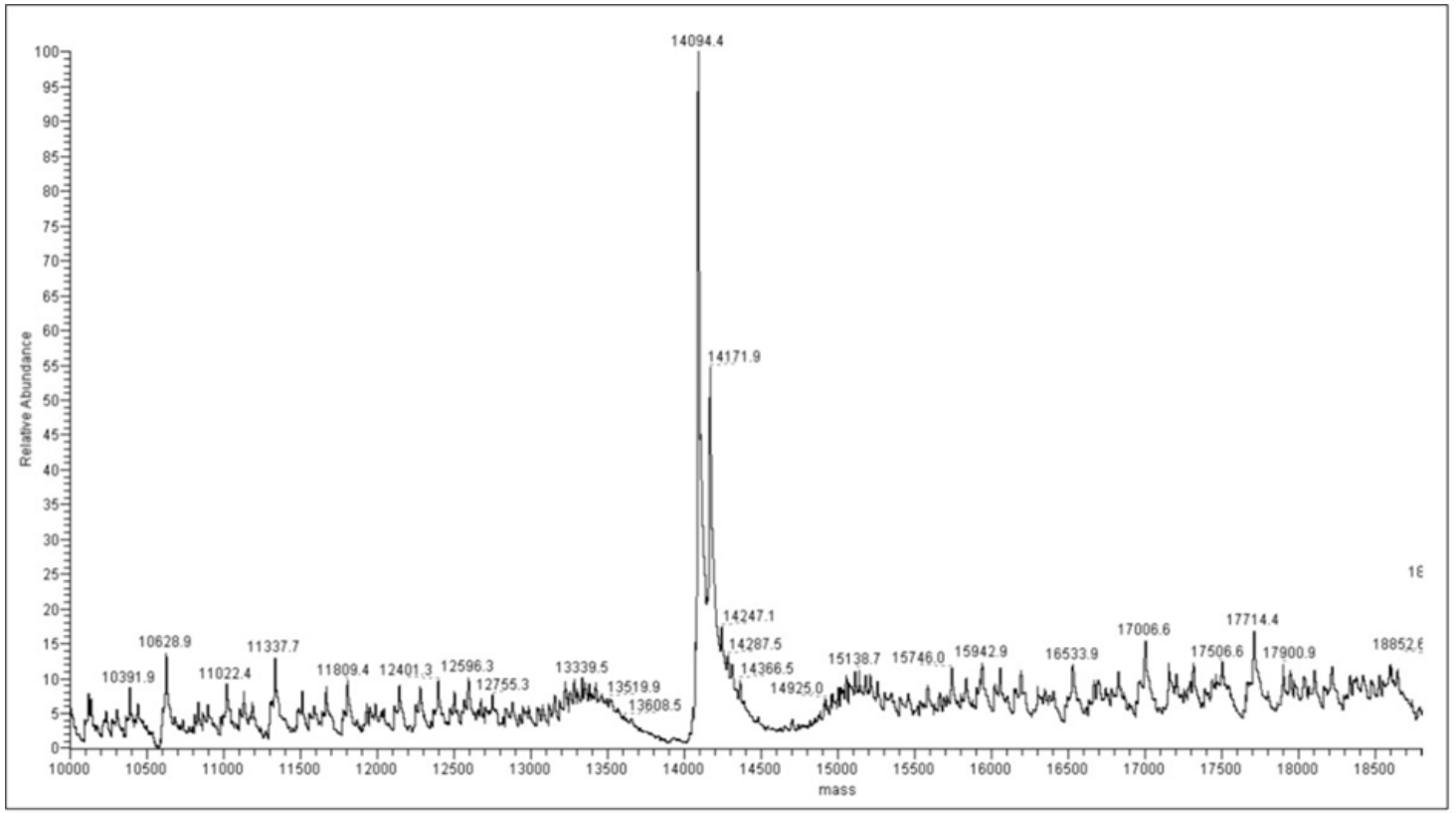

Figure 5.2: Deconvoluted whole-protein mass spectrum of thrombin-cleaved Survivin$_{1\text{-}120}$ with major species at 14094.4 Da, as identified by LTQ-FT mass spectrometry. The minor species, at 14171.9 Da, a mass difference of 77.5 Da, may correspond to the addition of two potassium ions to thrombin-cleaved Survivin$_{1\text{-}120}$. Percent relative abundance is depicted on the y-axis.

36 μM. The experimental design was such that the amount of bovine gamma globulin (BGG) was constant in each experiment, as above. The linear increase in percent fluorescence polarization and percent fluorescence anisotropy may have corresponded to non-specific binding of H3* to uncleaved $Survivin_{1-120}$. One possible source of non-specific binding may be uncleaved $Survivin_{1-120}$ aggregates: improperly folded uncleaved $Survivin_{1-120}$ may present non-specific binding opportunities to H3*, giving rise to the observed increase in percent fluorescence polarization and anisotropy (Figure 5.5).

Because the His_6- tag was at the extreme N-terminus of Survivin and histone-3 binds Survivin's BIR domain, the presumption was that the His_6-tag would not interfere with histone-3 peptide binding. The data presented in Figure 5.5, however, possibly suggests that uncleaved $Survivin_{1-120}$ did not adopt or retain its properly-folded tertiary conformation that facilitates specific H3* binding. Subsequent experiments utilized uncleaved His_6-$Survivin_{1-120}$, however, cleaved $Survivin_{1-120}$ would likely have yielded more reliable results.

Analysis of Survivin-Histone-3 Binding Specificity

The specificity of the Survivin:H3* binding interaction was evaluated by titrating unlabeled histone-3 peptide into 30 μM His_6-$Survivin_{1-120}$ and 1 μM H3* in 100 mM potassium phosphate, pH 7.5; as shown in Figure 5.6, the addition of an increasing amount of H3 decreased fluorescence polarization, however, a large standard deviation of 42% in the 0 nM H3 sample introduced question about the validity of the data. It is

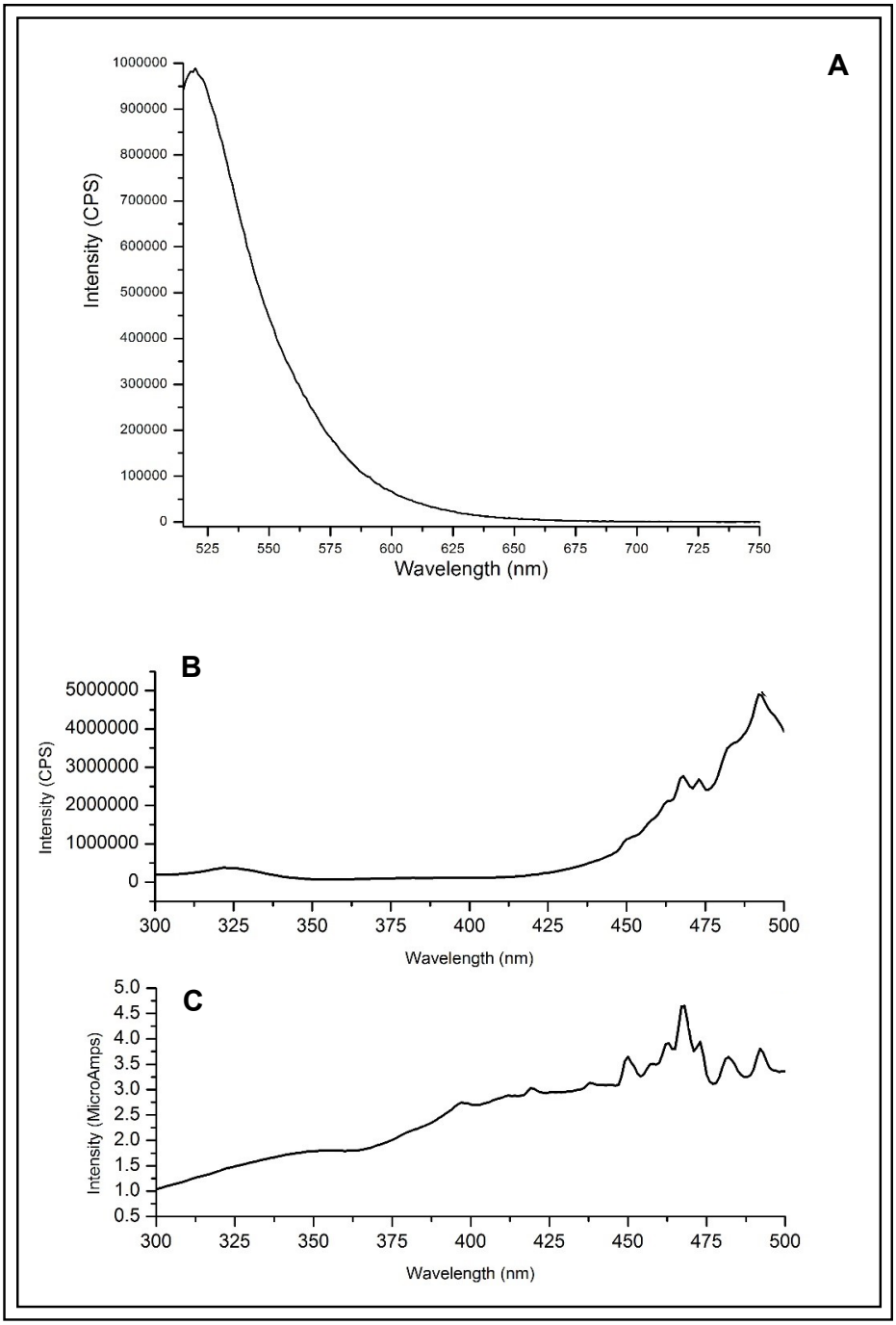

Figure 5.3: Emission scan (Panel A) and excitation scan (Panel B) of 100 nM carboxyfluorescein-labeled histone-3 (H3*) peptide in 100 mM potassium phosphate, pH 7.5, with excitation reference scan (Panel C). The emission and excitation maxima were 522 nm and 493 nm, respectively. Wavelength (nm) is depicted on each x-axis; intensity in counts per second (cps) is depicted on panels A and B y-axes while intensity in MicroAmps is depicted on Panel C y-axis.

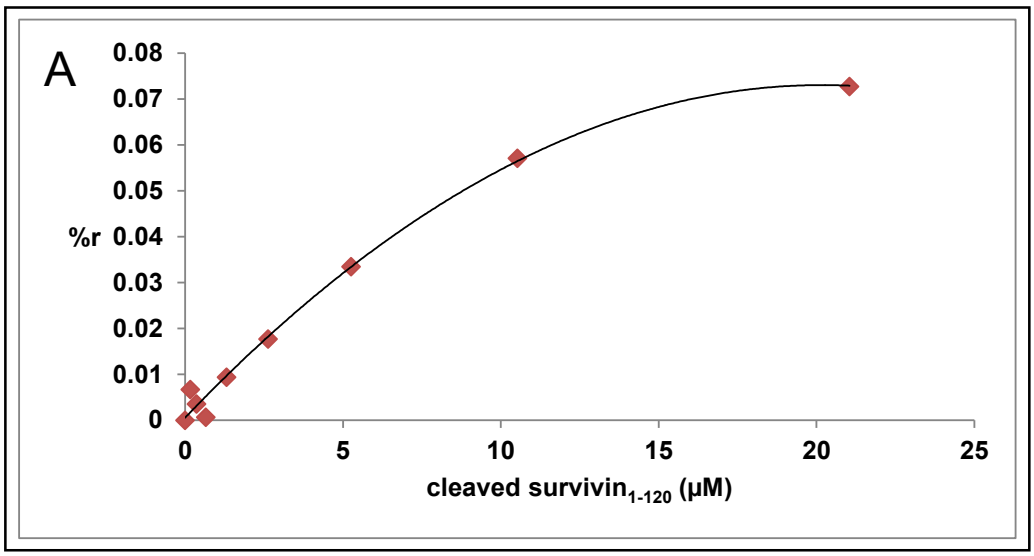

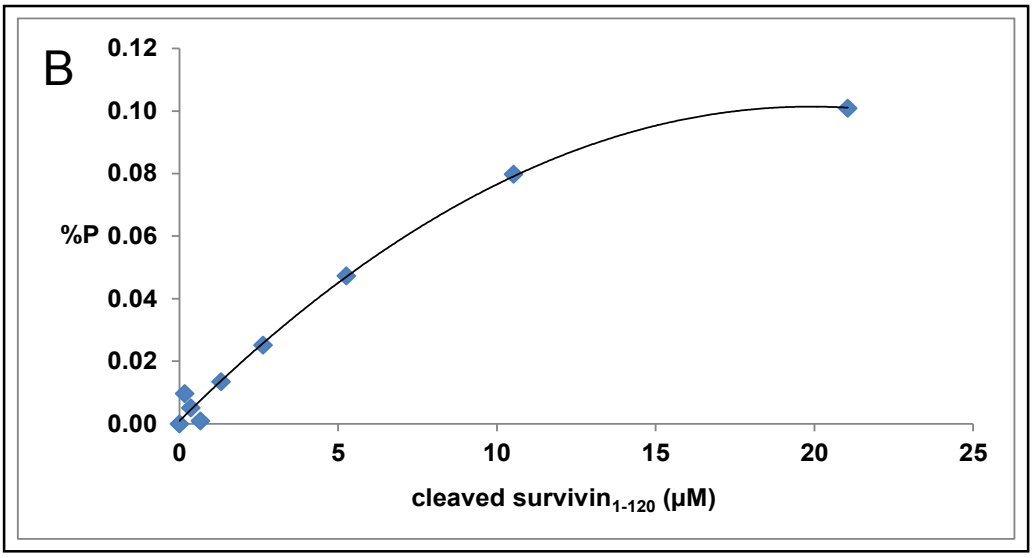

Figure 5.4: Percent fluorescence anisotropy (%r) (Panel A) and percent fluorescence polarization (%P) (Panel B) of thrombin-cleaved Survivin$_{1\text{-}120}$, in the presence of 100 nM fluorescein-labeled histone 3 peptide (H3*) in 100 mM potassium phosphate, pH 7.5, 100 µg/mL bovine gamma globulin, 0.02% (w/v) sodium azide. A: Percent fluorescence anisotropy (%r) with increasing concentration of thrombin-cleaved Survivin$_{1\text{-}120}$. B: Percent fluorescence polarization (%P) with increasing concentration of thrombin-cleaved Survivin$_{1\text{-}120}$. Fitted line is shown for reference only.

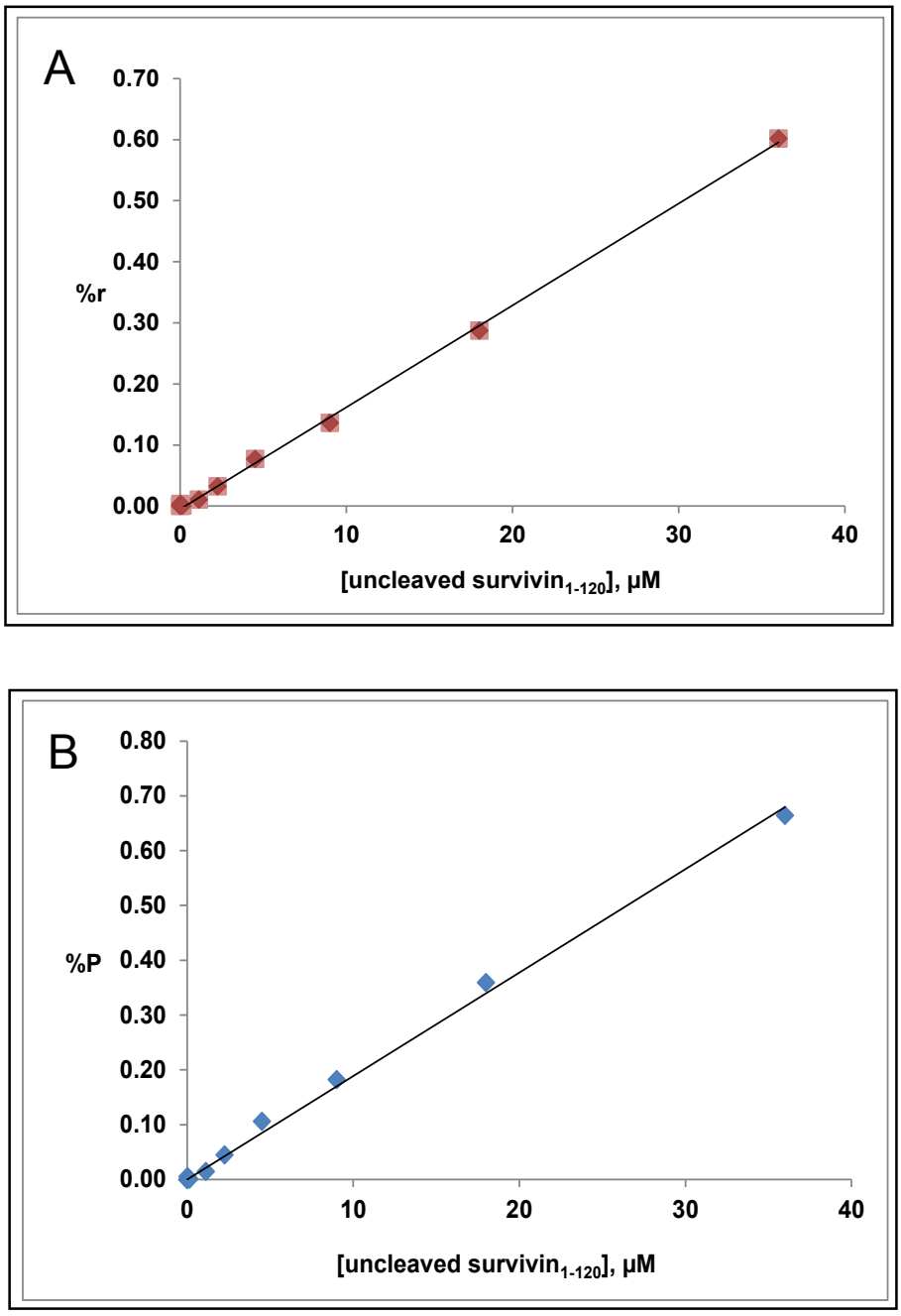

Figure 5.5: Percent fluorescence anisotropy (%r) (Panel A) and percent fluorescence polarization (%P) (Panel B) of uncleaved His_6-$Survivin_{1-120}$, in the presence of 100 nM fluorescein-labeled histone 3 peptide (H3*) in 100 mM potassium phosphate, pH 7.5, 100 µg/mL bovine gamma globulin, 0.02% (w/v) sodium azide. A: Percent fluorescence anisotropy (%r) with increasing concentration of uncleaved $Survivin_{1-120}$. B: Percent fluorescence polarization (%P) with increasing concentration of uncleaved $Survivin_{1-120}$. Line is only shown for reference purposes.

difficult to see a compelling trend of decreased fluorescence polarization with the addition of increased H3. In addition, the experiment included uncleaved Survivin$_{1\text{-}120}$, and as discussed previously, H3* may non-specifically bind uncleaved Survivin$_{1\text{-}120}$. Therefore, the conclusion that can be made from these results is that the experiment should be repeated using thrombin-cleaved Survivin$_{1\text{-}120}$.

Computational Screen Identifies Promising Survivin-Histone-3 Inhibitors

Computational screening of several hundred compounds using a Survivin conformation that binds histone-3 peptide was performed (Karanicolas Laboratory, University of Kansas, Lawrence, Kansas). Numerous compounds (Figure 5.7) were identified that bound Survivin at the Survivin-histone-3 binding interface. These compounds will be evaluated using the fluorescence polarization assay to determine if they displace histone-3 peptide from Survivin$_{1\text{-}120}$.

Identifying False Positives by Analyzing Candidate Inhibitor Propensity to Quench Fluorescence Polarization

As was described in chapter 1, the fluorescence polarization quantity is calculated using the instrument outputs of vertical and horizontal fluorescence intensities. Therefore, changes in fluorescence intensity, due to quenching, can alter the fluorescence polarization value. Quenching of fluorescence intensity can occur by a variety of processes. Non-radiative decay of the excited photon to the surrounding media can decrease fluorescence intensity. Because decreased fluorescence polarization can also result from disrupted protein-peptide binding, any compounds that

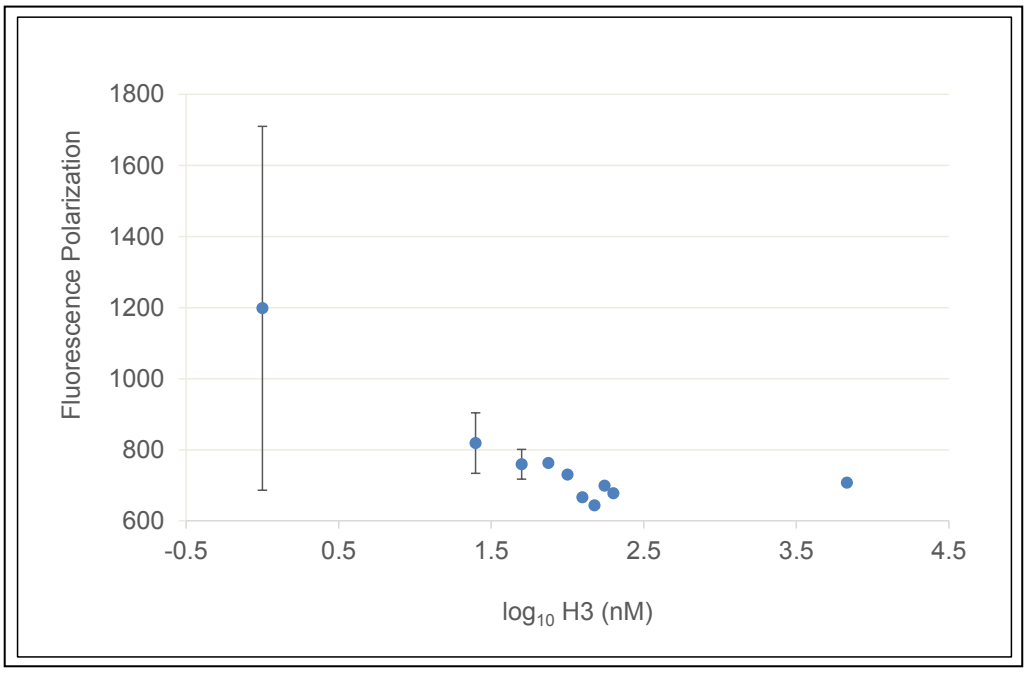

Figure 5.6: Fluorescence polarization (y-axis) as a function of increasing amounts of unlabeled histone-3 peptide (log nM, x-axis) added to 1 μM H3* and 30 μM uncleaved Survivin$_{1\text{-}120}$ to evaluate binding specificity of H3* for uncleaved Survivin$_{1\text{-}120}$.

Alias	Chemical name
JK15	5-[(1,3-benzothiazol-2-ylmethyl)sulfanyl]-4H-1,2,4-triazol-3-amine
JK16	1-[(1-phenyl-1,2,3,4-tetrazol-5-yl)methyl]-1,2,4-triazole-3-carbonitrile
JK18	1-methyl-4-[(3-phenyl-1H-pyrazol-4-yl)methyl]piperazine
JK19	2-amino-5-(4-chlorophenyl)-1,3-thiazole-4-carbohydrazide
JK20	4-(((3-(2-furyl)-5-mercapto-4H-1,2,4-triazol-4-yl)imino)methyl)phenol
JK21	6-[2-(1H-imidazol-4-yl)ethyl]-6,7-dihydro-5H-pyrrolo[3,4-b]pyridin-5-one

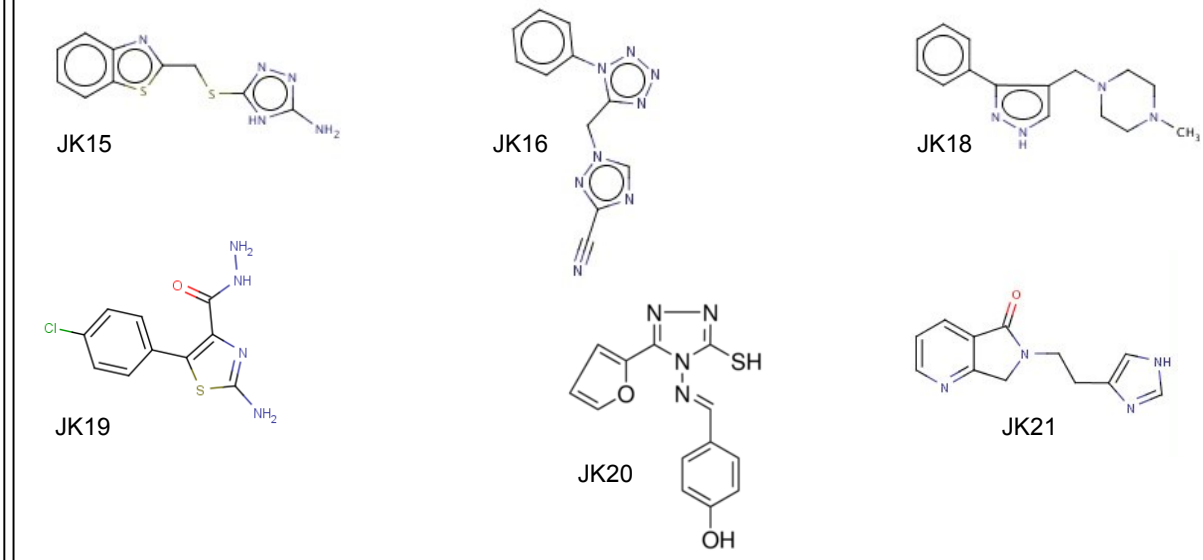

Figure 5.7: Candidate Survivin-histone-3 protein-protein interaction inhibitors identified by computational screening performed in the Karanicolas laboratory.

yield a decreased fluorescence signal would need to be evaluated for both their propensity to quench the fluorescence signal and their ability to disrupt protein-peptide binding, which may be completed in a secondary assay. Application of candidate inhibitors to the Survivin-histone-3 protein-peptide interaction may elicit decreased fluorescence polarization. Two interpretations of this outcome are possible. First, the candidate inhibitor displaces fluorescently-labeled histone-3 peptide from Survivin. Displaced fluorescently-labeled histone-3 peptide tumbles quickly and yields virtually no fluorescence polarization. Alternatively, the candidate inhibitor does not displace fluorescently-labeled histone-3 peptide from Survivin. Rather, the candidate inhibitor quenches the fluorescence signal of the fluorescently-labeled histone-3 peptide while it remains bound to Survivin protein. Consequently, the observed vertically and horizontally polarized fluorescence intensities are reduced and the ratio, the calculated fluorescence polarization value, approaches zero. This scenario represents the false positive, where the candidate did not displace the fluorescently-labeled peptide but the fluorescence polarization result suggested that the fluorescently-labeled histone-3 peptide was displaced from the Survivin protein. To rule out false positives, the candidate inhibitor is evaluated for its propensity to quench the fluorescence intensity of the fluorescently-labeled histone-3 labeled peptide, in the absence of Survivin. The experiment is performed by titrating increasing candidate inhibitor into a constant amount of fluorescently-labeled histone-3 peptide and monitoring fluorescence intensity of the labeled peptide. To evaluate the contribution of both vertically- and horizontally-polarized emission on the output of fluorescence polarization, it may be helpful to

determine the steady-state fluorescence intensities of the labeled peptide and candidate inhibitor, as well as the intensities using vertically- and horizontally-polarized light.

Identifying False Negatives by Analyzing Candidate Inhibitor Autofluorescence

In fluorescence polarization HTS, the drug candidate is tested at various concentrations. If the candidate does not decrease the observed percent fluorescence polarization, two explanations are possible. First, the candidate did not displace H3* from the Survivin protein, so the observed percent fluorescence polarization arises from the slowly tumbling, intact complex of H3* and Survivin. As an alternative, the candidate displaced H3* from the Survivin protein, but the candidate's fluorescence emission spectrum overlaps that of the monitored emission spectrum of H3*, so the observed percent fluorescence polarization arises from slowly tumbling candidate-bound Survivin protein. The second scenario represents the false negative where the candidate displaced H3*, but the fluorescence polarization result suggested that H3* still bound the Survivin protein. To analyze candidates for autofluorescence, the candidate compound's excitation and emission maxima should be determined in an experiment independent of the fluorescence polarization assay. It also may be beneficial to titrate increasing amounts of inhibitor to Survivin, alone, to evaluate increased percent fluorescence polarization in the absence of H3*.

Determination of Candidate Inhibitor IC_{50}

Candidates that 1) decrease fluorescence polarization 2) do not autofluoresce, and 3) do not quench H3* fluorescence will be further screened for their ability to disrupt

the Survivin:H3* binding interaction. The concentration of inhibitor that elicits half-maximal protein-peptide dissociation, IC_{50}, will be determined by titration of candidate inhibitor into constant Survivin-histone-3* using the fluorescence polarization screening assay.

Secondary Screen

To structurally characterize candidate molecule inhibition of His_6-$Survivin_{1-120}$:histone-3 peptide binding, nuclear magnetic resonance spectroscopy or x-ray crystallography experiments may be performed on ^{15}N-backbone-labeled thrombin-cleaved $Survivin_{1-120}$ or unlabeled thrombin-cleaved $Survivin_{1-120}$, respectively, with unlabeled histone 3 peptide, in the presence of the candidate inhibitor.

Our preliminary analyses using a cuvette-based fluorescence polarization platform indicated that H3* bound thrombin-cleaved $Survivin_{1-120,}$ however a dissociation contant should be determined from additional experiments with thrombin-cleaved $Survivin_{1-120}$. H3* bound uncleaved $Survivin_{1-120}$ apparently non-specifically. This cuvette-based finding regarding uncleaved $Survivin_{1-120}$ was corroborated in the plate fluorometer platform, where the polarization increased linearly with increased uncleaved $Survivin_{1-120}$ concentration. For this reason, conclusions made on histone-3 binding to uncleaved $Survivin_{1-120}$ regarding pH dependence, temperature, and DMSO content cannot be interpreted. Prior to screening to identify candidate inhibitors, these analyses will need to be repeated using thrombin-cleaved $Survivin_{1-120}$.

5.3 Conclusions

Fluorescence polarization-based screening presents advantages over other approaches for the identification of protein-protein interaction inhibitors, especially for non-enzymatic protein targets. The protein and peptide binding partner are combined in solution, rather than on a rigid substratum or via antibody-mediated recognition. In addition, the 96-well plate format utilizes relatively small sample volumes and relatively low protein concentrations compared to NMR or x-ray crystallography approaches, may be completed in a short period of time, can be optimized to yield sufficient signal:noise ratio, and can be performed at a variety of incubation temperatures as well as excitation and emission wavelengths different from those of naturally-occurring fluorophores. Several limitations and caveats, however, should be considered for the most conservative data interpretation, including that of non-specific fluorescently-labeled peptide binding and improper target protein folding within the experimental matrix. When considering these limitations and ruling out false positives and negatives, fluorescence polarization may be a useful method to identify candidate protein-peptide interaction inhibitors, presenting yet another avenue to bring therapeutics to the clinic for many human diseases.

Our objective was to establish a screening assay to identify inhibitors of the Survivin-histone-3 protein-peptide binding interaction. Herein is described the foundation for a fluorescence polarization assay for $Survivin_{1\text{-}120}$ and histone-3 peptide that can be used to evaluate candidate inhibitors identified by an *in silico* screen performed in the Karanicolas laboratory.

Chapter 6: Conclusions and Future Prospects

6.1 Introduction

Chapter 3 described efforts to utilize click chemistry to site-specifically label the Survivin protein with a fluorophore, with the ultimate goal of facilitating fluorescence-based protein-protein interaction studies of Survivin with its protein binding partners. Although the data described therein suggested that the fluorophore was adducted to the Survivin protein, additional analysis such as whole-protein mass spectrometry and tryptic digest followed by peptide mass spectrometry, could have augmented the data described in chapter 3. These and other suggestions are the subject of subsequent sections of this chapter.

Chapter 4 described efforts to synthesize a lanthanide chelator amenable to copper-free click chemistry, the ultimate goal of which was to expand the utility of protein structure-determination methods such as x-ray crystallography and nuclear magnetic resonance spectroscopy. Although fluorescence- and HPLC-based data described within chapter 4 suggest that synthesis of a clickable lanthanide chelator was successful, additional analyses that would corroborate this conclusion are described in subsequent sections of this chapter.

Chapter 5 concerned efforts to establish a fluorescence polarization assay to rapidly screen chemical libraries for the identification of candidate inhibitors of Survivin protein-protein interactions. Additional analyses may be considered as an alternative to the approaches described therein.

Collectively, although the methods described in chapters 3-5 may facilitate the development, through structure-aided design, or identification of small molecule inhibitor leads of selected protein targets, the proposed methods have limitations. The following

chapter will address whether or not the objectives of each specific aim were obtained, the limitations of the approaches proposed in preceding chapters, and additional strategies to overcome the methodological limitations of the proposed approaches.

6.2 Analyses to Evaluate Copper-free Click Chemistry Reaction Success with the Mutant Survivin Protein

Strategies to Confirm Mutant Survivin Protein Synthesis

Regarding the utility of copper-free click chemistry to site-specifically incorporate a fluorescent probe into the Survivin protein, DNA sequences of all seven plasmids encoding mutant Survivin genes with the amber stop codon were correct and all seven mutants yielded Survivin protein, as observed by western blotting (chapter 3, Figure 3.1). These results suggest that the translated $Survivin_{1\text{-}120}$ contained the unnatural amino acid paF, however, these results do not confirm inclusion of paF, nor do they provide information about the site of paF incorporation. Mass spectrometry could confirm that: 1) the Survivin protein contained the unnatural amino acid paF and 2) the copper-free click chemistry-mediated adduction of DBCO488 fluorophore to paF was site-specific.

The molecular weight of $His_6\text{-}Survivin_{1\text{-}120}$ (uncleaved Survivin) is 15978.0 Da and the cleaved product (14094.4 Da) was easily detected using Linear Trap Quadrupole-Fourier Transform (LTQ FT) mass spectrometry (chapter 5, Figure 5.2). Therefore, mass spectrometry could also be used to confirm that the $Survivin_{1\text{-}120}$ protein contained the unnatural amino acid paF. The seven paF-containing $Survivin_{1\text{-}120}$ mutants have following masses, and differences from the $His_6\text{-}Survivin_{1\text{-}120}$ mass, as outlined in Table

6.1. Insertions of paF at the N- and C-termini and mutations F93paF, F101paF, and G99paF elicit changes in mass that could be detected using LTQ FT mass spectrometry. The difference in mass of His_6-$Survivin_{1-120}$ and W10paF and W67paF, +1.975 Da, however, is more subtle. Using Thermo Electron Corporation's Finnegan LTQ FT instrument, which yields maximum resolution of 500,000 (FWHM) [Thermo Electron, 2003], it should be possible to detect a difference of 1.975 Da between tryptophan and paF, especially when evaluating peptide fragments instead of the whole protein mass spectrum shift. Therefore, tryptic digest may be performed on whole-protein W10paF or W67paF Survivin, and the resulting fragments evaluated to ascertain that positions 10 and 67 contain paF instead of tryptophan. These analyses could confirm site-specific incorporation of paF into the His_6-$Survivin_{1-120}$ protein.

As was described in chapter 2, BL21*DE3 *E. coli* expressing the unnatural amino acyl tRNA synthetase may occasionally insert arginine at the amber stop codon; compared to paF, arginine insertion would yield the following masses, which are smaller than the intended mutant mass by -32.0 Da (the difference between paF and arginine) (Table 6.2). As was discussed in chapter 2, this was the basis for selecting DH10B (TopTen) *E. coli* rather than BL21*DE3 *E. coli*.

Mutant	Mass (Da)	Difference from His_6-$survivin_{1-120}$ mass (Da)
NtermpaF, CtermpaF	16166.20	206.20
W10paF, W67paF	15979.98	1.98
F93paF, F101paF	16019.01	41.01
G99paF	15902.93	-75.07

Table 6.1: Masses of paF-containing His_6-$Survivin_{1-120}$ mutant proteins and differences from His_6-$Survivin_{1-120}$ mass.

Mutant	Mass (Da)
paFNtermR, paFCtermR	16134.20
paF10R, paF67R	15947.98
paF93R, paF101R	15987.01
paF99R	15870.93

Table 6.2: Mass differences between paF-containing His_6-$Survivin_{1-120}$ mutant proteins with arginine, rather than paF, incorporated at the amber stop codon.

A mass difference of 32.0 Daltons is detectable using LTQ FT mass spectrometry, and could be used to determine if arginine, instead of paF, was incorporated at the amber stop codon. The aforementioned approaches may address whether or not paF or arginine had been incorporated into the Survivin protein, in a site-specific manner.

Strategies to Confirm Copper-free Click Chemistry Reaction Success with Azide-Containing Survivin Protein

FPLC and fluorescence data suggested that the copper-free click chemistry reaction between N-terminal paF-containing His_6-$Survivin_{1-120}$ and DBCO488 was successful. To corroborate those data and to confirm that paF-containing His_6-$Survivin_{1-120}$ had been adducted with DBCO488, an aliquot of pure (Figure 3.12) uncleaved CtermpaF-DBCO488-$Survivin_{1-120}$ was submitted for mass spectrometry analysis (MS Bioworks, Ann Arbor, MI). Despite adequate sample purity, concentration, and preparation, satisfactory whole-protein mass spectrometry data were not obtained. Specifically, the MS Bioworks analyst had diluted the sample with 0.1% trifluoroacetic acid, which can suppress ionization [Balogh, 2009] and then indicated that the sample was of inadequate concentration and contained detergents and impurities, which was inconsistent with the sample preparation performed prior to shipment. In addition, the MS Bioworks analyst indicated that the sample was allowed to thaw at room temperature for 30 minutes, exposed to UV illumination, prior to analysis. These steps may have led to decomposition of the sample and/or photodestruction of the fluorophore prior to analysis. Therefore, LTQ FT mass spectrometry could be repeated using a

different collaborator or resource. The fluorescently-labeled construct would have a mass of 16818.26 Da, a difference of 840.26 Da from His_6-$Survivin_{1-120}$. Site-specific incorporation could be confirmed using tryptic digest followed by LTQ FT mass spectrometry.

Taken together, although the current findings indicate that Survivin gene sequences for insertion of paF were correct, Survivin protein was overexpressed, arginine incorporation was minimal, and fluorescence data suggest that a protein had been fluorescently labeled, the objectives of chapter 3, to site-specifically fluorescently label the Survivin protein, remain unconfirmed. Ascertaining that these objectives had been met would enable steady-state fluorescence intensity measurements of Survivin with histone-3 and fluorescence lifetime determinations of Survivin with histone-3 with more confidence than with the existing set of data and interpretations.

6.3 General Considerations for the Utility of Fluorescence-based Approaches to Evaluate Survivin Protein-Protein Interactions

As was described in chapter 3, fluorescence-based approaches including steady-state intensity, FRET, and fluorescence lifetime may be used to evaluate protein-protein interactions. Depending on the objective of the experiment, it may or may not be necessary to site-specifically fluorescently-label the protein of interest. When it is important to know the exact location of the fluorophore, site-specific labeling techniques such as genetic encoding or site-directed mutagenesis with unnatural amino acid incorporation followed by click chemistry may be utilized. Because the protein of interest is labeled with a fluorophore, considerations should be made in the placement

and size of the fluorophore, as well as of the excitation and emission maxima of endogenous fluorophores in the protein of interest, the fluorophore, and of any other fluorophores that may be present in the experimental assay buffer or biological matrix. If a relatively large fluorophore such as green fluorescent protein (GFP) is used, this may alter the conformation of the protein to which it is fused, which may prevent proper association of the target protein with its binding partner(s).

Additional considerations when selecting the fluorophore include fluorophore solubility, quantum yield, extinction coefficient, Stokes shift, factors that may affect its fluorescence lifetime (protonation state), and spectral overlap with potential donors and acceptors.

6.4 Label-Free Approaches to Evaluate Protein-Protein Interactions

Bio-Layer Interferometry

An alternative to fluorescence-based approaches to monitor protein-protein interactions is Bio-Layer Interferometry (BLI). This method relies on changes that occur in the interference pattern of white light upon protein binding. Briefly, target protein is immobilized on a biosensor tip; molecules that bind the target protein will cause a change in the interference pattern. These changes can be monitored as a wavelength shift. Some advantages of BLI are that measurements and output are in delivered real-time. Although labeling of the protein of interest is not a prerequisite for BLI experiments, a variety of different biosensor tips are available including nickel-NTA tips for analyzing His-tagged proteins. Each analysis uses a 4 microliter volume and because the platform rotates at 2000 rpm, the method is insensitive to changes in flow

rate and changes in the refractive index of the sample buffer. In addition, the sample may not be irreversibly damaged during analysis. A variety of analyses may be completed including identification of protein partner binding, identification of candidate protein-protein interaction inhibitors, and protein partner binding affinity. Given the difficulty obtaining sufficient quantities of thrombin-cleaved Survivin protein and the advantages with BLI, it may be worthwhile to pursue BLI for the high-throughput screening of candidate Survivin-histone-3 protein-protein interaction inhibitors.

Limitations of BLI include that the protein of interest may bind the tip in a conformation that is not physiologically relevant. This could be assessed using a variety of different BLI tips and considering the use of a labeled protein target (such as a His_6-tag and nickel-NTA BLI tip), positioning the label such that it would not hamper the target protein's folding and conformation, and altering the concentrations of target protein used in each experiment. In addition, non-specific binding of proteins to the BLI tip is also possible. To evaluate the specificity of protein target binding to the tip, antibodies against the protein target may be applied, the specificity of which should already be known (evaluated by western blotting, for example): binding of the antibody to the protein on the BLI tip will elicit a shift in the interference pattern. If the antibody does not bind the tip, this may suggest that the protein of interest is not bound to the BLI tip. An alternative interpretation is that the antibody does not recognize the protein in the conformation that binds the tip, either because the target protein is improperly folded or the interface to which the antibody binds is obscured by a tag or by binding to the BLI tip. Regarding the experimental conditions, the amount of salt and/or detergent should be considered in the buffer. For protein-protein interactions that are governed by

electrostatics, such as that between Survivin, borealin, and inner centromere protein (INCENP) [Jeyaprakash, *et al.,* 2007], salt content similar to that found in the intracellular mileu, ~150 mM [Lodish, 1999], would be ideal. Excess salt within the buffer would likely interfere with Survivin binding borealin and INCENP.

6.5 Analyses to Evaluate Clickable Chelator Synthesis

Chapter 4 described efforts to synthesize a small molecule clickable lanthanide chelator. Fluorescence-based and HPLC approaches yielded preliminary data that suggested that synthesis was successful, however, additional analyses are warranted. Specifically, small-molecule mass spectrometry data yielded peaks that corresponded to the clickable chelator as well as to the product of the copper-free click chemistry reaction between the clickable chelator and paF, the clicked chelator, however, the data contained many unassigned fragment peaks as well as substantial peaks from the matrix blanks, which precluded unequivocal assignment of the matrix and experimental sample peaks. In order to obtain more reliable small-molecule mass spectrometry data, several strategies could be pursued, as described below.

The current HPLC separation method utilized trifluoroacetic acid, which can suppress ionization [Balogh, 2009]. Potentially, replacement of trifluoroacetic acid with formic acid in the HPLC separation may improve mass spectrometry detection of the clickable chelator. In addition, using the C18 stationary phase and the existing method (chapter 2), the clicked chelator exhibited a retention time of approximately 6 minutes and the clickable chelator exhibited a retention time of approximately 7 minutes. Increasing the difference between these two species' retention times could improve

collection of single fractions containing each species; fractions submitted for mass spectrometry would then contain single species. Strategies to increase the difference between these two species' retention times may include varying the gradient, using a stepwise gradient, and/or altering the composition of the mobile phases used for separation. If satisfactory separation is not achieved using the C18 stationary phase, it may be possible to utilize a different stationary phase such as phenyl (Ascentis, Sigma).

In addition to modifications in the HPLC separation and fraction collection techniques, alternatives may be pursued in the choice of small-molecule mass spectrometry used. Compared to matrix-assisted laser desorption/ionization (MALDI), electrospray ionization (ESI) is more sensitive for studying molecules ~1 kD and smaller. Therefore, it may be beneficial to analyze the submitted fractions and samples by ESI.

An additional piece of information that would improve peak assignment of the clickable chelator is the mass spectra of DTPA and metallated DTPA. Using MALDI, terbium-metallated DTPA yielded convoluted mass spectrometry data, with multiple peaks present and uncertainty regarding whether or not terbium remained chelated during analysis. ESI mass spectrometry analysis of DTPA with and without terbium may yield improved mass spectrometry data. In addition, mass spectrometry data obtained on DTPA metallated with different lanthanides may yield fragmentation patterns that provide insight on whether or not DTPA remains metallated during analysis. The peak assignments that would result from these experiments may help peak assignments from analysis of the clickable chelator. Possible outcomes of mass

spectrometry analysis of DTPA:lanthanide are based on the protonation state of DTPA and the masses of the chelated lanthanides:

Unmetallated DTPA has a single pKa, at 1.8 [Moeller and Thompson, 1962]. DTPA chelates lanthanide at a 1:1 molar stoichiometry [Moeller and Thompson, 1962] and metallation of DTPA with lanthanide yields 5 distinct pKa, 1.80, 2.55, 4.33, 8.60, and 10.58 [Moeller and Thompson, 1962]. At a pH of 5.5, at which the metallation and syntheses were performed (chapter 4), metallated DTPA would fluctuate between two species, carrying -3 or -4 charge. The mass of fully protonated DTPA is 393.35 Da, so the masses of $DTPA^{-3}$ and $DTPA^{-4}$ are 390.35 and 389.35 Da, respectively. The mass of terbium is 158.93 Da. Therefore, the mass of metallated DTPA would be 552.28 Da (Table 6.3). If terbium becomes dissociated during analysis and DTPA accepts a proton, other combinations of masses may be possible, as indicated. If mass spectrometry yields a peak at 549.28 Da, this may suggest that the DTPA:Tb complex is intact. If the mass spectrometry yields peaks at 158.93 Da and 390.35 Da, this may suggest that the lanthanide became unbound during ionization. The mass of europium is 151.96 Da, so metallation of $DTPA^{-3}$ with europium would yield a mass of 542.31 Da. If mass spectrometry of europium-metallated DTPA yields peaks at 151.96 Da and 390.35 Da, this would corroborate the conclusion with terbium-metallated DTPA that the lanthanide becomes unbound during analysis. A fragmentation event within the DTPA molecule may also yield peaks of different masses depending on whether or not the lanthanide remains chelated during analysis. These and other interpretations should be considered if additional mass spectrometry analyses are performed. Ultimately, it will be important to fully utilize the available mass spectrometry opportunities to determine

whether or not the synthesis of the clickable chelator and clicked chelator were successful.

In addition, NMR analyses to evaluate the structure of the clickable chelator in a paF-containing ^{15}N-backbone-labeled Survivin$_{1\text{-}120}$ protein may provide additional information on copper-free click chemistry reaction success between the clickable chelator and paF-containing Survivin$_{1\text{-}120}$.

Taken together, the objectives of the efforts described in chapter 4 aimed to synthesize, using a two-step, aqueous synthesis, a small-molecule lanthanide chelator amenable to copper-free click chemistry-mediated incorporation into the target protein. Although the fluorescence and HPLC data suggested that the small-molecule chelator was synthesized and that the copper-free click chemistry reaction between the clickable chelator and the small-molecule paF were successful, the small-molecule mass spectrometry data were inconclusive. In addition, the clickable chelator has yet to be incorporated into a paF-containing Survivin$_{1\text{-}120}$ protein and NMR experiments are remaining, therefore the objectives of the aims described in chapter 4 were unmet.

DTPA	Mass (Da)	Terbium Mass (Da)	Complex Mass (Da)	Europium Mass (Da)	Complex Mass (Da)
uncharged	393.35	158.93	552.28	151.96	545.31
$DTPA^{-1}$	392.35	158.93	551.28	151.96	544.31
$DTPA^{-2}$	391.35	158.93	550.28	151.96	543.31
$DTPA^{-3}$	390.35	158.93	549.28	151.96	542.31
$DTPA^{-4}$	389.35	158.93	548.28	151.96	541.31

Table 6.3: Masses of uncharged and charged DTPA species, terbium, europium, and of different DTPA species metallated with terbium or europium.

6.6 Considerations for the Utility of Lanthanide Chelation in NMR Structure Determination

Optimizing Lanthanide Chelator Insertion

Chapter 3 describes the use of the unnatural amino acyl tRNA synthetase to facilitate site-specific incorporation of the unnatural amino acid paF. Optimization of the *Methanococcus jannaschii* (Chapter 2) bacterium, which encodes the tRNA synthetase, to modify unnatural amino acid recognition and retrieval has already been demonstrated for over seventy unnatural amino acids [Wang, *et al.*, 2006, Xie, *et al.*, 2007, Brustad, *et al.*, 2008, Lee and Schultz, 2008]. Therefore, it may be possible to optimize insertion of the clicked lanthanide chelator (clicked chelator) into the protein of interest. First, the clicked chelator synthesis and purification is completed *ex vivo*. Next, translation of the protein of interest is performed in an *Escherichia coli* culture in the presence of the *M. jannaschii* tRNA synthetase that retrieves the clicked chelator, with clicked chelator added to the incubation medium. This yields a protein with site-specific incorporation of the lanthanide chelator. Using this strategy negates the need to perform copper-free click chemistry on the protein of interest, minimizing the risk of non-specific incorporation of the chelator to the protein. If the tRNA synthetase can differentially select one stereoisoform of the clicked chelator, an additional advantage could also be that only one stereoisomer of the clicked chelator is retrieved for incorporation into the growing polypeptide chain. To determine whether or not the clicked chelator may cross the bacterial membrane, fluorescence analyses may be performed on lysed bacterium to ascertain the presence of the clicked chelator, which possesses fluorescence emission unique from that of the culture medium and bacterium.

One drawback to this proposed genetic incorporation of the clicked chelator, however, is that the clicked chelator is approximately 1 kD and contains an incompressible moiety in the DTPA chelation of terbium, so the ribosome peptidyl transferase center and amino acyl tRNA synthetase would need to be large enough to accommodate the clicked chelator. The risk of this approach is that many antibiotics including erythromycin (733.93 g/mol), telithromycin (812.03 g/mol), clindamycin (504.96 g/mol), and chloramphenicol (323.13 g/mol) are small molecules that block nascent polypeptide translocation through the bacterial ribosomal peptidyl transferase center or block the exit tunnel of the 50S ribosomal subunit [Dunkle, *et al.*, 2010]. Using ChemDraw, the clicked chelator structure was rendered using correct bond angles and lengths (Figure 4.1); the approximate length of the clicked chelator that extends perpendicularly from the polypeptide backbone is 13 Å. The approximate length from the central nitrogen in the triazole moiety to the carboxylic acids chelating the terbium is 24.5 Å. The approximate circumference of the chelated terbium is 33.8 Å. Because the chelator moiety of the 1 kD clicked chelator is incompressible, the clicked chelator may not traverse the peptidyl transferase center without inhibiting polypeptide synthesis.

Another consideration for this proposed approach is that it is not yet known whether or not the tRNA synthetase active site could accommodate the 1 kD size of the clicked chelator. Optimization of the tRNA synthetase using degenerate primers and efforts used to incorporate the over seventy unnatural amino acids already published [Wang, *et al.*, 2006, Xie, *et al.*, 2007, Brustad, *et al.*, 2008, Lee and Schultz, 2008] may be applied to optimization of the tRNA synthetase to accommodate the large size of the clicked chelator, however 1 kD may be beyond the capacity of the synthetase to

simultaneously 1) recognize and recruit the clicked chelator while 2) retaining ATP-mediated charging of the tRNA with the clicked chelator. For these reasons, it may be prudent to consider incorporation of a smaller unnatural amino acid.

It is appealing to consider truncating the clicked chelator to a smaller molecule that still retains the ability to 1) chelate lanthanide and 2) be incorporated site-specifically into the protein backbone. This may be accomplished by incorporating a portion of the clicked chelator as an unnatural amino acid. In this context, the smallest possible unit may be DTPA:Tb with the central carboxylic acid modified to an amide bond; this would facilitate incorporation into the growing polypeptide chain as the amino acid side chain is the DTPA:Tb construct. This amidated DTPA:Tb construct thus becomes an unnatural amino acid. Subsequently, tRNA synthetase optimization is performed using degenerate primers, as has been previously done with other unnatural amino acids [reviewed in Liu and Schultz, 2010] to generate a tRNA that retrieves the amidated DTPA:Tb lanthanide chelator for ribosomal insertion into the growing polypeptide chain.

Regarding the possibility of unnatural amino acid-mediated direct incorporation of the lanthanide chelator into the target protein during translation, our analyses indicate that the clickable chelator retains terbium fluorescence during purification, suggesting that terbium remains chelated during synthesis and purification. It is not known, yet, if terbium would remain chelated during protein translation or if it would be toxic to the bacterial culture. Analysis of the fluorescence of the protein after overexpression and purification would yield information about whether or not terbium remained chelated during translation. In addition, fluorescence and mass spectrometry analyses of the

resulting protein could yield information about whether or not the chelator had been incorporated with and without terbium.

These two strategies facilitate direct incorporation of a small-molecule lanthanide chelator into the protein of interest. They also negate the need to perform copper-free click chemistry on the protein of interest.

Optimizing Chelator Rigidity

Regarding lanthanide chelation, for NMR-based analyses, it is critical for the chelator to rigidly chelate the lanthanide to orient pseudocontact chemical shifts. One strategy to facilitate rigid chelation is that of "caged" lanthanide incorporation, as was demonstrated with a DTPA derivative and cysteine reactivity [Prudêncio, *et al.*, 2004]. This approach, however, does not address the issue of non-specific cysteine reactivity and the potential consequences of cysteine insertion or mutation on the target protein's tertiary structure. Therefore, it may be beneficial to consider other alternatives.

One strategy to incorporate a rigid chelator is to synthesize a chelator that contains bonds with low degrees of rotation. To date, such a molecule does not yet exist that can be site-specifically incorporated into the protein of interest. To fully harness lanthanide chelation and the pseudocontact chemical shift perturbation for structure determination, incorporation of a rigid small molecule lanthanide chelator without perturbing protein backbone or secondary structure is necessary; these properties may be mutually exclusive.

The aforementioned strategies describe optimization of lanthanide incorporation for NMR-based structural analyses. Lanthanides may also be employed for

fluorescence-based analyses. The potential utility of lanthanide chelation in high-throughput rational screening may also be considered.

6.7 Lanthanide Chelation for Fluorescence Polarization-based Rational Screening

Chapter 5 described the utility of fluorescence polarization-based rational screening to identify promising therapeutic candidates. Currently, peptide binding partners of the protein target may be commercially synthesized and may include fluorophores such as carboxyfluorescein. An alternative approach would be to synthesize peptides containing the unnatural amino acid paF, then perform copper-free click chemistry to adduct the clickable chelator to the peptide. This process would yield a peptide containing site-specific lanthanide incorporation, which could then be utilized in fluorescence polarization-based screening analyses. An additional application would be NMR-based protein-protein interaction studies where the lanthanide-labeled peptide is titrated into the ^{15}N-backbone-labeled protein of interest to evaluate consequences of titration of peptide on target protein structure; these complementary approaches, fluorescence polarization and NMR, would yield valuable information with streamlined effort because the same proteins could be evaluated in multiple approaches. Candidate molecules identified using fluorescence polarization may be applied to the protein in NMR-based structural analyses. These NMR analyses could provide structural information about candidate inhibitor binding to disrupt the protein-peptide interaction from the fluorescence polarization screen.

Limitations of Fluorescence Polarization to Identify Candidate Protein-Peptide Interaction Inhibitors

Although fluorescence polarization-based analyses can be utilized to identify candidate protein-peptide interaction inhibitors and offers many advantages to alternative approaches, the methodology is not without limitation. In addition to correcting for false positives and negatives, which add additional samples and expense, it may be difficult to procure pure protein in a physiologically-relevant conformation, in concentrations amenable to optimal signal:noise ratio of the experiment. In addition, although it may be possible to monitor fluorescence of endogenous amino acids such as tryptophan, tyrosine, or phenylalanine in the peptide binding partner, these amino acids are likely present in the protein target as well, thereby precluding use of these amino acids' fluorescence properties in fluorescence polarization. An alternative to endogenous fluorophores in fluorescence polarization is exogenous fluorophores such as carboxyfluorescein, which can be incorporated during synthesis of synthetic peptides. Peptide synthesis with and without fluorophore labeling can be quite expensive, costing thousands of dollars for approximately 15-amino acid-long peptides. As with other techniques that require labels, insertion or incorporation of a fluorophore into the peptide sequence may interfere with binding of the peptide to the protein target, so it is important to consider the location of the fluorophore within the peptide during synthesis and the potential consequences of peptide binding the protein target.

Finally, the objectives of the experiments described in chapter 5, to establish a fluorescence-polarization-based high-throughput screening assay of candidate Survivin-histone-3 protein-protein inhibitors, were unmet. Specifically, analyses described in

chapter 5 to determine fluorescently-labled histone-3 peptide dissociation constant, binding specificity, and effect of DMSO, temperature, and pH used His_6-$Survivin_{1-120}$, but it was determined that fluorescently-labeled histone-3 peptide bound His_6-$Survivin_{1-120}$ non-specifically. It will also be important to evaluate the incubation time of the assay. In order to establish the HTS platform, the experiments may be performed using thrombin-cleaved $Survivin_{1-120}$.

6.8 Summary and Conclusions

Fluorescence-based approaches including steady-state intensity, FRET, and fluorescence lifetime analyses to evaluate protein-protein interactions are useful indicators of local fluorophore environment. An appreciation for each approach's limitations and advantages is imperative for proper data interpretation; used correctly, fluorescent labeling of a protein of interest can be a useful technology that facilitates study of protein-protein interactions. To this end, fluorescent labeling of the Survivin protein, an important anti-cancer target, was achieved coupling site-directed mutagenesis, unnatural amino acid insertion, and copper-free click chemistry. These low-resolution fluorescence-based approaches may provide information about the fluorophore local environment that may complement structure determination methods such as x-ray crystallography and nuclear magnetic resonance spectroscopy.

Expanding the utility of x-ray crystallography and NMR using lanthanide chelation is promising. Current small-molecule lanthanide chelators originate from multi-step-organic syntheses that yield cysteine-reactive and other types of chelators that may or may not be site-specifically incorporated into the protein of interest. Described in

chapter 4 is the 2-step aqueous synthesis of a small-molecule lanthanide chelator amenable to copper-free click chemistry-mediated site-specific incorporation into the Survivin protein. Described within chapter 5 is a fluorescence polarization-based platform amenable to high-throughput screening of candidate protein-peptide interaction inhibitors.

The efforts of the experiments described in chapter 3 aimed to site-specifically label the Survivin protein with a fluorescent tag using copper-free click chemistry. Outstanding analyses include confirming synthesis of the paF-containing Survivin protein and the fluorescently-labeled Survivin protein using mass spectrometry. Also outstanding are experiments determining the steady-state fluorescence intensity and fluorescence lifetimes of fluorescently-labeled Survivin with its binding partners. The efforts of the experiments described in chapter 4 aimed to synthesize, using two steps and aqueous conditions, a small-molecule lanthanide chelator amenable to site-specific copper-free click chemistry-mediated incorporation into the Survivin protein. The goals of the aim were unmet as the small-molecule mass spectrometry experiments need to be repeated to confirm synthesis of the chelator. Additional outstanding experiments include clicking the chelator into a paF-containing Survivin protein and performing NMR experiments on Survivin with its binding partners. Finally, the goals of the experiments described in chapter 5 aimed to establish a high-throughput fluorescence polarization screening assay to identify putative inhibitors of the Survivin-histone-3 protein-protein interaction. The goals were unmet as the outstanding experiments include establishing fluorescence polarization assay robustness using thrombin-cleaved $Survivin_{1\text{-}120}$ then performing the screening experiments.

Collectively, the efforts described herein were undertaken to springboard improved structure-aided drug design and rapid identification of therapeutic candidate molecules. Although the protein target described within this dissertation, Survivin, is a promising anti-cancer target, the efforts to evaluate protein-protein interactions using these approaches could be applied to many different protein targets. Targeting protein-protein interactions is a promising strategy to expand therapeutic opportunities against proteins that are non-enzymatic and involved in many different intracellular pathways. Therefore, the efforts described herein have potential to expand therapeutic targeting beyond those of conventional approaches, offering hope for treatment of many human and animal diseases.

References

Adrain, C., Creagh, E. M., Martin, S. J., Apoptosis-associated release of Smac/DIABLO from mitochondria requires active caspases and is blocked by Bcl-2, *EMBO J.*, **2001**, 20, 6627 – 6636.

Alcala, J. R., Gratton, E., Prendergast, F. G., Fluorescence Lifetime Distributions in Proteins, *Biophys. J.,* **1987**, 51, 597 – 604.

Allen, K. N., Imperiali, B., Lanthanide-tagged proteins -- an illuminating partnership, *Curr. Opin. Chem. Biol*., **2010**, 14, 247 – 254.

Allen, J. E., McLendon, G. L., Tryptophan and tyrosine to terbium fluorescence resonance energy transfer as a method to “map” aromatic residues and monitor docking, *Biochemical and Biophysical Research Communications,* 2006, 349, 1264 – 1268.

Almeida, R. M., Geraldes, C. F. G. C., Pauleta, S. R., Moura, J. J. G., Gd(III) Chelates as NMR Probes of Protein-Protein Interactions. Case Study: Rubredoxin and Cytochrome c_3, *Inorg. Chem.*, **2011**, 50, 10600 – 10607.

Altieri, D., The molecular basis and potential role of Survivin in cancer diagnosis and therapy, *TRENDS in Molecular Medicine,* **2001**, 7, 12, 542 – 547.

Altieri, D., Survivin, cancer networks and pathway-directed drug discovery, *Nature Reviews*, **2008**, 8, 61 – 70.

Altieri, D., Marchisio, P. C., Lab. Invest., **1999**, 79, 1327 – 1333.

Ambrosini, G., Adida, C., Altieri, D., A novel anti-apoptosis gene, *Survivin*, expressed in cancer and lymphoma, *Nature Medicine*, **1997**, 3, 917 – 921.

American Cancer Society, Cancer Facts & Figures 2014, Atlanta: American Cancer Society; **2015**.

Arkin, M. R., Wells, J. A., Small-molecule inhibitors of protein-protein interactions: progressing towards the dream, *Nature Reviews Drug Discovery*, **2004**, 3, 301 – 317.

Balogh, M., The Mass Spectrometry Primer, Waters Corporation, **2009**, Milford, MA.

Beechem, J., Brand, L., Time resolved fluorescence decay in proteins. *Annu. Rev. Biochem*., **1985**, 54, 43 – 71.

Berezin, M. Y., and S. Achilefu, Fluorescence Lifetime Measurements and Biological Imaging, *Chem. Rev.*, **2010**, 110, 2641 – 2684.

Bertini, I., Luchinat, C., NMR of Paramagnetic Substances, *Coord. Chem. Rev.*, **1996**, 150, 77 – 110.

Bertini, I., Luchinat, C., Parigi, G., Paramagnetic constraints: An aid for quick solution structure determination of paramagnetic metalloproteins, *Concepts in Magnetic Resonance*, **2002**, 14, 259 – 286.

Bertini, I., Luchinat, C., Parigi, G., Solution NMR of Paramagnetic Molecules, *Current Methods in Inorganic Chemistry, V.2,* **2011***,* Elsevier Science Serials, 1 – 372.

Bertini, I., Luchinat, C., Piccioli, M., *Methods Enzymol*., **2001**, 339, 314.

Bloembergen, N., Morgan, L. O., Proton Relaxation Times in Paramagnetic Solutions. Effects of Electron Spin Relaxation, *J. Chem. Phys*., **1961**, 34, 842.

Branden, C., Tooze, J., Introduction to Protein Structure, 2nd Ed., Garland Publishing, Inc., New York, **1998**.

Brannon, J. H., Magde, D., Absolute Quantum Yield by Thermal Blooming. Fluorescein, *J. Physical Chemistry*, **1978**, 82, 705 – 709.

Brittain, H. G., Richardson, F. S., Martin, R. B., Terbium(III) emission as a probe of calcium(II) binding sites in proteins, *J. Am. Chem. Soc.*, **1976**, 98, 8255.

Brooker, L. G. S., Keyes, G. H., Sprague, R. H., VanDyke, R. H., VanLare, E., VanZandt, G., White, F. L., Studies in the Cyanine Dye Series. XI. The Merocyanines, *Journal of the American Chemical Society*, **1951**, 74, 5350.

Brustad, E., Bushey, M. L., Brock, A., Chittuluru, J., Schultz, P. G., A promiscuous aminoacyl-tRNA synthetase that incorporates cysteine, methionine, and alanine homologs into proteins, *Bioorganic & Medicinal Chemistry Letters,* **2008**, 18, 6004 – 6006.

Cacheris, W. P., Nickle, S. K., Sherry, A. D., Thermodynamic Study of Lanthanide Complexes of 1,4,7-Triazacyclononane-*N,N',N''*-triacetic Acid and 1,4,7,10-Tetraazacyclododecane-*N,N',N'',N'''*-tetraacetic Acid, *Inorg. Chem.*, **1987**, 26, 958 – 960.

Carmena, M., Wheelock, M., Funabiki, H., Earnshaw, W. C., The chromosomal passenger complex (CPC): from easy rider to the godfather of mitosis, *Nat. Rev. Mol. Cell Biol.,* **2012**, 13, 789 – 803.

Carvalho, A., Carmena, M., Sambade, C., Earnshaw, W. C., Wheatley, S. P., Survivin is required for stable checkpoint activation in taxol-treated HeLa cells, *J. Cell Science,* **2003**, 14, 2987 – 2998.

Chai, J., Du, C., Wu, J., Kyln, S., Wang, X., Shi, Y., Structural and biochemical basis of apoptotic activation by Smac/DIABLO, *Nature*, **2000**, 406, 855 – 862.

Chantalat, L., Skoufias, D. A., Kleman, J-P., Jung, B., Dideberg, O., Margolis, R. L., Crystal Structure of Human Survivin Reveals a Bow Tie-Shaped Dimer with Two Unusual α-Helical Extensions, *Molecular Cell*, **2000**, 6, 183 – 189.

Cheung, C. H. A., Chen, H-H., Kuo, C-C., Chang, C-Y., Coumar, M. S., Hsieh, H-P., Chang, J-Y., Survivin counteracts the therapeutic effect of microtubule de-stabilizers by stabilizing tubulin polymers, *Molecular Cancer,* **2009**, 8, 43, 1-15.

Chin, J. W., Santoro, S. W., Martin, A. B., King, D. S., Wang, L., Schultz, P. G., Addition of *p*-Azido-L-phenylalanine to the genetic code of Escherichia coli, *JACS communications*, **2002**, 124, 9026 – 9027.

Clore, G. M., Iwahara, J., Theory, practice, and applications of paramagnetic relaxation enhancement for the characterization of transient low-population states of biological macromolecules and their complexes, *Chem. Rev.*, **2009**, 109, 4108 – 4139.

Clore, G. M., Tang, C., Iwahara, J., *Curr. Opin. Struct. Biol*., **2007**, 17, 603.

Condon, S. M., The discovery and development of Smac mimetics – small-molecule antagonists of the inhibitor of apoptosis proteins, *Annual Reports in Medicinal Chemistry*, **2011**, 46, 211 – 226.

D'Abramo, C. M., Archambault, J., Small Molecule Inhibitors of Human Papilloma Virus – Protein Interactions, *Open Virol. J.,* **2011**, 5, 80 – 95.

DAS6 Fluorescence Decay Analysis Software User's Guide, Part Number J81119 ver. E, HORIBA Jobin Yvon IBH.

Deiters, A., Schultz, P. G., In vivo incorporation of an alkyne into proteins in *Escherichia coli, Bioorganic and Medicinal Chemistry Letters,* **2005**, 15, 1521 – 1524.

Deveraux, Q. L., Roy, N., Stennicke, H. R., Van Arsdale, T., Zhou, Q., Srinivasula, S. M., Alnemri, E. S., Galvesen, G. S., Reed, J. C., IAPs block apoptotic events induced by caspase-8 and cytochrome *c* by direct inhibition of distinct caspases, *The EMBO Journal*, **1998**, 17, 2215 – 2223.

Du, C., Fang, M., Li, Y., Li, L., Wang, X., Smac, a mitochondrial protein that promotes cytochrome c-dependent caspase activation by eliminating IAP inhibition, *Cell*, **2000**, 102, 33 – 42.

Dunkle, J. A., Xiong, L., Mankin, A. S., Cate, J. H. D., Structures of the *Escherichia coli* ribosome with antibiotics bound near the peptidyl transferase center explain spectra of drug action, *Proc. Natl. Acad. Sci.*, *U.S.A.,* **2010**, 107, 17152 – 17157.

Förster, T., Zwischenmolekulare Energiewanderung und Fluoreszenz [Intermolecular energy migration and fluorescence], *Annalen der Physik* (in German), **1948**, 437, 55 – 57.

Franz, K. J., Nitz, M., Imperiali, B., Lanthanide-Binding Tags as Versatile Protein Coexpression Probes, *ChemBioChem*, **2003**, 4, 265 – 271.

Ge, P., Selvin, P. R., Thiol-Reactive Luminescent Lanthanide Chelates: Part 2, *Bioconjugate Chem.,* **2003**, 14, 870 – 876.

Ghisaidoobe, A. B. T., Chung, S. J., Intrinsic Tryptophan Fluorescence in the Detection and Analysis of Proteins: A Focus on Förster Resonance Energy Transfer Techniques, *Int. J. Mol. Sci*, **2014**, 15, 22518 – 22538.

Giaccone, G., Zatloukal, P., Roubec, J., Floor, K., Musil, J., Kuta, M., van Klaveren, R. J., Chaudhary, S., Gunther, A., Shamsili, S., Multicenter Phase II Trial of YM155, a Small-Molecule Suppressor of Survivin, in Patients with Advanced, Refractory, Non-Small-Cell Lung Cancer, *Journal of Clinical Oncology*, **2009**, 27, 4481 – 4486.

Giodini, A., Kallio, M. J., Wall, N. R., Gorbsky, G. J., Tognin, S., Marchisio, P. C., Symons, M., Altieri, D., Regulation of Microtubule Stability and Mitotic Progression by Survivin, *Cancer Research*, **2002**, 62, 2462 – 2467.

Glover, C. J., Hite, K., DeLosh, R., Scudiero, D. A., Fivash, M. J., Smith, L. R., Fisher, R. J., Wu, J., Shi, Y., Kipp, R. A., McLendon, G. L., Sausville, E. A., Shoemaker, R. H., A high-throughput screen for identification of molecular mimics of Smac/DIABLO utilizing a fluorescence polarization assay, *Analytical Biochemistry*, **2003**, 320, 157 – 169.

Gordon, C. G., Mackey, J. L., Jewett, J. C., Sletten, E. M., Houk, K. N., Bertozzi, C. R., Reactivity of biarylazacyclooctynones in copper-free click chemistry, *Journal of the American Chemical Society,* **2012**, 134, 9199 – 9208.

Gribbon, P., Sewing, A., Fluorescence readouts in HTS: no gain without pain?, *Drug Discovery Today,* **2003**, 8, 1035 – 1043.

Groner, B., Weiss, A., Targeting Survivin in Cancer: Novel Drug Development Approaches, *BioDrugs*, **2014**, 28, 27 – 39.

Guéron, M., Nuclear relaxation in macromolecules by paramagnetic ions: a novel mechanism, *J. Magn. Reson*., **1975**, 19, 58 – 66.

Hagan, A. K., Zuchner, T., Lanthanide-based time-resolved luminescence immunoassays, *Anal Bioanal Chem*, **2011**, 400, 2847 – 2864.

Hammer, M., Schweitzer, D., Richter, S., Konigsdorffer, E., Sodium fluorescein as a retinal pH indicator?, *Physiol. Meas.*, **2005**, 26.

Häussinger, D., Huang, J., Grzesiek, S., DOTA-M8: An Extremely Rigid, High-Affinity Lanthanide Chelating Tag for PCS NMR Spectroscopy, *J. Am. Chem. Soc.,* **2009**, 131, 14761 – 14767.

He, M.M., Smith, A.S., Oslob, J.D., Flanagan, W.M., Braisted, A.C., Whitty, A., Cancilla, M.T., Wang, J., Lugovskoy, A.A., Yoburn, J.C., Fung, A.D., Farrington, G., Eldredge, J.K., Day, E.S., Cruz, L.A., Cachero, T.G., Miller, S.K., Friedman, J.E., Choong, I.C., Cunningham, B.C., Small-molecule inhibition of TNF-alpha, *Science*, **2005**, 310, 1022 – 1025.

Hebbink, G. A., Grave, L., Woldering, L. A., Reinoudt, D. N., van Veggel, F. C. J. M., Unexpected sensitization efficiency of the near-infrared Nd3+, Er3+, and Yb3+ emission by fluorescein compared to eosin and erythrosin, *J Phys Chem A,* **2003**, 107, 2483 – 2491.

Hemmila, I., Laitala, V., Progress in Lanthanides as Luminescent Probes, *J. Fluoresc*. **2005**, 15, 529 – 542.

Hiruma, Y., Hass, M. A. S., Kikui, Y., Liu, W. M., Olmez, S. P., Skinner, A., Blok, A., Kloosterman, A., Koteishi, H., Lohr, F., Schwalbe, H., Nojiri, M., Ubbink, M., The Structure of the Cytochrome P450cam-Putidaredoxin Complex Determined by Paramagnetic NMR Spectroscopy and Crystallography, *Journal of Molecular Biology*, **2013**, 425, 4353 – 4365.

Horrocks, W. D., Luminescence Spectroscopy, *Methods in Enzymology*, **1993**, 226, 495 – 538.

Hou, L., Honaker, M. T., Shireman, L. M., Balogh, L. M., Roberts, A. G., Ng, K., Nath, A., Atkins, W. M., Functional Promiscuity Correlates with Conformational Heterogeneity in A-class Glutathione S-Transferases, *J. Biol. Chem.*, **2007**, 282, 23264 – 23274.

Hristov, G., Marttila, T., Durand, C., Niesler, B., Rappold, G. A., Marchini, A., SHOX triggers the lysosomal pathway of apoptosis via oxidative stress, *Hum. Mol. Genet*., **2014**, 23, 1619 – 1630.

Huisgen, R., Centenary Lecture – 1,3-Dipolar Cycloadditions, Proceedings of the Chemical Society of London, **1961**, 357.

Irwin, J. J., Shoichet, B. K., ZINC—a free database of commercially available compounds for virtual screening, *J. Chem. Inf. Model*, **2005**, 45, 177 – 182.

Iwahara, J., Clore, G. M., Detecting transient intermediates in macromolecular binding by paramagnetic NMR, *Nature*, **2006**, 440, 1227 – 1230.

Iwamoto, T., Grove, A., Montal, M.O., Montal, M. and Tomich, J.M. (1994) Chemical synthesis and characterization of peptides and oligomeric proteins designed to form transmembrane ion channels. *Int.J.Pept.Protein Res.*, **1994**, 43, 597-607.

Jewett, J. C., Bertozzi, C. R., Cu-free click cycloaddition reactions in chemical biology¸ *Chem. Soc. Rev.*, **2010**, 39, 1272 – 1279.

Jeyaprakash, A. A., Klein, U. R., Lindner, D., Ebert, J., Nigg, E. A., Conti, E., Structure of a Survivin-Borealin-INCENP core complex reveals how chromosomal passengers travel together, *Cell,* **2007**, 131, 271 – 285.

Jeyaprakash, A. A., Basquin, C., Jayachandran, U., Conti, E., Structural Basis for the Recognition of Phosphorylated Histone H3 by the Survivin Subunit of the Chromosomal Passenger Complex, *Structure*, **2011**, 19, 1625 – 1634.

Jiang, X., Wilford, C., Duensing, S., Munger, K., Jones, G., Jones, D., Participation of Survivin in mitotic and apoptotic activities o fnormal and tumor-derived cells, *J. Cell. Biochem.*, **2001**, 83, 342 – 354.

Johnson, D. K., Karanicolas, J., Druggable protein interaction sites are more predisposed to surface pocket formation than the rest of the protein surface, *PLoS Comput. Biol*., **2013***,* 9, 1 – 10.

Jorgensen, W. L., The many roles of computation in drug discovery, *Science*, **2004**, 303, 1813 – 8.

Kasha, M., Characterization of electronic transitions in comlex molecules, *Disc Faraday Soc*, **1950**, 9, 14 – 19.

Kempe, M. and Barany, G., CLEAR: A Novel Family of Highly Cross-Linked Polymeric Supports for Solid Phase Synthesis, *J. Am. Chem. Soc.,* **1996** , 118, 7083 - 7093.

Kim, B. E., Nevitt, T., Thiele, D. J., Mechanisms for copper acquisition, distribution and regulation, *Nat Chem Biol*, **2008**, 4, 176 – 185.

Kolb, H. C., Finn, M. G., Sharpless, K. B., Click chemistry: Diverse chemical function from a few good reactions, *Angewandte Chemie International Edition*, **2001**, 40, 2004 – 2021.

Kota, S., Takahashi, V., Ni, F., Snyder, J. K., Strosberg, A. D., Direct Binding of a Hepatitis C Virus Inhibitor to the Viral Capsid Protein, *PLoS One,* **2012**, 7, 1 – 10.

Kuppens, S., Hellings, M., Jordens, J., Verheyden, S., Engelborghs, Y., Conformational states of the switch I region of Ha-*ras*-p21 in hinge residue mutants studied by fluorescence lifetime and fluorescence anisotropy measurements, *Protein Science*, **2003**, 12, 930 – 938.

Lakowicz, J. R., Principles of Fluorescence Spectroscopy, Second Edition, **1999**, Plenum Publishers.

Lampe, J. N., Brandman, R., Sivaramakrishnan, S., Ortiz de Montellano, P. R., Two-dimensional NMR and All-atom Molecular Dynamics of Cytochrome P450 CYP119 Reveal Hidden Conformational Substates, *J. Biol. Chem.*, **2010**, 285, 9594 – 9603.

Lea, W. A., Simeonov, A., Fluorescence Polarization Assays in Small Molecule Screening, *Expert Opin. Drug Discovery*, **2011**, 6, 17 – 32.

Lemos, M. A. and G. Hungerford, The Binding of *Curcuma Longa* Extract with Bovine Serum Albumin Monitored *via* Time-Resolved Fluorescence, *Photochem. Photobiol.,* **2013**, 89, 1071 – 1078.

Li, F., Ambrosini, G., Chu, E. Y., Plescia, J., Tognin, S., Marchisio, P. C., Altieri, D. C., Control of apoptosis and mitotic spindle checkpoint by Survivin, *Nature*, **1998**, 396, 580 – 584.

Lim, K., Jameson, D. M., Gentry, C. A., Herron, J. N., Molecular Dynamics of the Anti-Fluorescein 4-4-20 Antigen-Binding Fragment. 2. Time-Resolved Fluorescence Spectroscopy, *Biochemistry*, **1995**, 34, 6975 – 6984.

Lipinski, C. A., Lombardo, F., Dominy, B. W., Feeney, P. J., Experimental and computational approaches to estimate solubility and permeability in drug discovery and development settings, *Adv. Drug Deliv. Rev.*, **2001**, 46, 3 – 26.

Liu, Z., Sun, C., Olejniczak, E. T., Meadows, R. P., Betz, S. F., Oost, T., Herrmann, J., Wu, J. C., Fesik, S. W., Structural basis for binding of Smac/DIABLO to the XIAP BIR3 domain, *Nature,* **2000**, 408, 1004 – 1008.

Lodish, Harvey F., Molecular Cell Biology, **1999**, New York, Scientific American Books.

Madl, T. Bermel, W., Zangger, K., Use of Relaxation Enhancements in a Paramagnetic Environment for the Structure Determination of Proteins Using NMR Spectroscopy, *Angew. Chem. Int. Ed.,* **2009**, 48, 8259 – 8262.

Madsen, U., Krogsgaard-Larsen, P., Liljefors, T., *Textbook of Drug Design and Discovery*, **2002**, Washington, DC, Taylor & Francis.

Magde, D., Rojas, G. E., Seybold, P. G., Solvent Dependence of the Fluorescence Lifetimes of Xanthene Dyes, *Photochemistry and Photobiology*, **1999**, 70, 737 – 744.

Martin, M. E., Parameswarappa, S. G., O'Dorisio, M. S., Pigge, F. C., Schultz, M. K., A DOTA-peptide conjugate by copper-free click chemistry, *Bioorganic & Medicinal Chemistry Letters,* **2010**, 20, 4805 – 4807.

Martin, M. M., Lindqvist, L, The pH dependence of fluorescein fluorescence, *Journal of Luminescence*, **1975**, 10, 381 – 390.

Mathis, G., Rare earth cryptates and homogeneous fluoroimmunoassays with human sera, *Clin Chem*, **1993**, 39, 1953 – 1959.

Moeller, T., Thompson, L. C., Observations on the rare earths—LXXV(1): The stabilities of diethylenetriaminepentaacetic acid chelates, *Journal of Inorganic and Nuclear Chemistry*, **1962**, 24, 499.

Morley, Fundamental Studies on Brooker's Merocyanine, *J. Am. Chem. Soc.*, **1997**, 119, 10192 – 10202.

Muchmore, S. W., Chen, J., Jakob, C., Zakula, D., Matayoshi, E. D., Wu, W., Zhang, H., Li, F., Ng S. C., Altieri, D. C., Crystal structure and mutagenic analysis of the inhibitor-of-apoptosis protein Survivin, *Mol. Cell,* **2000**, 6, 173 – 182.

Murphy, C. J., Barton, J. K., Luminescence Spectroscopy, *Methods in Enzymology*, **1993**, 226, 495 – 538.

Nakahara, T., Takeuchi, M., Kinoyama, I., Minematsu, T., Shirasuna, K., Matsuhisa, A., Kita, A., Tominaga, F., Hatakeyama, S., Yamanaka, K., Kudoh, M., Sasamata, M., YM155, a Novel Small-Molecule Survivin Suppressant, Induces Regression of Established Human Hormone-Refractory Prostate Tumor Xenografts, *Cancer Res.*, **2007**, 67, 8014 – 8021.

Niedzialkowska, E., Wang, F., Porebski, P. J., Minor, W., Higgins, J. M. G., Stukenberg, P. T., Molecular basis for phosphospecific recognition of histone H3 tails by Survivin paralogues at inner centromeres, *Molecular Biology of the Cell,* **2012**, 23, 1457 – 1466.

Nikolovska-Coleska, Z., Wang, R., Fang, X., Pan, H., Tomita, Y., Li, P., Roller, P. P., Krajewski, K., Saito, N. G., Stuckey, J. A., Wang, S., Development and optimization of a binding assay for the XIAP BIR3 domain using fluorescence polarization, *Analytical Biochemistry*, **2004**, 332, 261 – 273.

Nikolovska-Coleska, Z., Meagher, J. L., Jiang, S., Kawamoto, S. A., Gao, W., Yi., H., Qin, D., Roller, P. P., Stuckey, J. A., Wang, S., Design and characterization of bivalent Smac-based peptides as antagonists of XIAP and development and validation of a fluorescence polarization assay for XIAP containing both BIR2 and BIR3 domains, *Analytical Biochemistry,* **2008**, 374, 87 – 98.

Nitz, M., Sherawat, M., Franz, K. J., Peisach, E., Allen, K. N., Imperiali, B., Structural Origin of the High Affinity of a Chemically Evolved Lanthanide-Binding Peptide, *Angew. Chem.*, **2004**, 116, 3768 – 3771.

Oikawa, T., Unno, Y., Matsuno, K., Sawda, J., Ogo, N., Tanaka, K., Asai, A., Identification of a small-molecule inhibitor of the interaction between Survivin and Smac/DIABLO, *Biochemical and Biophysical Research Communications*, **2010**, 393, 253 – 258.

Otting, G., Prospects for lanthanides in structural biology by NMR, *J. Biomol NMR,* **2008**, 42, 1 – 9.

Pandya, S., Yu, J., Parker, D., Engineering emissive europium and terbium complexes for molecular imaging and sensing, *Dalton Trans*., **2006**, 2757 – 2766.

Pietraszkiewicz, M., Karpiuk, J., Kumar, R. A., Lanthanide complexes of macrocyclic and macrobicyclic N-oxides; light-converting supramolecular devices, *Pure Appl. Chem.*, **1993**, 65, 563 – 566.

Poupart, S., Boudou, C., Peixoto, P., Massonneau, M., Renard, P., Romieu, A., Aminopropargyl derivative of terpyridine-bis(methyl-enamine) tetraacetic acid chelate of europium (Eu (TMT)-AP3): a new reagent for fluorescent labeling of proteins and peptides, *Org. Biomol. Chem.,* **2006**, 4, 4165 – 4177.

Prudêncio, M., Rohovec, J., Peters, J. A., Tocheva, E., Boulanger, M. J., Murphy, M. E. P., Hupkes, H., Kosters, W., Impagliazzo, A., Ubbink, M., A Caged Lanthanide Complex as a Paramagnetic Shift Agent for Protein NMR, *Chem. Eur. J.*, **2004**, 10, 3252 – 3260.

Rajapakse, H. E., Reddy, D. R., Mohandessi, S., Butlin, N. G., Miller, L. W., Luminescent Terbium Protein Labels for Time-Resolved Microscopy and Screening, *Angew. Chem. Int. Ed.,* **2009,** 48, 4990 – 4992.

Ryu, Y., Schultz, P. G., Efficient incorporation of unnatural amino acids into proteins in *Escherichia coli*, *Nature Methods,* **2006,** 3, 263 – 265.

Saha, A. K., Kross, K., Kloszewski, E. D., Upson, D. A., Toner, J. L., Snow, R. A., Black, C. D. V., Desai, V. C., Time-Resolved Fluorescence of a New Europium Chelate Complex: Demonstration of Highly Sensitive Detection of Protein and DNA Samples, *J. Am. Chem. Soc.*, **1993**, 115, 11032 – 11034.

Sambrook, J., Russell, D. W., Molecular Cloning, A Laboratory Manual, 3rd Edition, **2001**, Cold Spring Harbor Laboratory Press, Cold Spring Harbor, NY.

Sandtner, W., Bezanilla, F., Correa, A. M., In Vivo Measurement of Intramolecular Distances Using Genetically Encoded Reporters, *Biophysical Journal*, **2007,** L45 – L47.

Saupe, A., Englert, G., High-Resolution Nuclear Magnetic Resonance Spectra of Orientated Molecules, *Physical Review Letters,* **1963**, 11, 462 – 464.

Schneider, G., Fechner, U., Computer-based de novo design of drug-like molecules, *Nat Rev Drug Discov,* **2005,** 4, 649 – 63.

Serrano, A. L., Bilsel, O., Gai, F., Native State Conformational Heterogeneity of HP35 Revealed by Time-Resolved FRET, *J. Phys. Chem.*, **2012**, 116, 10631 – 10638.

Skoufias, D. A., Mollinari, C., Lacroix, F. B., Margolis, R. L., Human Survivin is a kinetochore-associated passenger protein, *J. Cell. Biol.,* **2000**, 151, 1575 – 1582.

Solomon, I., Relaxation Processs in a System of Two Spins, *Phys. Rev*., **1955**, 99, 559.

Speers, A. E., Cravatt, B. F., Profiling Enzyme Activities In Vivo Using Click Chemistry Methods, *Chemistry & Biology*, **2004**, 11, 535 - 546.

Su, X-C., Huber, T., Dixon, N. E., Otting, G., Site-Specific Labelling of Proteins with a Rigid Lanthanide-Binding Tag, *ChemBioChem*, **2006**, 7, 1599 - 1604.

Su, X., Man, B., Beeren, S., Liang, H., Simonsen, S., Schmitz, C., Huber, T., Messerle, B. A., Otting, G., A dipicolinic acid tag for rigid lanthanide tagging of proteins and paramagnetic NMR spectroscopy, *J. Am. Chem. Soc.*, **2008**, 130, 10486 – 10487.

Su, X.-C., Otting, G. J. Paramagnetic labelling of proteins and oligonucleotides for NMR, *J. Biomol. NMR,* **2010**, 46, 101 – 112.

Sukthankar, P., Gudlur, S., Avila, L.A., Whitaker, S.K., Katz, B.B., Hiromasa, Y., Gao, J., Thapa, P., Moore, D., Iwamoto, T., Chen, J. and Tomich, J.M., Branched Oligopeptides Form Nanocapsules with Lipid Vesicle Characteristics, *Langmuir,* **2013**, 29, 14648 – 14654.

Sun, C., Cai, M., Meadows, R. P., Xu, N., Gunasekera, A. H., Herrmann, J., Wu, J. C., Fesik, S. W., NMR Structure and Mutagenesis of the Third Bir Domain of the Inhibitor of Apoptosis Protein XIAP, *J. Biol. Chem.*, **2000**, 275, 33777 – 33781.

Sun, C., Nettesheim, D., Liu, Z., Olejniczak, E. T., Solution Structure of Human Survivin and Its Binding Interface with Smac/Diablo, *Biochemistry*, **2005**, 44, 11 – 17.

Thermo Electron Corporation, Finegan LTQ FT Instrument Manual, Thermo Electron **2003**, Printed in USA, 04/03, B-1248.

Uren, A. G., Wong, L., Pakusch, M., Fowler, K. J., Burrows, F. J., Vaux, D. L., Choo, K. H. A., Survivin and the inner centromere protein INCENP show similar cell-cycle localization and gene knockout phenotype, *Curr. Biol*, **2000**, 10, 1319 – 1328.

Velculescu, V. E., Madden, S. L., Zhang, L., Lash, A. E., Yu, J., Rago, C., Lal, A., Wang, C. J., Beaudry, G. A., Ciriello, K. M., Cook, B. P., Dufault, M. R., Ferguson, A. T., Gao, Y., He, T. C., Hermeking, H., Hiraldo, S. K., Hwang, P. M., Lopez, M. A., Luderer,

H. F., Mathews, B., Petroziello, J. M., Polyak, K., Zawel, L., Kinzler, K. W., Analysis of human transcriptomes, *Nat. Genet.,* **1999**, 23, 387 – 388.

Verdecia, M. A., Huang, H., Dutil, E., Kaiser, D. A., Hunter, T., Noel, J. P., Structure of the human anti-apoptotic protein Survivin reveals a dimeric arrangement, *Nature Structural Biology,* **2000**, 7, 602 – 608.

Verhagen, A. M., Ekert, P. G., Pakusch, M., Silke, J., Connolly, L. M., Reid, G. E., Moritz, R. L., Simpson, R. J., Vaux, D. L., Identification of DIABLO, a mammalian protein that promotes apoptosis by binding to and antagonizing IAP proteins, *Cell*, **2000**, 102, 43 – 53.

Wang, L., Xie, J., Schultz, P. G., Expanding the Genetic Code, *Annural Review of Biophysics and Biomolecular Structure*, **2006**, 35, 225 – 249.

Wang, R., Gao, Y., Lai, L., LigBuilder: A Multi-Purpose Program for Structure-Based Drug Design, *Journal of Molecular Modeling,* **2000**, 6, 498 – 516.

Weisberg, E., Manley, P. W., Breitenstein, W., Bruggen, J., Cowan-Jacob, S. W., Ray, A., Huntly, B., Fabbro, D., Fendrich, G., Hall-Meyers, E., Kung, A. L., Mestan, J., Daley, G. Q., Callahan, L., Catley, L., Cavazza, C., Mohammed, A., Neuberg, D., Wright, R. D., Gilliland, D. G., Griffin, J. D., Characterization of AMN107, a selective inhibitor of native and mutant Bcr-Abl, *Cancer Cell*, **2005**, 7, 129 – 141.

Werts, M. H. V., Hofstraat, J. W., Geurts, F. A. J., Verhoeven, J. W., Fluorescein and eosin as sensitizing chromophores in near-infrared luminescent ytterbium (III), neodymium (III) and erbium (III) chelates, *Chem Phys Lett*, **1997**, 276, 196 – 201.

Werts, M. H. V., Verhoeven, J. W., Hofstraat, J. W., Efficient visible light sensitisation of water-soluble near-infrared luminescent lanthanide complexes, *J Chem Soc Perkin Trans,* **2000**, 2, 433 – 439.

Wüthrich, K., Protein structure determination in solution by NMR spectroscopy, *J. Biol. Chem.*, **1990,** 265, 22059 – 22062.

Xie, J., Liu, W., Schultz, P. G., A Genetically Encoded Bidentate, Binding Amino Acid, *Angew. Chem. Int. Ed.*, **2007**, 46, 9239 – 9242.

Young, T. S., Schultz, P. G., Beyond the Canonical 20 Amino Acids: Expanding the Genetic Lexicon, *J. Biol. Chem.*, **2010**, 285, 11039 – 11044.

Zhang, K., Wang, M., Potential effects of CRM1 inhibition in mantle cell lymphoma, *Chin. J. Cancer Res.*, **2012**, 24, 372 – 387.

Zhang, W., Luo, X., Liu, Y., Shao, X., Wade, J. D., Bathgate, R. A., Guo, Z., Site-specific DOTA/europium-labeling of recombinant human relaxin-3 for receptor-ligand interaction studies, *Amino Acids,* **2011**, 43, 983 – 992.

Zhu, M. L., Horbinski, C. M., Garzotto, M., Qian, D. Z., Beer, T. M., Kyprianou, N., Tubulin-targeting chemotherapy impairs androgen receptor activity in prostate cancer, *Cancer Res.*, **2010**, 70, 7992 – 8002.